
21 Proton-Conducting Membranes for Fuel Cells

Vineet Rao, Norbert Kluy, Wenbo Ju, and Ulrich Stimming

CONTENTS

21.1	Introduction	568
21.1.1	Basic Principle of Operation of PEMFCs.....	568
21.2	Physiochemical Requirements for the Membranes in Fuel Cell Applications	569
21.2.1	Specific Fuel Cell Applications	569
21.2.1.1	Automotive Application.....	569
21.2.1.2	Stationary Application.....	573
21.2.1.3	Portable Applications (H ₂ -Fueled PEMFC)	574
21.2.2	Porous Structure and Permeability Requirements.....	574
21.2.3	Catalyst Utilization and Interfacial Aspects.....	578
21.2.4	Membrane Requirements for Direct Methanol Fuel Cells	580
21.2.4.1	Methanol Crossover	580
21.2.4.2	Water Permeation.....	580
21.3	Mechanistic Aspects of Proton Conductivity (Nafion and PFSA).....	580
21.3.1	Microscopic Structure	581
21.4	Materials: Physiochemical Properties and Fuel Cell Performance	582
21.4.1	PFSA Membranes	582
21.4.1.1	Properties of Nafion PFSA Membranes.....	583
21.4.1.2	Performance of DuPont Nafion® Membranes.....	583
21.4.1.3	Synthesis of PFSA Monomers and Polymers	586
21.4.1.4	Reinforced Membrane	589
21.4.1.5	Chemical Stabilization.....	589
21.4.1.6	Fluoride Emission Rate: Reinforced and Chemically Stabilized Membrane.....	589
21.4.2	Mechanically Reinforced Perfluorinated Membranes.....	590
21.4.2.1	PFSA Ionomer in Expanded Porous PTFE (Gore-Select Membranes)	590
21.4.2.2	PFSA Ionomer with PTFE Fibril Reinforcement (AGC, Flemion)	592
21.4.2.3	PFSA Ionomer and PTFE Reinforcement at Asahi Kasei (Aciplex Membranes)	594
21.4.3	Partially Fluorinated Ionomers.....	594
21.4.3.1	FuMA-Tech Membranes	594
21.4.3.2	Poly(α, β, γ-Trifluorostyrene) and Copolymers (Ballard Advanced Materials)	594
21.4.3.3	Radiation-Grafted Membranes	595
21.4.4	Inorganic/Organic (Fluorinated) Composite Ionomer Membranes.....	596
21.4.4.1	Hydrophilic Fillers (SiO ₂ , TiO ₂ , ZrO ₂) and ORMOSIL Networks	596
21.4.4.2	Properties of Recast Membranes with Inorganic Fillers	597
21.4.4.3	Heteropoly Acid Additive	599
21.4.4.4	Phosphate and Phosphonate Additives.....	599
21.4.4.5	Proton-Conducting Membranes Based on Electrolyte-Filled Microporous Matrices/ Composite Membranes	600
21.4.4.6	Other Concepts	601
21.4.5	Polymer Membranes with Inorganic Acid Impregnation	602
21.4.5.1	PEMEAS (Celanese) Membranes	603
21.4.6	Sulfonated Hydrocarbon Polymer Electrolyte Membranes.....	603
21.5	Summary	608
	References.....	609

21.1 INTRODUCTION

Polymer electrolyte-based fuel cells are emerging as attractive energy conversion systems suitable for use in many industrial applications, starting from a few milliwatts for portables to several kilowatts for stationary and automotive applications. The ability of polymer electrolyte membrane fuel cells (PEMFCs) to offer high chemical to electrical fuel efficiency and almost zero emissions in comparison to today's prevailing technology based on internal combustion engines (ICEs) makes them an indispensable option as environmental concerns rise.¹⁻⁶

Although the basic principles of fuel cells have been known for at least a century, the introduction of solid polymer electrolyte membranes a few decades ago revolutionized fuel cell technology. Initially, poly(styrenesulfonic acid) (PSSA) and sulfonated phenol-formaldehyde membranes were used, but the useful service life of these materials was limited because of their tendency to degrade in fuel cell operating conditions.^{7,8} A critical breakthrough was achieved with the introduction of Nafion[®], a perfluorinated polymer with side chains terminating in sulfonic acid moieties, which was invented in the 1960s for the chlor-alkali industry at DuPont. This material and its close perfluorosulfonic acid (PFSA) relatives are currently the state of the art in PEMFCs. PFSA-based membranes have good proton conductivity, high chemical and mechanical stability, high tear resistance, and very low gas permeability in fuel cell operating conditions.^{9,10}

But some problems associated with PFSA-based membranes have precluded large-scale market adoption of fuel cells. Their relatively high cost, limits to the range of temperature over which they can be reliably used (the upper limit is considered to be somewhat above 100°C, because the glass transition temperature is around 120°C; at higher temperatures >100°C, membranes have low water content and thus low proton conductivity), faster oxidative degradation and faster deterioration in mechanical properties at elevated temperatures, and a stringent requirement for external humidification of reactant gases under these conditions make the fuel cell balance of a plant more complicated. Additionally, for liquid-phase direct methanol fuel cells (DMFCs), the PFSA membrane is permeable to methanol and water, whose presence on the cathode side seriously degrades the DMFC performance.

All these drawbacks have led researchers to make more efforts to discover membranes with improved characteristics on all these accounts. In the past decade, researchers all around the world have reported success in exploring new concepts for improving the properties of proton-conducting membranes. Companies like DuPont, Dow Chemical, W.L. Gore & Associates, PolyFuel, Asahi Glass Co., Ltd. (AGC), Asahi Chemical, Ion Power, and Ballard have brought improved membranes onto the market. The main goal of this chapter is to review some of these new ideas in the field of proton-conducting membranes.

21.1.1 BASIC PRINCIPLE OF OPERATION OF PEMFCs

A fuel cell consists of two electrodes sandwiched around an electrolyte. Air (or oxygen) is supplied to the cathode and

hydrogen to the anode, generating electricity, water, and heat. The electrocatalyst is either platinum or a platinum alloy, usually supported on high-surface-area carbon. The hydrogen atom splits into a proton and an electron, which take different paths to the cathode. The proton passes through the electrolyte, while the electrons pass through the external circuit. At the cathode catalyst, oxygen reduction takes place to produce water molecules. The electrons passing through the external load are available for useful work before they return to the cathode, to be reunited with the proton and oxygen in a molecule of water. The theoretical open-circuit potential for a H₂/O₂ fuel cell is 1.23 V at 25°C and unit activity, but because of kinetic losses in the oxygen reduction process at the cathode and ohmic losses in the electrolyte membrane, the workable potential available from this fuel cell is usually around 0.7 V.

The heart of a fuel cell is the membrane electrode assembly (MEA). In the simplest form, the electrode component of the MEA would consist of a thin film containing a highly dispersed nanoparticle platinum catalyst. This catalyst layer is in good contact with the ionomeric membrane, which serves as the reactant gas separator and electrolyte in this cell. The membrane is about 25–100 μm thick. The MEA then consists of an ionomeric membrane with thin catalyst layers bonded on each side. Porous and electrically conducting carbon paper/cloth current collectors act as gas distributors. Since ohmic losses occur within the ionomeric membrane, it is important to maximize the proton conductivity of the membrane, without sacrificing the mechanical and chemical stabilities.

Existing polymer membranes, for example, PFSA-based membranes, operate most effectively within a limited temperature range and require that the membrane must remain constantly hydrated with water, resulting in complex and expensive engineering solutions (cf. Section 21.2.1.1). More efficient and better-performing polymer membranes are needed for continued advancement of PEMFCs. An additional challenge in developing materials for PEMs is that these materials need to endure prolonged exposure to the fuel cell environment. Electrolyte membrane materials must resist oxidation, reduction, and hydrolysis. A further challenge is that the material should be affordable. Finally, it is desirable that the material will permit operation at a higher temperature (>120°C).

Carbon monoxide (CO) is formed as a by-product when organic fuels are thermally reformed to produce H₂ that can then be used in a fuel cell. For such reformat gas-supplied fuel cell systems, high-temperature membranes offer an important advantage because the MEAs based on high-temperature membranes are less susceptible to CO poisoning. Better CO tolerance of high-temperature MEAs results in relatively less stringent demand on purification of the reformat gas to hydrogen. This results in easier and more cost-effective balance of plant (BOP) for the fuel cell system. Fuel cells with high-temperature PEMs need smaller and less expensive cooling systems.

Over the last few years, membrane development has intensified, and numerous new developments have been reported.¹⁰

This increase in the interest in novel proton-conducting membranes for fuel cell applications has resulted in several studies and review publications on the overall subject and also on some related topics (e.g., nonfluorinated membranes). The content of these reviews has been used and is cited in the appropriate text passages.

Fuel cells, especially PEMFCs, can be used for various applications ranging from portable power supply for use in consumer electronics devices to stationary deployment for combined heat and power generation. Another potential application is transportation, in which fuel cells systems are developed for the propulsion of cars. The performance, operating conditions, costs, and durability requirements differ depending on the application. Transportation applications demand stringent requirements on fuel cell systems. Only the durability requirement in the transportation field is not as rigorous as the stationary application, although cyclic durability is necessary.

21.2 PHYSIOCHEMICAL REQUIREMENTS FOR THE MEMBRANES IN FUEL CELL APPLICATIONS

The fuel cell principle is based on the spatial separation of the reaction between hydrogen and oxygen by an electrolyte. The electrolyte needs to conduct either positively charged hydrogen ions (protons) or negatively charged oxygen (or hydroxide or carbonate) ions. For a technical realization, the specific ionic conductivity of the electrolyte has to be in the range of 50–200 mS cm⁻¹ and the electronic conductivity of the electrolyte should be minimal. It is obvious from the principle of fuel cells that the electrolyte should be mostly gas impermeable in order to effectively separate the reaction volumes. Furthermore, a high chemical stability in oxidizing and reducing atmospheres is required. Often, the MEA made from electrolyte membranes and catalysts has to be pressed against flow field/bipolar plates to minimize contact resistance or for sealing purposes. This necessitates good mechanical stability for the membrane. Because of these requirements, only a few systems are suitable for technical applications.

The main requirement—a high specific conductivity of the electrolyte—is illustrated in Figure 21.1, which shows the conductivity of selected electrolytes used in fuel cells. As can be seen in Figure 21.1, suitable materials are available for different operating temperatures and are also quite different ranging from solid-state ceramics to molten salts and aqueous electrolytes. Interestingly, the specific conductivities differ considerably, being higher for the liquids. It should be noted, however, that the important value is the area-specific resistance with a target value of <0.15 Ω cm². Therefore, although the specific conductivity of the oxygen ion-conducting, yttria-stabilized zirconia (YSZ) is lower compared to the other electrolytes, it can be integrated into a planar fuel cell with a thickness of about 15 μm. In order to restrict the resistance to 0.15 Ω cm², the associated specific ionic conductivity should exceed 10⁻² S cm⁻¹. Figure 21.1 indicates that this

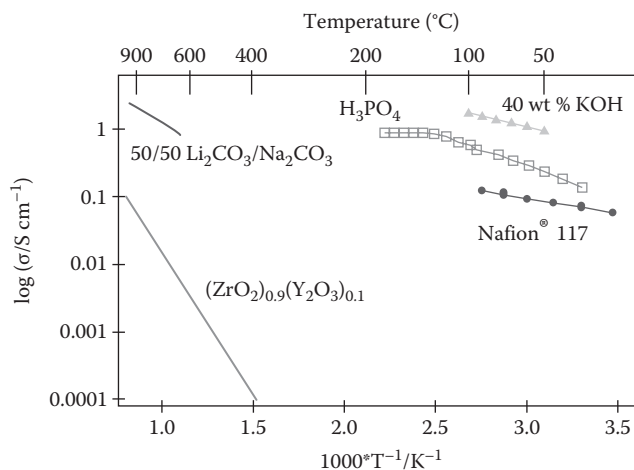


FIGURE 21.1 Specific conductivities of electrolytes used in fuel cells in different temperature ranges. (Data from Spedding, P.L., *J. Electrochem. Soc.*, 120, 1049, 1973; Horvath, A.L., *Handbook of Aqueous Electrolyte Solutions*, Ellis Horwood Ltd., Chichester, U.K., 1985; Brandon, N.P. et al., *Annu. Rev. Mater. Res.*, 33, 183, 2003; Dimitrova, P. et al., *Solid State Ionics*, 150, 115, 2002.)

value is attained at ca. 700°C for YSZ. The liquid electrolytes generally need a stabilizing matrix, and therefore, the resulting electrolyte layer is thicker. As a consequence, the specific conductivity has to be higher for these types.

21.2.1 SPECIFIC FUEL CELL APPLICATIONS

21.2.1.1 Automotive Application

21.2.1.1.1 Cooling Requirements

The main focus in membrane development for automotive applications is the search for membranes that can operate at higher temperatures and lower relative humidity (RH). The major issues have been published in a series of publications by automotive experts and fuel cell developers.^{11–13} The main statements are recapitulated here: assuming the availability of a hydrogen infrastructure, fuel cell-based systems might offer better efficiency than the ICE, which is one of the driving forces behind the development of fuel cells for this application. However, the ICE has the advantage that the waste heat can be removed more efficiently compared to fuel cell stacks. As a rule of thumb, it is stated that in ICEs, one-third of the fuel energy is converted into mechanical energy, and two-thirds is converted into heat. Half of the heat is removed by the coolant and half by the exhaust. Conversely, in a fuel cell system, typically less than 10% of the heat is rejected with the exhaust gases. Although the fuel cell system efficiency of about 50% is higher compared to ICEs, the coolant load is considerably larger. Furthermore, the PEM stack temperature is significantly lower, in the range of 60°C–80°C as compared to ICE peak coolant temperatures of 120°C. Since radiator performance is nearly proportional to the initial temperature difference (ITD) between the coolant and ambient temperatures, an ICE has about two to four times the heat rejection capacity during operation at elevated ambient

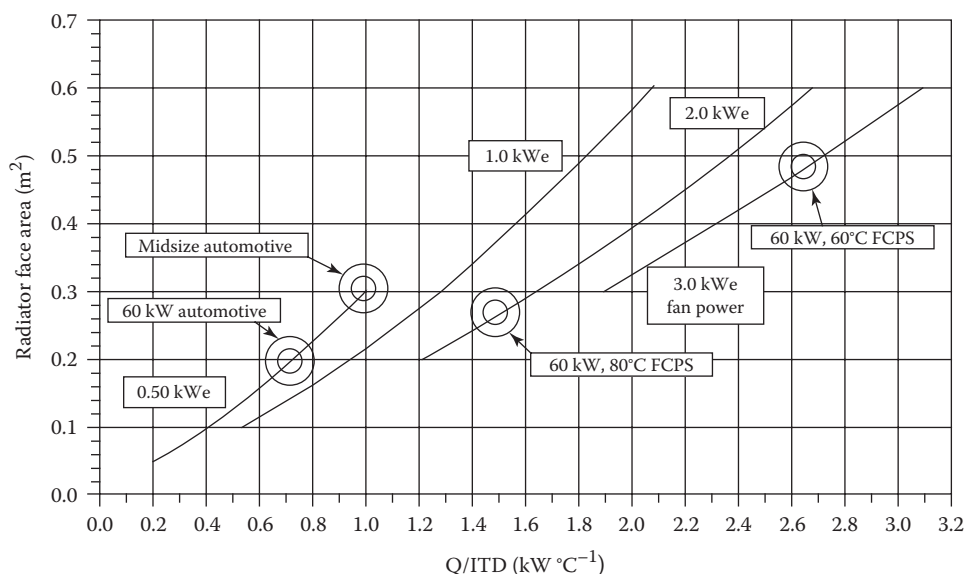


FIGURE 21.2 Thermal rejection requirements of automotive and fuel cell systems ($T_{\text{amb}} = 38^{\circ}\text{C}$). Solid lines are lines of constant radiator fan power. (Reproduced from Masten, D.A. and Bosco, A.D., in: *Handbook of Fuel Cells: Fundamentals, Technology and Applications*, Vielstich, W., Gasteiger, H.A., and Lamm, A., eds., Vol. 4, John Wiley & Sons, Chichester, U.K., 2003. With permission.)

temperatures of 32°C – 40°C (an ambient temperature of 38°C is the design value for radiators). The thermal rejection requirements for automotive power trains are shown in Figure 21.2. The necessary radiator face area is plotted versus the ratio of heat power and ITD. The solid line represents the radiator fan's constant electrical power. As can be seen with the present technology, even a modest-sized fuel cell power system in cars requires cooling systems that challenge normal car design. Consequently, stack temperatures coincident with or even higher than normal ICE coolant temperatures would be highly desirable in order to achieve more efficient cooling. Another aspect is that well-developed automotive hardware could be used enabling more cost-effective stack sizing and compact packaging.

21.2.1.1.2 Humidification Requirements

The operating temperature ranges of PEMFCs are determined by the humidification requirement of the electrolyte membranes. Also, current membranes have glass transition temperatures in the range of 80°C – 120°C and are thus subject to creep and hole formation at temperatures in that range. The implications of operating PEMFCs at higher temperatures and at 100% RH will be discussed in detail in the following section.

The membrane and ionomer humidification requirements are of paramount importance for PEMFC operation since the proton conductivity is a fundamental necessity in the membrane as well as in the electrode for the fuel cell to function. The operating conditions of current PEMFCs are dictated by the properties of the membranes/ionomers. At present, the most important membrane type (e.g., Nafion membranes from DuPont) is based on PFSA ionomers that are used in the membrane and the catalyst layers. Figure 21.3 shows the proton conductivity versus RH for three different

electrolyte systems, which are either presently available or are being developed for fuel cells. The often used PFSA system is represented by 1100 equivalent weight (EW) Nafion as measured by Alberti et al.¹⁴ Values at 80°C and 120°C are provided. Further results on sulfonated polyetherketone (s-PEEK) membranes are shown; the pure system is compared to an Aerosil®-filled membrane. The third system is a high-temperature membrane based on polybenzimidazole (PBI) filled (*doped*) with phosphoric acid by Ma et al.¹⁵ The PBI/ H_3PO_4 conductivity at four different temperatures 80°C , 160°C , 180°C , and 200°C is given. The minimum conductivity for fuel cell application was stated earlier in this section as 50 mS cm^{-1} . This conductivity is achieved for all membrane systems at different temperatures and different humidification conditions. For Nafion, the conductivity is above 0.1 S cm^{-1} for RH values greater than 90% for both 80°C and 120°C , but drops to 0.01 S cm^{-1} at 40% RH. Also represented on the right-hand axis of the plot is the ohmic loss for a $25\text{ }\mu\text{m}$ membrane at 1 A cm^{-2} . At 0.1 S cm^{-1} , the loss is 25 mV, which corresponds to a voltage efficiency loss of about 2%. Although this loss appears relatively small, overall voltage efficiency is a critical issue and should be kept as high as possible in automotive applications. The problem with the PFSA systems is the need for nearly 100% humidification, which is an important constraint in the system design. An alternative polyarylene membrane system—here s-PEEK membranes are shown—has the advantage of being potentially more cost effective compared to the fluorinated material, but the humidification requirements are similar to or even more stringent than (at least in this example) the Nafion case. A hypothetical advanced membrane with more suitable properties is represented by the blue line: such an advanced membrane should exhibit conductivity well over 50 mS cm^{-1} at RH of the gases below 50%. A membrane operating in a stable fashion at

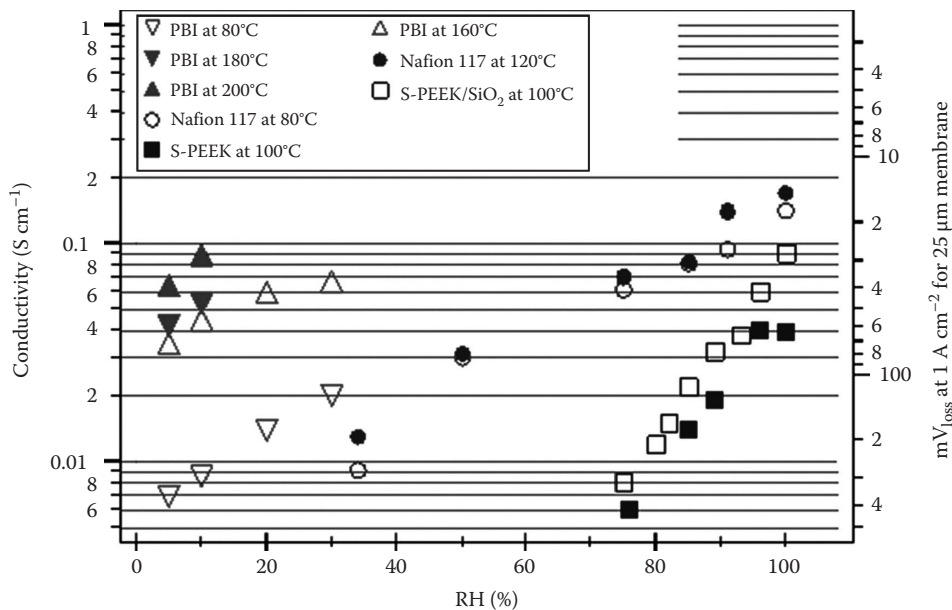


FIGURE 21.3 Conductivity of different membranes as a function of humidity. Requirements for an advanced membrane. (Data from Alberti, G. et al., *J. Membr. Sci.*, 185, 73, 2001; Ma, Y.L. et al., *J. Electrochem. Soc.*, 151, A8, 2004; Wainright, J.S. et al., in: *Handbook of Fuel Cells: Fundamentals, Technology and Applications*, Vielstich, W., Gasteiger, H.A., Lamm, A., eds., Vol. 3, John Wiley & Sons, Chichester, U.K., 2003.)

50% RH and at 120°C would be the ideal candidate for a future automotive fuel cell power system. The PBI/H₃PO₄ attains appropriate conductivity only above 160°C at 30% RH. At this high temperature, 30% RH is also critical as will be discussed later. Furthermore, this membrane system has performance disadvantages in dynamic load and temperature operation as will be discussed later. As a consequence, this system is better suited to stationary applications.

Figure 21.4 displays the water content of air given as the ratio g (H₂O)/g (dry air) for saturation humidity as a function of temperature and as a function of pressure. The 100%

RH requirement of the membrane means that a low-pressure system is restricted to temperatures below 100°C since the saturation partial pressure of water increases exponentially with temperature. In addition, it would be highly desirable to have a water-neutral situation in order to obtain a compact and simple system where the water produced at the cathode of the fuel cell as well as the permeated water is collected completely (a condenser would be necessary) to humidify the gases. In this respect, it would be an ideal situation to operate the fuel cell at the intersections of solid and dashed lines, which are the water-neutral operating conditions. The only

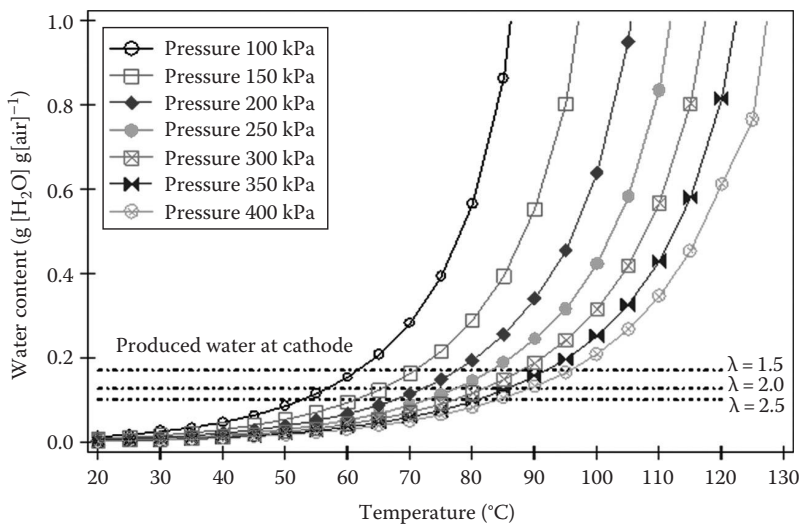


FIGURE 21.4 Water content required for membrane saturation versus temperature for different pressures of air. The dashed lines indicate the water produced for different air stoichiometries. (Zentrum für Sonnenenergie- und Wasserstoff-Forschung [ZSW] measurements, Stuttgart, Germany, Internal publication.)

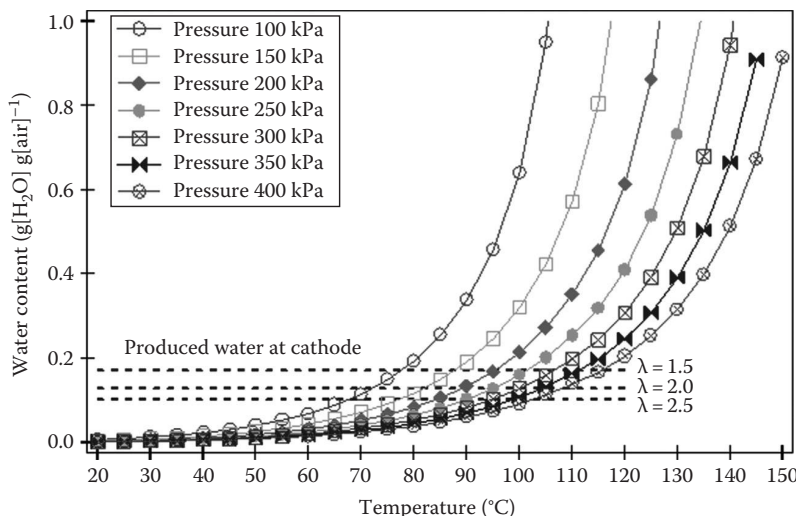


FIGURE 21.5 Water content required for 50% RH in air for advanced membranes versus temperature for different air pressures. The dashed lines indicate the water produced for different air stoichiometries. (ZSW measurements, Stuttgart, Germany, Internal publication.)

way to achieve such an operation while maintaining the 100% RH demand at temperatures near 100°C is to increase the pressure to 400 kPa. However, this means a drastic reduction in system efficiency due to the heavy losses associated with pressurization. These simple relationships exacerbate design complications and have been summarized thus by Masten and Bosco: “At higher temperatures and lower pressures, the humidification energy duty and associated condensate water requirements will overwhelm the water and thermal management capabilities of an automotive thermal system.” Increased stoichiometry and increased pressure may help in diminishing the water load but are associated with increased complexity and costs for the compressors and expanders.

Figure 21.5 shows the analogous relationships for 50% RH of the air. If a membrane tolerated such operation conditions over a long time, water-neutral operation would be feasible

at 100°C at moderate overpressures of 250 kPa. Ideally, a membrane should operate at 15%–20% RH that would enable water-neutral operation at ambient pressure and 110°C. However, such a membrane would probably be based on a radically different conduction mechanism compared to the present membranes where the proton conductivity is based on the liquid water environment. Such a membrane would be very welcome but at present is far from being realized. Realistically, it has to be assumed that progress in membrane development will consist of gradually improving membrane humidification and temperature stability.

In this respect, however, it is interesting to examine to exactly what degree 100% RH requirement is really necessary for state-of-the-art MEAs in the anode as well as in the cathode compartment under different operating conditions. Figure 21.6 shows single-cell measurements with GORE

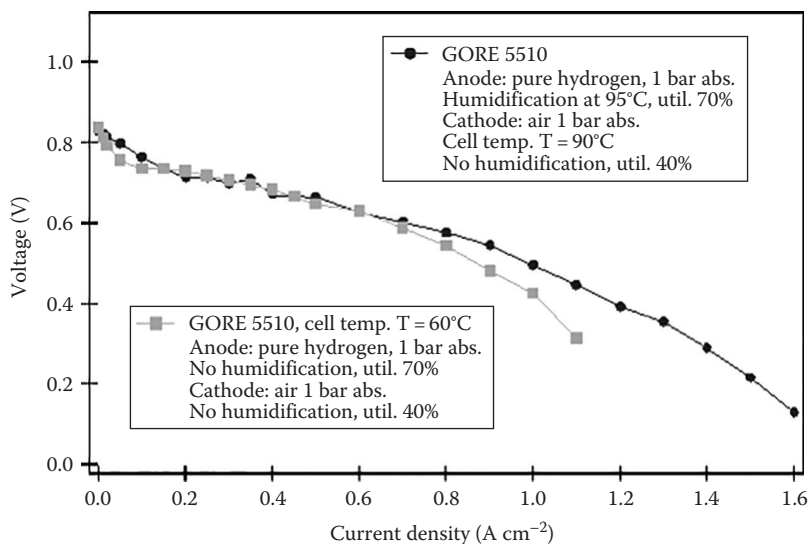


FIGURE 21.6 Performance of a GORE 5510 MEA in a single cell at a temperature of 60°C as well as of 90°C under reduced humidification conditions. (ZSW measurements, Stuttgart, Germany, Internal publication.)

5510 membrane electrode assemblies under low-humidification conditions. The membranes in these MEAs have a thickness of about 25 μm , which is a low value for PEMFCs. Therefore, it is possible to efficiently humidify the membrane by back diffusing the liquid product water into the membrane from cathode to anode side. The normal drying-out effect at the anode is diminished in this case because the membrane is thin and does not represent any significant diffusion resistance. With thin membranes, high current densities are also achievable due to their low ionic resistance. These attributes can be seen in Figure 21.6, which shows U–I curves at a high temperature of 90°C at the anode with humidification only at the anode as well as at a lower temperature of 60°C with no humidification at all. The U–I curves exhibit relatively low open-circuit voltages (OVCs) due to a high crossover of the gases, and therefore, the temperature difference does not influence the U–I curve much at lower current densities. At high current densities, humidification is improved, and stable operation is observed over about 12 h due to more water formation at the cathode. However, at present, it is not clear if this performance can be maintained over prolonged operation of more than 1000 h and if the power density is sufficient for transportation applications.

This example shows that efficient management of the liquid water produced at the cathode can be used to attenuate the 100% RH requirement of the membrane. Besides thin membranes, other strategies (described later) involving wicks or water produced by catalysts introduced into the membrane are well known. However, all of these strategies involve compromising other properties for water management; for example, thin membranes are not as durable since the mechanical properties are inferior or the performance of the MEAs is reduced in conjunction with reduced humidification.

The common way of improving the water management is to humidify the gases coming into the fuel cell. A less common approach is the direct hydration of the membrane by mounting porous fiber wicks within the membrane itself.¹⁶ Membranes with wicks are developed using twisted threads of porous polyester fibers that are then placed between the membrane and a cast thin film of Nafion ionomer and hot pressed at 150°C. Such membranes with porous fiber wicks are supplied with water directly through the wicks. The parts of the wicks outside the membrane are kept in contact with a water source such as a humidifier or condenser outside the membrane. Water diffuses through the porous fibers into the membrane, thus keeping it humidified. Similar approaches have also been reported by other authors.^{17,18}

21.2.1.2 Stationary Application

Fuel cells are promising candidates for energy conversion systems used for distributed power generation, which can guarantee uninterrupted power supply and thus cut unnecessary dependence on the grid. Fuel cells are quite efficient at around 60% electrical energy conversion efficiency, and the use of waste heat from the fuel cells to houses would make them more efficient. The efficiency of such a CHP

fuel cell system depends on the operating temperature of the system, which dictates the amount of recoverable heat. A fuel cell–based system makes very low noise and produces almost zero emissions when direct H_2 from non-fossil fuel sources is used. These are important advantages in comparison to conventional systems based on ICEs. But high costs and problems in long-term durability are major obstacles in the path of wide-scale introduction to the market. Polymer electrolyte membranes contribute a significant cost factor. The membranes are also primarily responsible for the degradation of the performance of the fuel cell system, being one of the most vulnerable components in the fuel cells. An effective heat removal system and a humidification management system are still very important in stationary fuel cell systems. But stationary applications put the strongest demand on the durability of the polymer electrolyte membranes. To understand the durability of the membrane, it is imperative to discuss various modes of its degradation.

21.2.1.2.1 Mechanical Degradation

Mechanical parameters related to preparing an MEA contribute significantly to the overall service life of the membrane.⁷ A high degree of cleanliness and quality control must be maintained to ensure that no foreign particles or fibers that may perforate the membrane during the MEA fabrication process are introduced. Generally, perforation can also take place at the fuel cell reactant inlets where mechanical stress may be highest. Care must be taken to design the fuel cell flow field to avoid local drying due to nonuniform distribution of reactant gases in the cell. Uniform contact pressure should also be maintained between the current collector system and the MEA. Excessive penetration of the catalyst layer into the membrane during MEA fabrication or due to high localized pressure exertion by the current collector can lead to high local current density and stresses. Excessive localized pressure close to the edge of the electrode/membrane may also lead to perforation and tearing of the membrane. Care must be taken in designing the fuel cell to avoid unsupported regions in the MEA flow field support structure into which the membrane could extrude and ultimately fail. Generally, when a membrane is perforated, hydrogen and oxygen will cross over to the other sides and react chemically on the catalyst producing only heat. The cell potential will decrease because of this mixing of reactants. The excessive heat produced due to the chemical reaction between hydrogen and oxygen may lead to more holes in the membrane.⁷

21.2.1.2.2 Thermal Degradation

PEMFCs generally operate at temperatures <100°C. PFSA-based polymer ionomer membranes like Nafion, Gore®, Aciplex®, and Flemion® are not significantly affected by temperatures up to 150°C where most of the water is lost and membranes may suffer irreversible dry out. Chemical degradation of these membranes in the H^+ form usually starts with the loss of sulfonate groups at over 220°C.⁷

21.2.1.2.3 Chemical and Electrochemical Degradation

In the case of properly designed and cleanly operated PEMFCs, polymer electrolyte membrane degradation by electrochemical and chemical mechanisms generally occurs relatively slowly over a period of several hundred hours. Polymer electrolyte membranes are especially sensitive to metal ions, which may get into the fuel cell via dust particles in the air or even rust. Even the platinum ions ever present in the electrode are not completely benign. Metal ions within the fuel cell would exchange with protons, thereby drastically reducing the proton conductivity of the membrane. It is also known that peroxide radicals are produced at very low levels during fuel cell operation, and these radicals are responsible for the chemical and physical deterioration of the membrane after extended use.^{19,20} Based on these findings, methods have been developed to perform accelerated chemical tests to simulate this type of PEM degradation. Peroxide radical-assisted degradation has been extensively studied for early PSSA membranes.²¹ It was shown that oxygen crossing over to the hydrogen side may lead to the formation of peroxide and hydroperoxide radicals, which can slowly deteriorate the membrane. The per(flurosulfonic acid) membranes are, relatively speaking, much better in terms of performance and service life. But peroxide radicals can still degrade the membrane, albeit to a smaller extent, as the basic backbone $-CF_2$ is less susceptible to peroxide attack. The susceptibility to peroxide attack has been attributed to traces of groups such as $-CHF_2$, which are inadvertently introduced into the perfluorocarbon sulfonyl structure during synthesis and can be converted into a carboxyl group by peroxo insertion.^{22,23}

The sum effect of mechanical, thermal, and chemical degradation of the membrane along with the degradation of catalysts will take its toll on the long-term performance of the fuel cell. A lot of effort is being put into improving membrane service life as well as MEA service life by many players in this field. For example, W.L. Gore has demonstrated service lives exceeding 28,000 h for membrane electrode assemblies targeted for stationary fuel cell systems.

21.2.1.3 Portable Applications (H_2 -Fueled PEMFC)

Portable applications are one of the most attractive segments in terms of fuel cell commercialization as the number of possible units required for consumer electronics market is high and cost limitations are much easier to meet than automotive or stationary applications. Fuel cells in the low power range can be used either as a complete substitute for batteries or in fuel cell/battery hybrid power supply systems. Fuel cells for portable applications usually operate under ambient conditions. For portable power supply applications based on hydrogen-fueled PEMFC, the most important issue is the power-to-volume/weight ratio, as more and more miniaturized power sources are needed for consumer electronics devices like laptops, mobile phones, palmtops, video cameras, and a host of military applications. To a large extent, the power-to-volume/weight ratio depends on the energy density of the fuel from which H_2 is extracted. Possible options for

hydrogen sources could be metal hydride, chemical hydride, or a thermal reformer, for example, methanol reformer. But the basic size of a fuel cell system also has a fair share in determining the overall energy density of portable fuel cell-based power supply. Thus, to meet these miniaturization challenges, passive thermal and water management and also suitable components for hydrogen/air feeding and pressure control must be realized. In meeting these requirements, the PEM has a big role to play, at least in water management. Water management requires the synergetic action of the gas diffusion layer (GDL) and the PEM. To meet the requirement of complete passive water management, the fuel cell should run on dry H_2 and dry air and retain just enough water in the membrane.

21.2.1.3.1 Membrane Humidification by Cathode Back Diffusion

One such approach employs a microporous layer (MPL) with an average pore size of around $1\ \mu\text{m}$ between the GDL (with an average pore size of $10\ \mu\text{m}$) and the catalyst layer. The MPL is made up of conducting carbon and is hydrophobized with a small amount of Teflon[®]. MPLs do not allow the escape of water as liquid drops because of surface tension in small pores. This builds up hydrostatic pressure on the cathode side. This hydrostatic pressure buildup allows back diffusion to the anode side. The positive role of MPLs in water management in PEMFCs has been investigated theoretically and experimentally in the literature.^{24–28} For the back diffusion to humidify, the whole membrane requires a thin and obviously stable membrane. With pure PFSA-based membranes, it has not been possible to reduce the thickness without compromising mechanical strength. To achieve this goal, several new ideas have been pursued, which will be discussed later in this chapter. One such approach is to reinforce the membranes with poly(tetrafluoroethylene) (PTFE) fibers, a technique pioneered by W.L. Gore, which can reduce membrane thickness to only a few microns. Figure 21.7 shows the $I-U$ characteristics of a fuel cell using Gore membranes, under completely dry conditions.

21.2.2 POROUS STRUCTURE AND PERMEABILITY REQUIREMENTS

The important chemical reactions take place at the interface between the electrode and the electrolyte. Since reactants in fuel cells are mostly gaseous and poorly soluble in the electrolyte, a third phase, the gaseous one, has to be in contact with the interface, leading to a three-phase boundary. Furthermore, a certain solubility and diffusivity of the reactant within the ionomer material in the electrode are needed to achieve greater utilization of the catalyst. This permeability in the ionomer helps to extend the electrochemically active surface area of the catalyst that belongs to the three-phase boundary. A diagram of this zone in a PEMFC is shown in Figure 21.8. Presently, differing opinions exist on the structure of the active layer; it is unclear if the ionomer is present at the interface as a third bulk phase or as a thin film

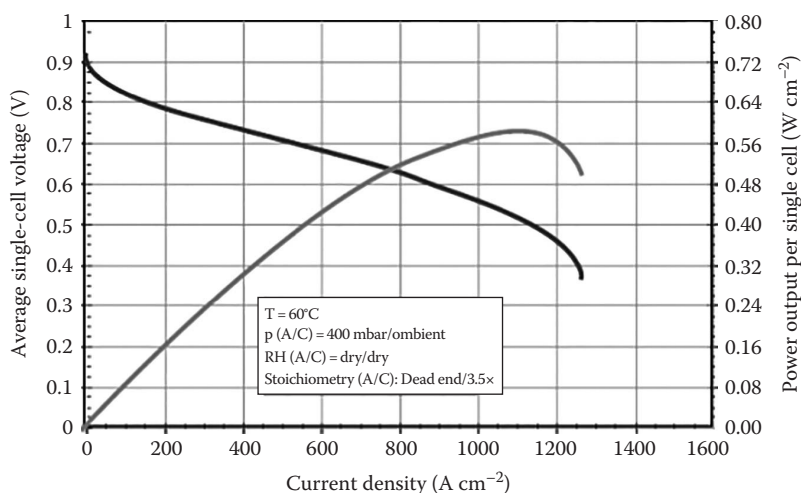


FIGURE 21.7 Performance of the Gore 58 series in completely dry conditions. (Courtesy of W.L. Gore & Associates, Elkton, MD.)

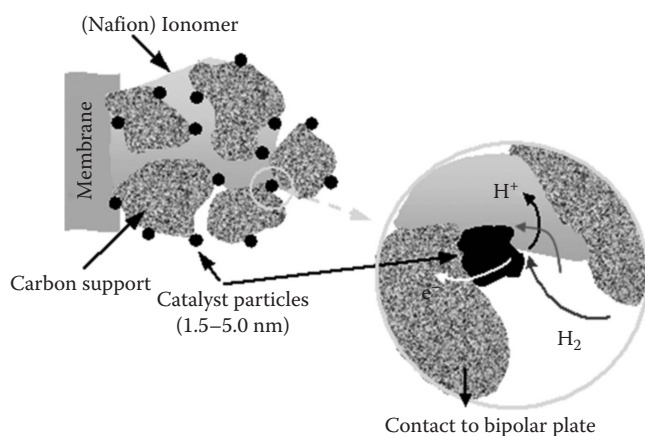


FIGURE 21.8 Diagram of the active layer of a gas diffusion electrode in a PEMFC.

of about 20–50 nm covering the catalyst. Such differences would have considerable implications for the optimization of this interfacial region.

To optimize the kinetics in this area, the following features are required:

- High, electrochemically active surface area of the catalyst
- Good access for the reactants to the electrode–electrolyte interface and sufficient permeability in the ionomer
- Effective water removal from the three-phase zone
- Good electric and ionic contact at the reaction sites

These requirements can be achieved best with a porous structure, but the realization depends strongly on operating temperature. Since costly precious metals (Pt and Pt alloys) are used as a catalyst, high dispersion of these metals is necessary in order to optimize the surface-to-mass ratio. Starting from metal salts, various chemical routes are usually used to achieve very small metal catalyst particles and thus high dispersion. The metal particle sizes are of the order

of a few nanometers (platinum surface areas in the range of 20–60 m² g⁻¹ are common). In the case of supported catalysts, the metal clusters are supported on larger electron-conducting and porous carbon particles (usually about 50–100 nm in diameter) in order to achieve better dispersion of the metal catalyst and higher active surface area and to prevent agglomeration of metal catalyst nanoparticles. The catalyst is introduced into the electrocatalyst layer along with the proton-conducting ionomer component. The ionomer content increases the metal catalyst utilization in the catalyst layer, but normally, an optimum content is found, and further increase in ionomer content leads to lower catalyst surface utilization. Largely varying utilizations of catalyst surfaces (varying between 50% and 90%) in PEMFC electrodes have been reported.²⁹ Usually, the catalyst layer has a thickness in the range of about 5–30 μm.

Gasteiger and Mathias have analyzed the requirements of membranes for automotive applications and have stressed that—in addition to proton conductivity—other critical ionomer properties include the H₂ and O₂ permeability.¹² Of course, the membrane material must not be too permeable to the reactive gases to avoid excessive gas crossover and resulting fuel efficiency loss. In the other extreme, the ionomer in the electrode must have sufficient gas permeability so that the reactant transport through it occurs without significant concentration gradients and associated mass transfer losses. Standard perfluorinated membranes allow permeation of gases at a rate proportional to the product of a permeability coefficient (dependent on temperature and RH, normalized by membrane thickness) multiplied by a partial pressure driving force and divided by the membrane thickness. This permeation leads to fuel efficiency loss with two components: direct reaction at the anode determined by the O₂ crossover rate and direct reaction at the cathode determined by the H₂ crossover rate. This fuel loss can be expressed in terms of an equivalent current that would be observed externally, if the H₂ consumed by crossover had reacted electrochemically. A tolerable fuel efficiency loss due to crossover was set at <10% for a low load and <1% for a high load of the MEA.

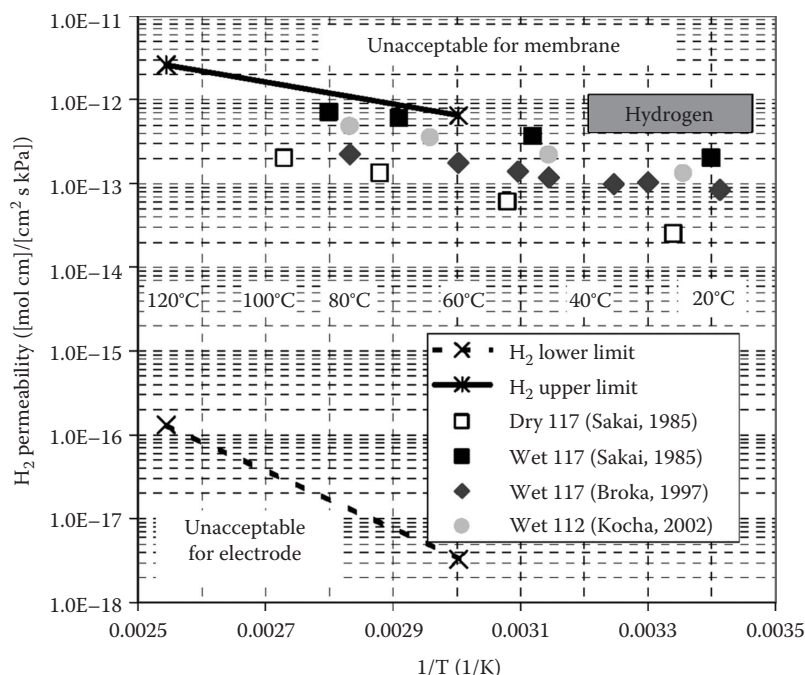


FIGURE 21.9 H_2 permeability as a function of temperature and RH. Upper limit (solid line) defined by crossover losses (assuming no contribution from O_2 crossover) and lower limit (dotted line) defined by electrode ionomer film transport requirements; data are for wet and dry Nafion® 1100 EW-based membranes. (From Kocha, S.S., in: *Handbook of Fuel Cells: Fundamentals, Technology and Applications*, Vielstich, W., Gasteiger, H.A., Lamm, A., eds., John Wiley & Sons, Chichester, U.K., 2003; Sakai, T. et al., *J. Electrochem. Soc.*, 133, 88, 1986; Sakai, T. et al., *J. Electrochem. Soc.*, 132, 1328, 1985; Broka, K. and Ekdunge, P., *J. Appl. Electrochem.*, 27, 281, 1997; Broka, K. and Ekdunge, P., *J. Appl. Electrochem.*, 27, 117, 1997; Reproduced from Gasteiger, H.A. and Mathias, M.F., *Proceedings of the Proton Conducting Membrane Fuel Cells III Symposium*, 2003. With permission of The Electrochemical Society, Inc.)

Gasteiger and Mathias assume a thin-film structure of the ionomer of 0.5–2 nm covering the entire solid catalyst surface. Experimental support for this electrode structure comes from double-layer capacitance measurements using cyclic voltammetry and AC impedance techniques. Gasteiger and Mathias observed values that are typical of Pt and carbon interfaces with electrolyte and imply that the entire solid surface was in contact with electrolyte for these electrodes. Under several assumptions regarding structure, diffusion, and reactivity, a minimum permeability was derived for a maximum of 20 mV loss.

These considerations regarding the membrane permeation properties have been summarized by Gasteiger and Mathias in Figures 21.9 and 21.10, with literature data of gas permeation measurements of Nafion membranes. Following their evaluation, the present membranes are close to the upper limit of gas permeation, which is acceptable, but a further increase in these properties at higher temperatures cannot be tolerated.

Besides the traditional methods of measuring gas permeation by way of gas analysis (a volumetric method or gas chromatography), an electrochemical methodology to determine the gas permeability and solubility of membranes is also used, which seems to have become more popular recently. Using microelectrodes that are pressed onto a membrane in a solid-state electrochemical cell, electrochemical reactions are investigated by chronoamperometry (recording of

current transients) of the diffusion-limited potential ranges. From the transients, gas concentrations (solubility) and diffusion coefficients in various proton exchange membranes can be measured, and diffusion-limited current densities can be determined.^{30–36} This is an interesting and simple way of measuring permeabilities since it may enable in situ measurement in a running fuel cell and also a local resolution. However, in contrast to the permeation measurement by gas analysis, no driving force in the form of a partial pressure gradient is applied to the membrane. The comparison of both techniques is, therefore, not straightforward. Under diffusion-limited conditions, the concentration at the microelectrode interface is zero, and therefore, a partial pressure gradient corresponding to the pressure in the cell (e.g., 100 kPa for ambient conditions) is assumed. Under this assumption, the results from both measurements should be comparable, and a comparison of selected measurements is shown in Figure 21.11.

As can be seen in Figure 21.11, the permeability measurements of Nafion-like membranes do vary considerably, probably because the state of the membranes is difficult to control (e.g., the dryness of the membrane). There is a pronounced difference in the permeabilities for wet and dry membranes, but the method of measurement does not yield consistent variation in the measured values. It can, therefore, be concluded that the electrochemical method is equivalent to the gas analysis method, even though the measurement conditions are different from those in fuel cell applications.

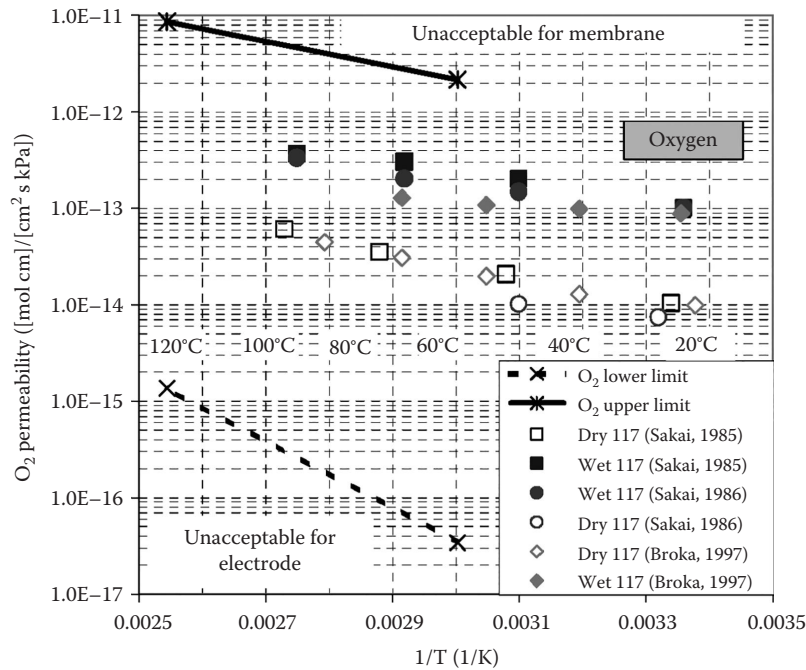


FIGURE 21.10 O₂ permeability as a function of temperature and RH. Upper limit (solid line) defined by crossover losses (assuming no contribution from H₂ crossover) and lower limit (dotted line) defined by electrode ionomer film transport requirements; data are for wet and dry Nafion 1100 EW-based membranes. (From Kocha, S.S., in: *Handbook of Fuel Cells: Fundamentals, Technology and Applications*, Vielstich, W., Gasteiger, H.A., Lamm, A., eds., John Wiley & Sons, Chichester, U.K., 2003; Sakai, T. et al., *J. Electrochem. Soc.*, 133, 88, 1986; Sakai, T. et al., *J. Electrochem. Soc.*, 132, 1328, 1985; Broka, K. and Ekdunge, P., *J. Appl. Electrochem.*, 27, 281, 1997; Broka, K. and Ekdunge, P., *J. Appl. Electrochem.*, 27, 117, 1997; Reproduced from Gasteiger, H.A. and Mathias, M.F., *Proceedings of the Proton Conducting Membrane Fuel Cells III Symposium*, 2003. With permission of The Electrochemical Society, Inc.)

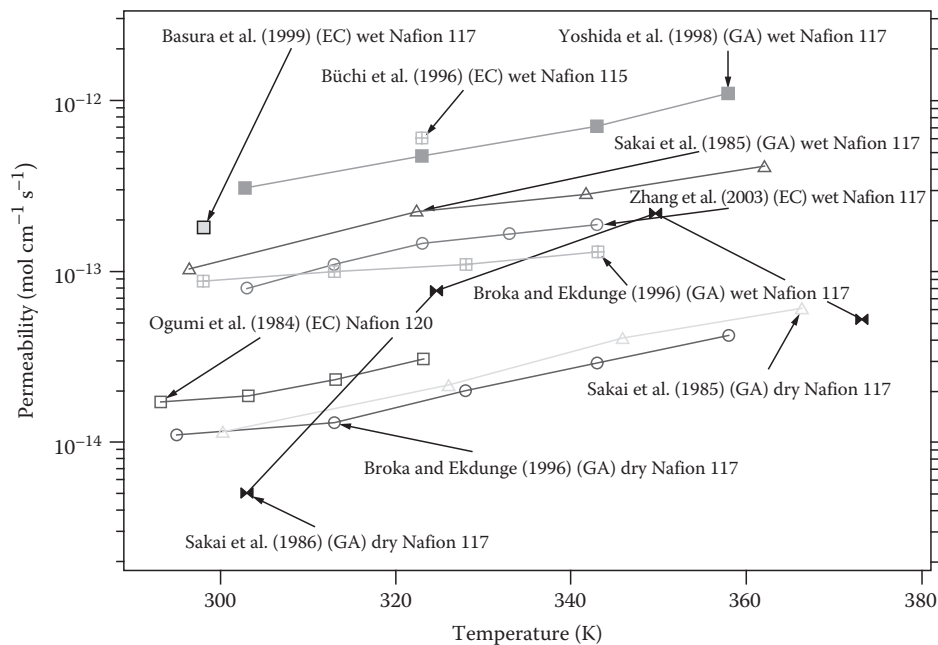


FIGURE 21.11 O₂ permeability as a function of temperature measured using an electrochemical method (microelectrodes, EC) and a gas permeation (gas analysis, GA) method. Permeability calculated for a partial pressure gradient of 100 kPa. (From Sakai, T. et al., *J. Electrochem. Soc.*, 133, 88, 1986; Sakai, T. et al., *J. Electrochem. Soc.*, 132, 1328, 1985; Broka, K. and Ekdunge, P., *J. Appl. Electrochem.*, 27, 281, 1997; Broka, K. and Ekdunge, P., *J. Appl. Electrochem.*, 27, 117, 1997; Gode, P. et al., *J. Electroanal. Chem.*, 518, 115, 2002; Büchi, F.N., Wakizoe, M., Srinivasan, S., *J. Electrochem. Soc.*, 143, 927, 1996; Zhang, L. et al., *Electrochimica Acta*, 48, 1845, 2003; Basura, V.I. et al. *J. Electroanal. Chem.*, 501, 77, 2001; Ogumi, Z. et al., *J. Electrochem. Soc.*, 131, 769, 1984.)

21.2.3 CATALYST UTILIZATION AND INTERFACIAL ASPECTS

The importance of the ionomer in the electrode for the performance of the PEMFC has been well known since the pioneering work of Raistrick et al.³⁷ In the PEMFC, the electroosmotic drag of water due to the proton transport from the anode to the cathode leads to the membrane drying out from the anode side (back diffusion of water from cathode to anode compensates partly for the water loss from the anode side of the membrane). Therefore, the loss of conductivity of the ionomer at the anode is also an additional important issue related to the membrane topic, since the ionomer in the electrode needs to connect ionically and chemically to the membrane. In an investigation of the transverse water profile in Nafion in PEMFCs with a sheet-partitioned membrane, Büchi and Scherer found that the increase in resistance is always confined to the membrane sheet contacting the anode.³⁸ It cannot be excluded that the main contribution to increased resistance of the MEA at high temperatures is from the ionomer in the electrode. To obtain clarification, cyclic voltammograms (CVs) of a commercial MEA with about 25 μm thick membranes were performed as a function of temperature at 100% RH in order to detect the influence of these interfacial structures on the performance of PEMFCs. Figure 21.12 shows the CVs of the anode as a working electrode (catalyst loading of 0.3 mg cm^{-2}) under nitrogen purging. The cathode was used as a combined counter and reference electrode and purged with hydrogen. Due to the small thickness of the membrane, hydrogen permeates the anode leading to an almost linear slope in the CVs. This current was subtracted in order to obtain more information regarding the interfacial properties of the MEA. The humidification of nitrogen/hydrogen was achieved by gas bubblers, which were invariably kept at 5°C higher than the cell.

Condensation of water was avoided by choosing adequate temperatures for the gas distribution system. Interestingly, the features due to hydrogen adsorption/desorption decrease with increasing temperature, indicating a loss of active catalyst surface area.

From these CVs, the reduction of Pt oxide in the negative-going scan can also be used to estimate the contacted catalyst surface area. The integration of the respective areas is not highly accurate, and an integration error of ± 15 mC is displayed in the charges plotted against temperature in Figure 21.13.

As can be seen from both Figures 21.12 and 21.13, the hydrogen desorption charge decreases almost monotonically with increasing temperature, indicating a loss of active surface with increasing temperature. At variance with the linear decrease, the charges from Pt oxide first increase up to 60°C, and then a strong decrease is observed at higher temperatures of 90°C. The charges from hydrogen desorption are considered to be of higher significance for the active surface determination, since the Pt oxide reduction may be influenced by kinetic and mass transport properties of the interface, which are strongly affected by the temperature increase. The form of the CV in the oxide region indicates mass transport limitations due to diffusion in a polymer film. Especially strong is the decrease in active catalytic area when the pressure is increased, for example, at the same temperature. This is demonstrated in Figure 21.14 for the temperature of 90°C where the pressure was increased from 1 to 2 bar (abs.).

The loss of surface area when increasing the pressure is probably associated with the water content depicted in Figures 21.13 and 21.14. With increasing pressure, the water content decreases and may lead to the ionomer in the electrode drying out. Since the membrane swells considerably with the

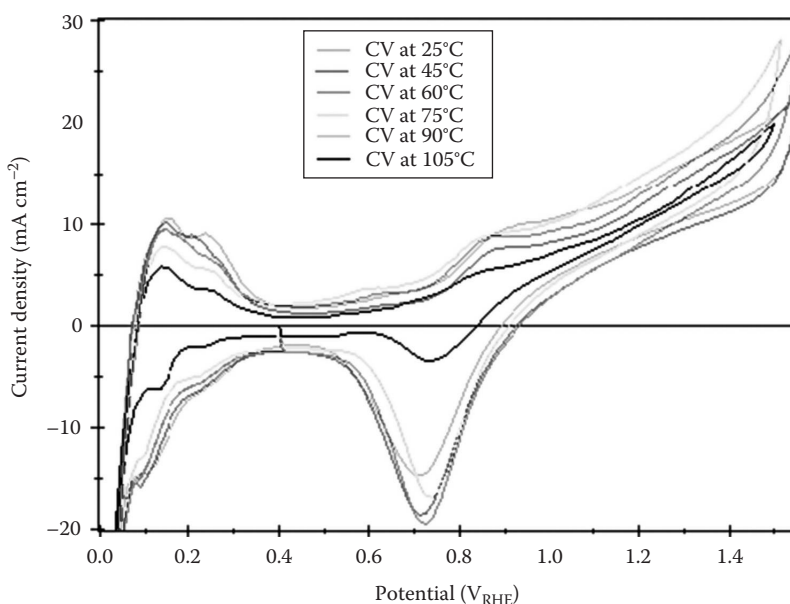


FIGURE 21.12 CVs of a commercial MEA with a 25 μm thick membrane as a function of temperature. Scan rate 50 mV s^{-1} . (ZSW measurements, Stuttgart, Germany, Internal publication.)

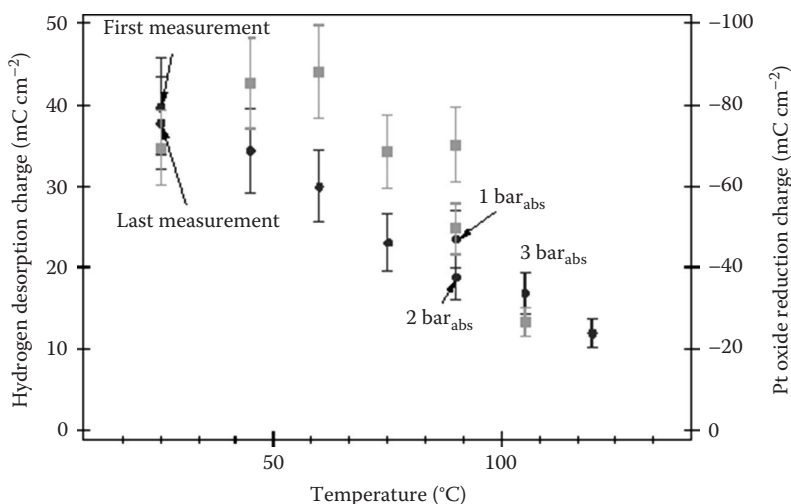


FIGURE 21.13 Hydrogen desorption charge (left-hand side, circles) and Pt oxide reduction charge (right-hand side, squares) as a function of temperature and pressure. (ZSW measurements, Stuttgart, Germany, Internal publication.)

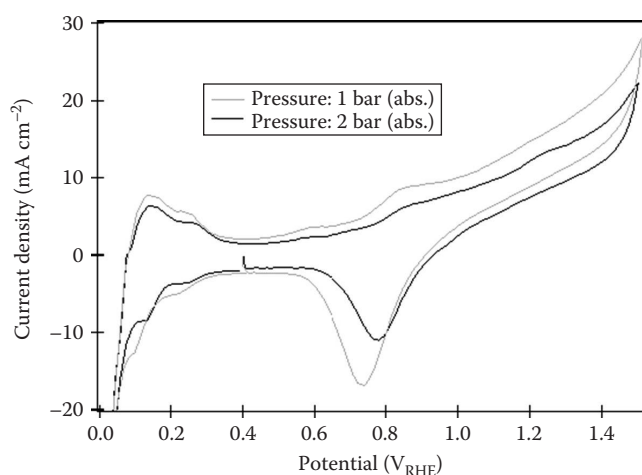


FIGURE 21.14 CVs of a commercial MEA at 90 °C for 1 and 2 bar absolute pressures. Scan rate 50 mV s⁻¹. (ZSW measurements, Stuttgart, Germany, Internal publication.)

water content, the higher pressure conversely leads to the ionomer in the electrode shrinking and thereby to reduced catalyst utilization. But then, the question remains why the catalyst surface utilization decreases with increasing temperature, although the water content of air/nitrogen increases considerably with temperature. It is well known that the water uptake of Nafion membranes is lower in the gaseous phase compared to the liquid phase (16 vs. 22 water molecules per sulfonic acid group). This is an effect that has been discussed for numerous membranes and is termed *Schroeder's paradox*.³⁹ Furthermore, Nafion has also been reported by Broka and Ekdunge to adsorb less water with increasing temperature even at constant humidity.⁴⁰ The reasons are not yet completely understood but are associated with the nanoporous structure and the phase-separated hydrous and anhydrous regions of Nafion. This effect is shown in Figure 21.15 for the temperature range of 20 °C–70 °C. If such dependence also exists in the ionomer present in the electrode, it is

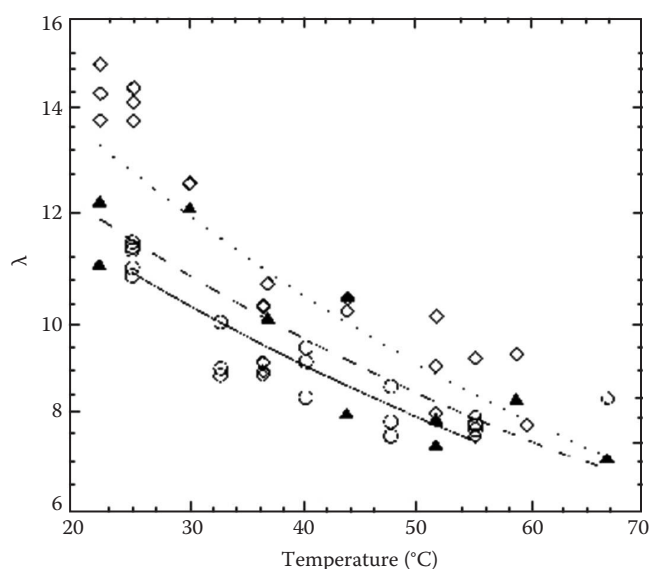


FIGURE 21.15 Water uptake from vapor phase (100% RH) by Nafion 117 membrane and recast Nafion film at different equilibration temperatures: (M) Nafion 117 membrane, (7) recast Nafion film, and (–) heat-treated Nafion 117 membrane. Fitted curves: second-order polynomial; 8 is the number of water molecules per sulfonate site. (Reproduced with permission from Springer Science + Business Media: *J. Appl. Electrochem.*, Oxygen and hydrogen permeation properties and water uptake of Nafion(R) 117 membrane and recast film for PEMFC, 27, 1997, 117, Broka, K. and Ekdunge, P.)

understandable why, with increasing temperature, the catalyst surface utilization also decreases.

It can be concluded that there are various problems associated with the standard PFSA membranes with increasing temperature:

- Loss of conductivity of membrane
- Loss of conductivity of ionomer in the electrode
- Loss of active catalyst surface area

21.2.4 MEMBRANE REQUIREMENTS FOR DIRECT METHANOL FUEL CELLS

DMFCs have potential near-term applications mainly in the portable power source market, as they are smaller, lighter, simpler, and cleaner than conventional batteries. Liquid methanol is consumed directly in a DMFC, which implies a higher energy density of the fuel cell system. But the power densities achievable with state-of-the-art DMFCs are still very small in comparison to hydrogen-fuelled PEMFCs. One of the major problems lies in the use of liquid methanol solution on the anode of the DMFC, which, on the one hand, keeps the ionomeric membrane water saturated (and thus no humidification is needed) but, on the other hand, does not keep fuel (methanol or any other organic fuel, e.g., formic acid, ethanol) and water from permeating to the cathode side, since the basic PFSA membranes are permeable to both methanol and water.^{41,42} The fuel and water crossover from anode to cathode hampers the performance of the air cathode.

21.2.4.1 Methanol Crossover

One of the most challenging issues that prevent DMFCs from being used in practical applications is the crossover of methanol fuel through typical polymer electrolyte membranes, for example, Nafion, from the anode to the cathode. It has been found that nearly 30%–40% of methanol can be wasted due to this crossover to the cathode depending on operating conditions like temperature, concentration of methanol in the anode feed, and current density in the cell. The mechanisms responsible for this transport of methanol to the cathode are diffusion due to concentration gradient and electroosmotic drag as moving protons also drag methanol like water, both being polar in nature. Methanol transported through the membrane by diffusion and electroosmotic drag recombines chemically with oxygen at the cathode, and therefore, fuel utilization efficiency is lowered. Additionally, methanol present at the cathode depolarizes the oxygen electrode and establishes a mixed potential thus lowering the cathode potential. Methanol competes with the oxygen reduction reaction at the cathode and predominantly reacts with oxygen. This undesired reaction increases the demand for oxygen and, therefore, requires higher stoichiometric flow rates. To minimize the negative impact of the methanol crossover, fuel cell developers are forced to use thicker membranes that reduce the fuel crossover but increase the specific cell resistance.^{8,41,43–46}

21.2.4.2 Water Permeation

Water permeation to the air cathode in liquid methanol solution-fed DMFCs creates a barrier for air diffusion to active sites in the cathode catalyst layer by flooding the electrode. The water transport mechanisms from the aqueous anode to the gaseous cathode are electroosmotic drag and diffusion. The Nafion membrane is saturated with water in the case of DMFCs, which gives rise to high electroosmotic drag coefficients⁴⁷ in comparison to partially saturated membranes,

as in the case of H₂/air PEMFCs. At lower current densities, diffusion due to a huge concentration gradient of water between anode and cathode is the dominant water transport mechanism. But with increasing current density, the electroosmotic drag becomes the dominant mechanism as the water transported by electroosmotic drag is proportional to current density. The water transport properties of different types of membranes have been widely investigated by several research groups.^{45,46,48–54} The permeated water hampers the performance of the air cathode by flooding the cathode catalyst and GDL, and it also makes the self-sustainable high-temperature operation of DMFCs difficult due to excessive heat loss by water vaporization from the air cathode.^{55,56} Additionally, it puts a huge demand on the air blower to remove water, making the DMFC's design more complicated and less energy efficient.^{42,43} In this vein, DMFCs or any direct liquid oxidation fuel cells using methanol, formic acid, ethanol, etc., as fuel should have membranes that are more liquid tight and still have sufficient proton conductivity.

21.3 MECHANISTIC ASPECTS OF PROTON CONDUCTIVITY (NAFION AND PFSA)

It is very important that the perfluorinated membrane has sufficient water content to be able to function in fuel cells. The interaction of the perfluorinated membrane with water and the resulting water content of the membrane determine the proton conductivity of the membrane. The mechanistic aspects have been discussed in numerous publications that cannot be completely recapitulated here.^{43,57–66} When in contact with water vapor or liquid water, Nafion or similar membranes show a pronounced swelling of 20%–50% associated with a considerable water uptake. Due to the ambivalent nature of the polymer, as it has a hydrophobic backbone and hydrophilic head groups, a spontaneous phase separation takes place in the membrane. In a hydrated condition, hydrophilic ionic clusters that are connected through water channels are formed, thereby forming a water network. The hydrophilic clusters contain the solvated SO₃ groups, water, and the cations (normally H⁺; but for cation exchange membranes, Na⁺, K⁺, or Li⁺ can naturally also be introduced). This water-filled network in a hydrophobic backbone yields high proton conductivity, which resembles an aqueous electrolyte (similar conductivities as well as activation energies for the proton conduction are observed). The ambivalent property of the membranes assists their mechanical stability, as the strong electrostatic interactions of the ionic clusters are apparently responsible for this stability. Importantly, Nafion can absorb more water from the liquid. For Nafion[®] 117, saturated with liquid water, 22 mol of water is absorbed per mole of sulfonic acid groups. It is detrimental for the applications that Nafion can take up only a maximum of 14 mol of water per mole of sulfonic acid groups from the water in the gaseous phase. As discussed earlier, the conductivity of Nafion membranes is strongly dependent on water content, which is displayed in [Figure 21.16](#) for two different EWs. The membrane

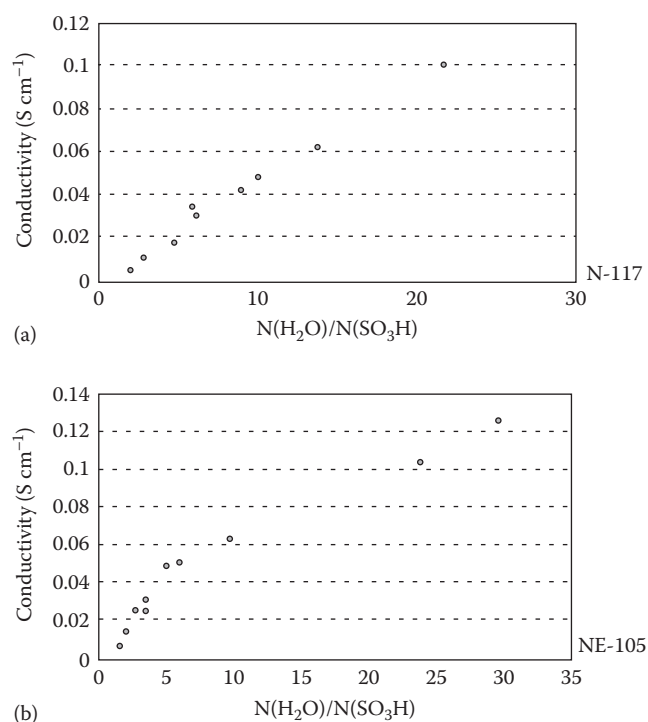


FIGURE 21.16 Conductivity of Nafion 117 (a) and 105 (b) as a function of water content expressed as the ratio of water molecules per sulfonic acid group. (From Zawodzinski, T.A. et al., *J. Phys. Chem.*, 95, 6040, 1991; Zawodzinski, T.A. et al., *J. Electrochem. Soc.*, 140, 1981, 1993.)

with the lower EQ shows the higher conductivity since the concentration of sulfonic acid groups is higher. A dried-out membrane possesses lower proton conductivity. Thus, water management in the membrane is one of the major issues in PEM technology. Processes influencing the water content in the membrane are electroosmotic drag and back diffusion of product water from the cathode into the membrane.

Water in a PEMFC is usually provided by the humidification of the reactant gases or from the cathode reaction. The amount of water fed into a cell by humidifying the reactant gases depends on gas temperature, pressure, and the flow rate. Water production at the cathode is directly proportional to the current density. Water carried to the cathode side by electroosmotic drag combined with the production of water at the cathode results in a gradual accumulation of water at the cathode. The water at the cathode can be carried to the flow channel through the GDL or through the membrane to the anode by back diffusion due to the water concentration gradient between the anode and cathode of the PEMFC. Water transport to the anode by back diffusion, which helps in keeping the membrane humidified, depends strongly on the thickness of the membrane and the properties of the GDL.

21.3.1 MICROSCOPIC STRUCTURE

The differences between PFSA membranes and nonfluorinated polyaromatic membranes are discussed on the basis

of publications by Kreuer.⁶⁴ Perfluorosulfonic polymers naturally combine the extremely high hydrophobicity of the perfluorinated backbone with the extremely high hydrophilicity of the sulfonic acid functional groups in one macromolecule. Especially in the presence of water, this gives rise to some hydrophobic/hydrophilic nanoseparation. The sulfonic acid functional groups aggregate to form a hydrophilic domain. When this is hydrated, protons form within inner space charge layers by dissociation of the acidic functional groups. While the well-connected hydrophilic domain is responsible for the transport of protons and water, the hydrophobic domain provides the polymer with the morphological stability and prevents the polymer from dissolving in water. Kreuer's group found the situation in s-PEEKs to be distinctly different with respect to both transport properties and morphological stability. In s-PEEKs, the hydrophilic/hydrophobic difference is less pronounced. This was inferred from the results of small-angle x-ray scattering (SAXS) experiments.⁶⁴ For a hydrated s-PEEK compared to Nafion, the ionomer peak is broadened and shifted toward higher scattering. This indicates a smaller characteristic separation length with a wider distribution and a larger internal interface between the hydrophobic and hydrophilic domains for the hydrated s-PEEK. As schematically illustrated in Figure 21.17, the water-filled channels in s-PEEK are narrower compared to those in Nafion. They are less separated and more branched with more dead-end *pockets*. These features correspond to the larger hydrophilic/hydrophobic interface and, therefore, also to a larger average separation of neighboring sulfonic acid functional groups. The stronger confinement of the water in the narrow channels of the aromatic polymers leads to a significantly lower dielectric constant of the water of hydration (about 20 compared to almost 64 in fully hydrated Nafion).⁵⁹

The different water interactions of the s-PEEK membranes are both advantageous and disadvantageous: on the one hand, a disadvantageous swelling behavior and a stronger decrease in water and proton transport coefficients with decreasing water content are observed; on the other hand, the hydrodynamic flow of the water, that is, electroosmotic drag and water permeation, is reduced compared to Nafion, which is an essential advantage, especially for DMFC applications.⁶⁴ Blending s-PEEKs with inert or basic polymers (e.g., PBI) significantly improves the swelling behavior without reducing the high proton conductivity at high water contents. Blending also further reduces the hydrophilic/hydrophobic separation and, therefore, also hydrodynamic solvent transport (water and methanol permeation). Therefore, polymers based on sulfonated polyarylenes not only are interesting, low-cost, alternative membrane materials for hydrogen PEM fuel cell applications but may also help to reduce the problems associated with high water and methanol crossover in DMFCs using aqueous solutions of methanol as a fuel. An important drawback is their reduced chemical stability, which may well lead to reduced durability of the membranes.⁶⁷

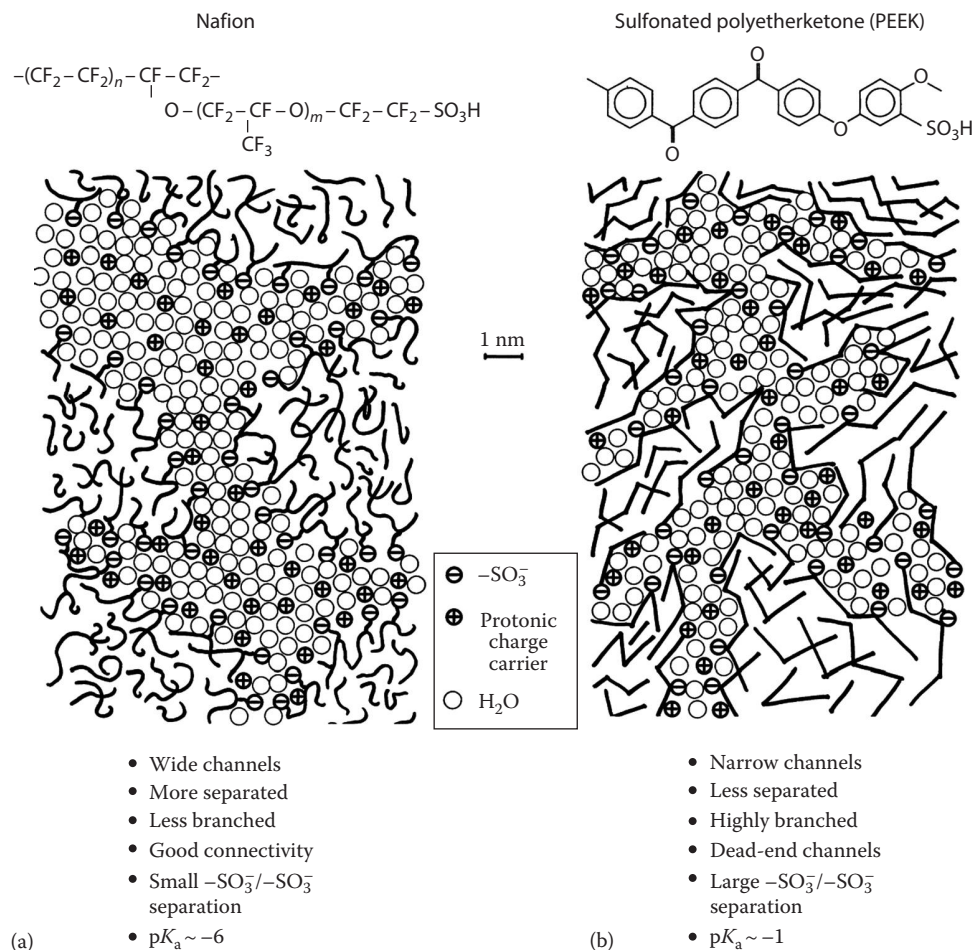


FIGURE 21.17 Schematic representation of the microstructures of (a) Nafion and (b) an s-PEEK illustrating the less pronounced hydrophobic/hydrophilic separation of the latter compared to the former. (Reprinted from *J. Membr. Sci.*, On the development of proton conducting polymer membranes for hydrogen and methanol fuel cells, 185, 2001, 29, Kreuer, K.D. et al. With permission from Elsevier; Kreuer, K.D., *J. Membr. Sci.*, 185, 29, 2001.)

21.4 MATERIALS: PHYSIOCHEMICAL PROPERTIES AND FUEL CELL PERFORMANCE

The commercial development of single-ion-conducting polymer membranes has changed the field of electrochemical devices in a significant way. Traditional systems such as sulfuric acid and potassium hydroxide combine excellent conductivity and cost-effectiveness, but the disadvantages are extreme corrosivity and challenging confinement. In this respect, the ion-conducting membranes exhibit excellent stability and processability, allowing the flexible design of electrochemical devices.

21.4.1 PFSA MEMBRANES

PFSA membranes possess high proton conductivity in the range of 0.1 S cm^{-1} at 80°C and good chemical as well as mechanical stability. The superior stability of Nafion is a consequence of the PTFE-based structure that is chemically

inert in reducing and oxidizing environments. The best-known examples of this class of proton-conducting membranes are the Nafion-type membranes from DuPont de Nemours. The most common commercial perfluorinated ionomer membranes used today in various industrial processes are listed in [Table 21.1](#). Asahi, Dow, and DuPont electro dialysis (ED) membranes have similar compositions and structures based on PFSA. The active ionomer component of the Gore-Select membrane is also a PFSA. In their usual form, these polymer membranes require water for conductivity. As long as these PEMs are kept hydrated, they function well; but when these membranes dry out, resistance rises sharply. A PTFE backbone is supplemented by regularly spaced perfluorovinyl ether pendant side chains terminated by a sulfonic acid group with the chemical structure shown in [Figure 21.18](#).

Hydrated Nafion 117 ($175 \mu\text{m}$ thick) has conductivities in the range of $10^{-1} \text{ S cm}^{-1}$ at 80°C . Nafion has a high electroosmotic drag coefficient that can lead to problems with water management in a PEMFC. Nafion has been

TABLE 21.1
Commercial Perfluorinated Ionomer Membranes Listed by Trade Name

Trade Name	Company	Membrane Type
Nafion XR resin	DuPont	PFSA
Nafion CR resin	DuPont	Perfluorocarboxylic acid
Flemion XR resin	AGC	PFSA
Flemion CR resin	AGC	Perfluorocarboxylic acid
Aciplex XR resin	Asahi Chemical	PFSA
Aciplex CR resin	Asahi Chemical	Perfluorocarboxylic acid

Source: Doyle, M. and Rajendran, G., in: *Handbook of Fuel Cells: Fundamentals, Technology and Applications*, Vielstich, W., Gasteiger, H.A., Lamm, A., eds., Vol. 3, John Wiley & Sons, Chichester, U.K., 2003, pp. 351–395.

DuPont de Nemours: Nafion membranes.

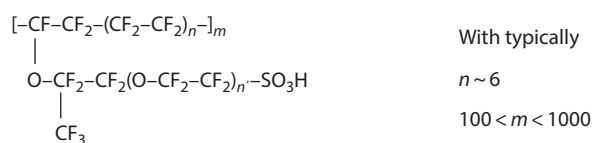


FIGURE 21.18 Structure of Nafion. The characteristic value of proton-conducting polymer membranes is the EW that is defined as the weight of polymer that will neutralize one equivalent of base and is inversely proportional to the IEC. The values n , m , and n' can be varied to produce materials with different EWs.

extensively studied because of its electrochemical applications such as chlor-alkali production and, more recently, fuel cells. Continued research has sought to explain the high level of the ionomer ionic conductivity. Fuel cell membrane developers are focusing on thinner membranes in order to decrease resistance and to alleviate the water management problems. Popular Nafion membrane products for fuel cells include NE-112, NE-1135, N-112, N-105, N-115, and N-117. In fuel cell applications, Nafion serves as a solid electrolyte to selectively transport protons across the cell junction. Tables 21.2 through 21.5 summarize the presently

TABLE 21.2
Thickness and Basis Weight Property Measurements Taken with Membrane Conditioned to 23°C, 50% RH

Membrane Type	Typical Thickness (μm)	Basis Weight (g m^{-2})	EW of Polymer That Will Neutralize One Equivalent of Base
N-112	51 (ca. 2 mil)	100	1100
NE-1135	89 (ca. 3.5 mil)	190	1100
N-115	127 (ca. 5 mil)	250	1100
N-117	183 (ca. 7 mil)	360	1100
NE-1110	254 (ca. 10 mil)	500	1100
N-105	127 (ca. 5 mil)	n.a.	1000

available product information provided by DuPont for Nafion® PFSA polymers.

21.4.1.1 Properties of Nafion PFSA Membranes

One activity at DuPont Fuel Cells business center is the development of a thinner membrane with sufficient mechanical stability. Thinner membranes translate into higher current density, which in turn means a higher electrical efficiency. The trade-off is a less mechanically robust membrane. Nafion membranes are nonreinforced films based on Nafion resin, a PFSA/PTFE copolymer in the acid (H^+) form. DuPont is especially marketing Nafion® PFSA NR-111 and NR-112 membranes as nonreinforced dispersion-cast films for that purpose. These membranes are delivered as a composite with the membrane positioned between a backing film and a coversheet. This composite is wound on a 6 in. ID plastic core, with the backing film facing out, as shown in Figure 21.19.

The backing film facilitates transporting the membrane into automated MEA fabrication processes, while the coversheet protects the membrane from exposure to the environment during intermediate handling and processing. In addition, the coversheet (in combination with the backing film) eliminates rapid changes in the membrane's moisture content and stabilizes the dimensions of the membrane as it is removed from the roll. A roll core leader is attached to the membrane, as shown in Figure 21.19, when this option is desired by the customer. The roll core leader material is the same as the backing film. The properties of these thin membranes are specified in Table 21.5.

21.4.1.2 Performance of DuPont Nafion® Membranes

It is assumed that DuPont's Nafion membranes are used in about 80% of all publications on PEMFCs. The simple reason is that this was the only commercially available material for long time. Therefore, it is not possible to present here a complete overview of performance data with Nafion or other membranes. Furthermore, the performance depends strongly on the conditions used as well as MEA preparation (catalyst loading, etc.). As a consequence, only the performance data from the membrane manufacturer itself are reported. Figure 21.20 exhibits performance reports by DuPont in 2002 for a three-layer MEA for neat hydrogen and reformate operation.

According to DuPont, good progress has been made in developing high-temperature operating membranes. Exploratory research membranes in the temperature range of 110°C–140°C have been developed. A further development focus of DuPont membranes is the DMFC application. Besides performance increase, the reduction in methanol permeation is an important aspect of the development. In a presentation, DuPont showed the advantage of using thicker (7 mil) membranes compared to the thinner (2 mil) Nafion® 112 that shows good performance for hydrogen/air operation. Figure 21.21 demonstrates this observation.

TABLE 21.3
Physical and Other Properties for EW1100 Membranes

Property	Typical Value	Test Method
Physical properties		
Tensile modulus, MPa (kpsi)		
50% RH, 23°C	249 (36)	ASTM D 882.
Water soaked, 23°C	114 (16)	ASTM D 882.
Water soaked, 100°C	64 (9.4)	ASTM D 882.
Tensile strength, maximum, MPa (kpsi)		
50% RH, 23°C	43 (6.2) in MD, 32 (4.6) in TD	ASTM D 882.
Water soaked, 23°C	34 (4.9) in MD, 26 (3.8) in TD	ASTM D 882.
Water soaked, 100°C	25 (3.6) in MD, 24 (3.5) in TD	ASTM D 882.
Elongation at break, %		
50% RH, 23°C	225 in MD, 310 in TD	ASTM D 882.
Water soaked, 23°C	200 in MD, 275 in TD	ASTM D 882.
Water soaked, 100°C	180 in MD, 240 in TD	ASTM D 882.
Tear resistance—initial, g mm ⁻¹		
50% RH, 23°C	6000 in MD, TD	ASTM D 1004.
Water soaked, 23°C	3500 in MD, TD	ASTM D 1004.
Water soaked, 100°C	3000 in MD, TD	ASTM D 1004.
		Tear resistance (g mm ⁻¹) of dry membrane increases with thickness. Values given are typical for 0.05 mm membrane.
Tear resistance—propagating, g mm ⁻¹		
50% RH, 23°C	>100 in MD, >150 in TD	ASTM D 1922.
Water soaked, 23°C	92 in MD, 104 in TD	ASTM D 1922.
Water soaked, 100°C	74 in MD, 85 in TD	ASTM D 1922.
Specific gravity	1.98	
Other properties		
Conductivity, S cm ⁻¹	0.083	Conductivity measurement as described by Zawodzinski et al., ^{183,184} membrane conditioned in 100°C water for 1 h, measurement cell submersed in 25°C DI water during experiment, membrane impedance (real) taken at zero imaginary impedance.
Acid capacity, mequiv. g ⁻¹	0.89	A base titration procedure measures the equivalents of sulfonic acid in the polymer and uses the measurement to calculate the acid capacity or EW of the membrane.
Conditioning state of membrane given. Measurements taken at 23°C and 50% RH. MD, machine direction; TD, transverse direction.		

TABLE 21.4
Hydrolytic Properties

Property	Typical Value	Test Method
Water content, % water	5	ASTM D 570. Water content of membrane conditioned to 23°C and 50% RH, compared to dry weight basis.
Water uptake, % water	38	ASTM D 570. Water uptake from dry membrane to water soaked at 100°C for 1 h (dry weight basis).
Thickness change, % increase		
From 50% RH, 23°C, to water soaked, 23°C	10	ASTM D 756.
From 50% RH, 23°C, to water soaked, 100°C	14	ASTM D 756.
Linear expansion, % increase		
From 50% RH, 23°C, to water soaked, 23°C	10	ASTM D 756.
From 50% RH, 23°C, to water soaked, 100°C	15	ASTM D 756.

TABLE 21.5
Properties of Nafion NR-111 and NR-112 Membranes

Thickness and basis weight properties					
Membrane type	Typical thickness, μm				Basis weight, g m^{-2}
NR-111	25.4				50
NR-112	50.8				100
Physical properties					
MD, machine direction; TD, transverse direction	NR-111		NR-112		Test method
Property, measured at 50% RH, 23°C	MD	TD	MD	TD	
Tensile strength, max., MPa	23	28	32	32	ASTM D 882
Non-std modulus, MPa	288	281	266	251	ASTM D 882
Elongation to break, %	252	311	343	352	ASTM D 882
Other properties, hydrogen crossover measured at 22°C, 100% RH, and 50 psi delta pressure					
Specific gravity, 23°C, 50% RH	1.97		1.97		DuPont
Acid capacity, mequiv. g^{-1}	0.95 ± 0.04		0.95 ± 0.04		DuPont
Hydrogen crossover, $\text{mL min}^{-1} \cdot \text{cm}^2$	<0.020		<0.010		DuPont
Hydrolytic properties, water content of membrane conditioned to 23°C and 50% RH (dry weight basis); water uptake from dry membrane to conditioned in water at 100°C for 1 h (dry weight basis)					
Water content, % water	5 ± 3				ASTM D 570
Water uptake, % water	50 ± 5				ASTM D 570
Linear expansion, % increase					
From 50% RH, 23°C, to water soaked, 23°C	10				ASTM D 756
From 50% RH, 23°C, to water soaked, 100°C	15				ASTM D 756

Source: Courtesy of DuPont, Wilmington, DE.

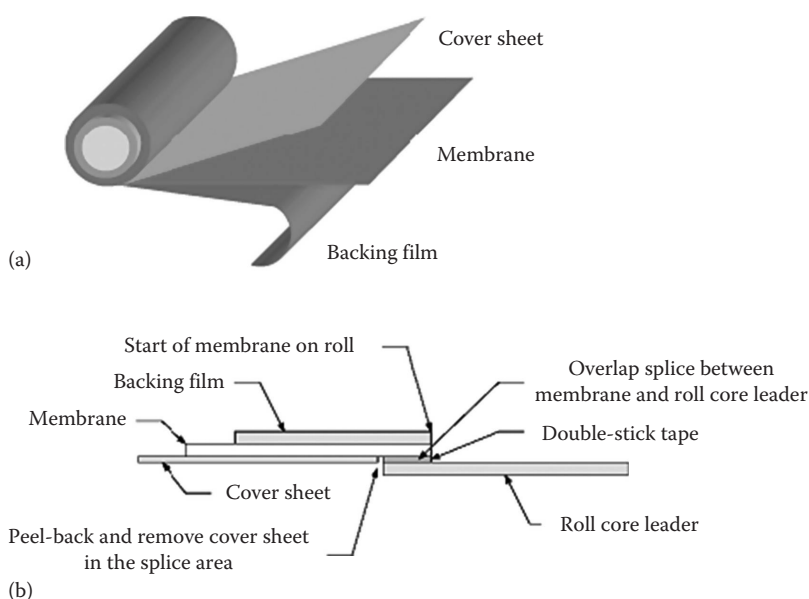


FIGURE 21.19 (a) Diagram of DuPont's Nafion PFSA NR-111 and NR-112 membranes showing roll unwind orientation (backing film facing out). (b) Splice design for attaching roll core leader to membrane. (Courtesy of DuPont, Wilmington, DE.)

Another finding reported by DuPont is that the EW exhibits a pronounced influence on performance and methanol permeation. Whereas the highest performances were found with low EW membranes, the membranes with high EW had the lowest relative methanol permeation (cf. Figure 21.22). According to DuPont, a 2 mil experimental membrane that exhibits better performance for DMFCs compared to the 7 mil commercial membrane is in development.

Recently, DuPont has introduced a new membrane that is an improvement in comparison to earlier versions NR-111, NR-112, and NR-211. DuPont Nafion® XL membrane is an extended-lifetime reinforced membrane based on chemically stabilized PFSA/PTFE copolymer in the acid (H⁺) form. The reinforcement improves the handling of the membrane and its physical properties. When the reinforcement is combined with the chemically stabilized polymer, the membrane

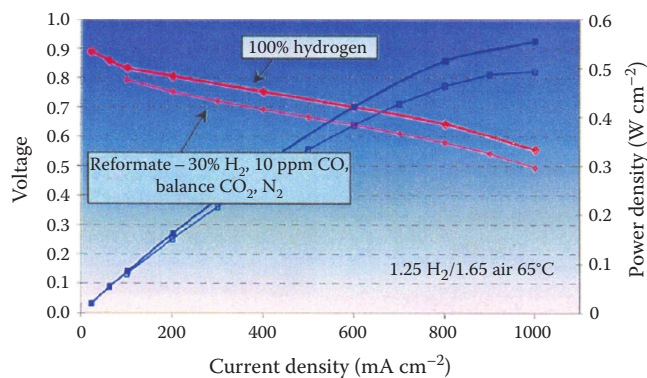


FIGURE 21.20 Performance for DuPont three-layer MEA. (DuPont, 2002.)

exhibits both substantially lower fluoride-ion release rate and longer operating durability under fuel cell conditions.

Features

- Performance is equivalent to MEAs made with Nafion® NR-211 membrane.
- Membrane tensile strength increased by a factor of 1.5 and hydration expansion reduced by 50% compared to NR-211 membranes.
- Reduction in fluoride emissions by over a factor of 40 compared to MEAs made with nonreinforced, chemically stabilized membrane.

Benefits

- Extended MEA lifetime—lasts 20 times longer in demanding load and humidity cycling applications

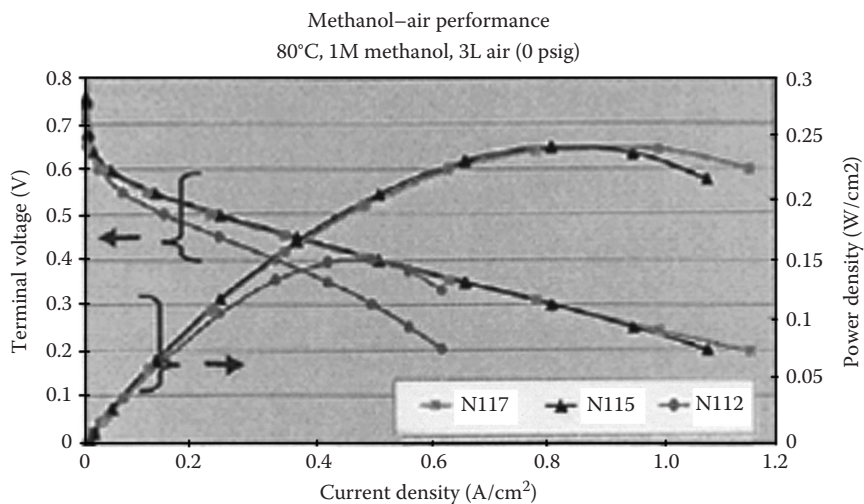
The mechanical durability and enhanced chemical stability of MEAs made with Nafion XL membrane are the result of

an advanced stabilization system that increases mechanical strength and provides resistance to peroxide attack, resulting in improved membrane life and performance (Table 21.6).

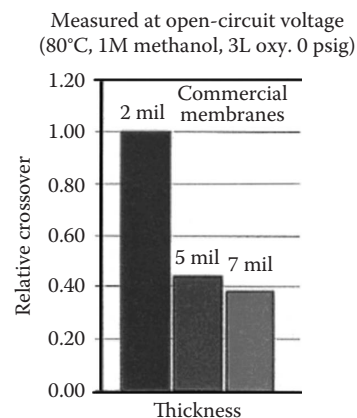
21.4.1.3 Synthesis of PFSA Monomers and Polymers

The synthesis of the monomers as well as the polymerization of PFSA membranes involves dangerous reactions under conditions of high pressure and temperature. Additionally, the synthesis of the comonomer that is commonly referred to as perfluoro sulfonylfluoride ethyl propyl vinyl ether (PSEPVE) involves numerous steps with low yields. These factors contribute to the cost of these materials. The synthesis routes are described in detail by Doyle and Rajendran and will only be briefly summarized here. The synthesis of the long-chain PFSA monomers used in commercial systems like Nafion, Flemion, and Aciplex proceeds through the reaction of SO_3 with tetrafluoroethylene (TFE) to form a cyclic sultone. A rearrangement of the cyclic compound yields the so-called rearranged sultone (RSU), which is reacted with hexafluoropropylene oxide (HFPO) to produce sulfonyl fluoride adducts. Heating these compounds in the presence of sodium carbonates yields the comonomer PSEPVE. The synthesis is illustrated in Figure 21.23 from Doyle and Rajendran.⁸ Polymerization is typically performed in perfluorocarbon solvents with a perfluorinated free radical initiator such as perfluoroperoxide.

The short-chain version of the perfluoro sulfonylfluoride vinyl ether monomer is highly desirable for obtaining membranes with improved functionalities. Ionomers with a short chain were intensively developed by Dow Chemical in the early 1990s and almost obtained commercial status. However, the development was abandoned, partly because the synthesis of the short-chain monomer is substantially more challenging. The Dow membrane was based on a copolymer of TFE and $\text{CF}_2=\text{CFOCF}_2\text{CF}_2\text{SO}_2\text{F}$. Since the shorter side chain makes the ionic concentration higher for the



→It appears, 2 mil membrane experiences a serious mass transport limitation as a result of high methanol and water crossover to the cathode particularly when operating with air.



Commercial 7 mil membrane (N117) shows →62% lower methanol crossover compared to 2 mil commercial membrane (N112).

FIGURE 21.21 Comparison of DMFC performance of Nafion 117, Nafion 115, and Nafion 112. (DuPont, 2002.)

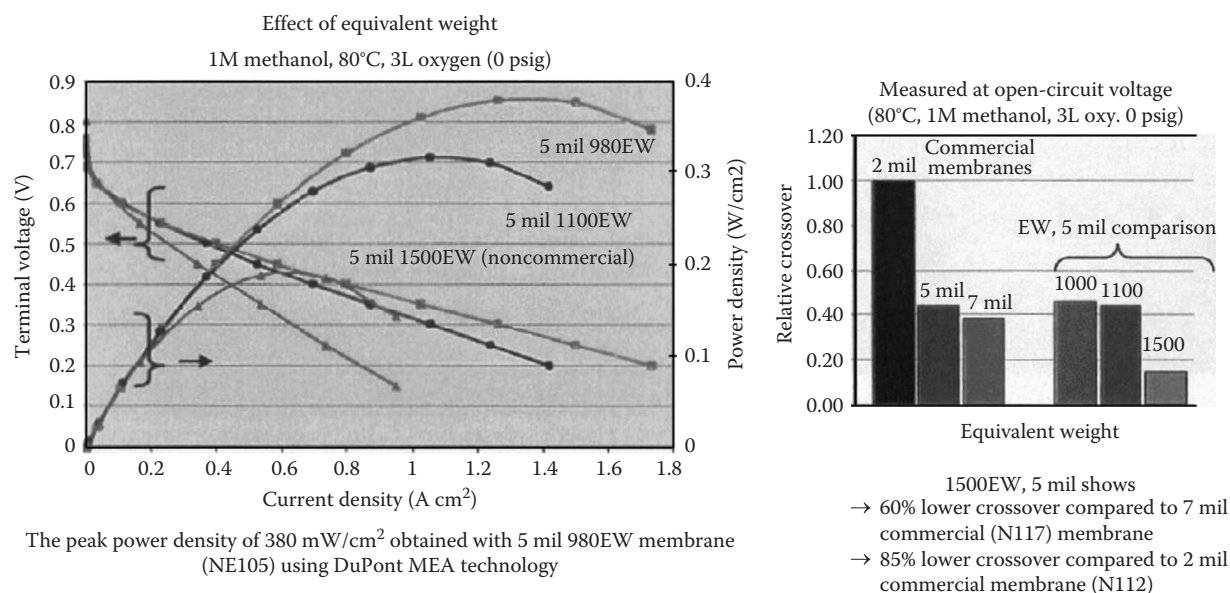


FIGURE 21.22 Comparison of DMFC performance of 5 mil membranes with different EWs. (DuPont, 2002.)

TABLE 21.6

Summary of Recent DuPont Membrane Development

Thickness and basis weight properties^a

Membrane type	Typical thickness (μm)		Basis weight (g m ⁻²)
XL	27.4		55

Physical properties^b

Property, measured at 50% RH, 23°C	MD	TD	Test method
Tensile strength, max., MPa	45	40	ASTM D 882
Non-std modulus, MPa	613	400	ASTM D 882
Elongation to break, %	200	185	ASTM D 882

Other properties, hydrogen crossover measured at 22°C, 100% RH, and 50 psi delta pressure

Conductivity, ^c mS cm ⁻¹	1.97	DuPont
In plane	>72.0	DuPont
Through plane	>50.5	DuPont
Hydrogen crossover, ^d mL min ⁻¹ · cm ²	<0.015	DuPont

Hydrolytic properties, water content of membrane conditioned to 23°C and 50% RH (dry weight basis); water uptake from dry membrane to conditioned in water at 100°C for 1 h (dry weight basis)

Water content, % water ^e	5 ± 3	ASTM D 570
Water uptake, % water ^f	50 ± 5	ASTM D 570
Linear expansion, % increase		
From 50% RH, 23°C, to water soaked, 23°C	1% (MD), 5% (TD)	DuPont
From 50% RH, 23°C, to water soaked, 100°C	3% (MD), 11% (TD)	DuPont

^a Measurements taken with membrane conditioned to 23°C and 50% RH.

^b Where specified; MD, machine direction; TD, transverse direction. Condition state of membrane given.

^c Conductivity measurements a 23°C and 100% RH.

^d Hydrogen crossover measured at 65°C and 100% RH. This is not a routine test.

^e Water content of membrane conditioned to 23°C and 50% RH (dry weight basis).

^f Water uptake from dry membrane to conditioned in water at 100°C for 1 h (dry weight basis).

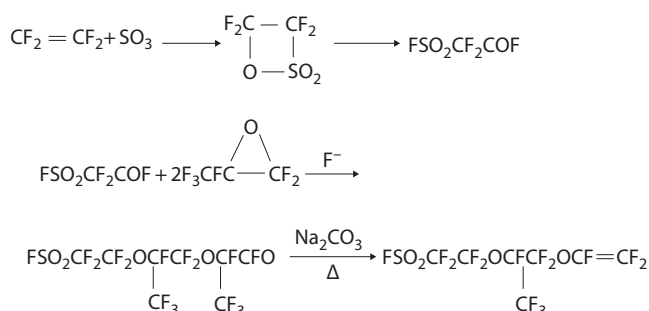
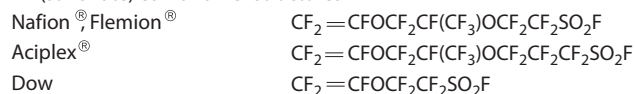


FIGURE 21.23 Synthesis process for Nafion membrane comonomer PSEPVE. (Reproduced from Doyle, M. and Rajendran, G., in: *Handbook of Fuel Cells: Fundamentals, Technology and Applications*, Vielstich, W., Gasteiger, H.A., and Lamm, A., eds., Vol. 3, John Wiley & Sons, Chichester, U.K., 2003. With permission.)

same EW, the Dow membrane showed higher conductivity and higher water uptakes under similar conditions. Testing of the Dow polymer in PEMFCs by Ballard in 1987–1988 showed significant improvement in performance compared to Nafion 117 (three times better current density at 0.5 V was reported). The typical functional comonomers of the relevant perfluorinated membranes are given in Figure 21.24 from Doyle and Rajendran.

Industrial production of perfluorinated ionomers, Nafion membranes, and all perfluorinated membranes is costly due to several factors: Firstly, the monomers used are expensive to manufacture, since the synthesis requires a large number of steps and the monomers are dangerous to handle. The precautions for safe handling are considerable and costly. Secondly, the PSEPVE monomer is not used for other applications, which limits the volume of production. The most significant cost driver is the scale of production. Today, the volume of the Nafion market for chlor-alkali electrolysis ($150,000 \text{ m}^2 \text{ year}^{-1}$) and fuel cells ($150,000 \text{ m}^2 \text{ year}^{-1}$) is about $300,000 \text{ m}^2 \text{ year}^{-1}$, resulting in a production capacity of $65,000 \text{ kg year}^{-1}$. When compared to large-scale production of polymers like Nylon

XR (sulfonate) comonomer structures



CR (carboxylate) monomer structures

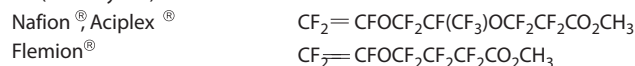


FIGURE 21.24 Typical functional comonomer structures for each ionomer system. (Reproduced from Doyle, M. and Rajendran, G., in: *Handbook of Fuel Cells: Fundamentals, Technology and Applications*, Vielstich, W., Gasteiger, H.A., and Lamm, A., eds., Vol. 3, John Wiley & Sons, Chichester, U.K., 2003. With permission.)

($1.2 \times 10^9 \text{ m}^2 \text{ year}^{-1}$), the perfluorinated ionomer membrane is a specialty polymer produced in small volumes.

DuPont predicted in a communication from 1998 that they consider a price of no more than $\$10 \text{ kW}^{-1}$ realistic in mass production. This prediction was, however, based on optimistic forecasts for transportation applications. The volumes quoted in the press release were 150,000 midsize vehicles (which corresponds to more than 1 million m^2 worldwide for economics of scale). In 2002, DuPont's expectation for a production volume of 1 million m^2 was about $\$25 \text{ kW}^{-1}$ (cf. Figure 21.25). The rule of thumb is to keep the membrane at 5% of the total fuel cell cost. A fairly common figure presently quoted for Nafion is $\$500 \text{ m}^{-2}$, although that varies depending on volume and on customer's buying power. Several small-scale users have reported much higher costs. DuPont claims that process improvements combined with increasing market volume have yielded, on average, a 50% reduction in the market price of Nafion over the past 3 years. The company has in place a comprehensive, long-term technology and capital investment plan to continue this trend in price reduction. DuPont has reported a market price of Nafion membranes at about $\$100 \text{ kW}^{-1}$ for the membrane material in a typical reformed hydrogen fuel cell system.

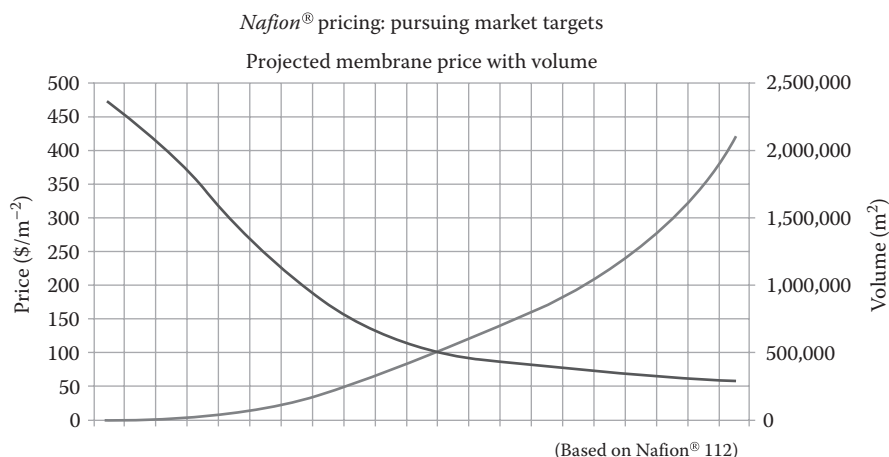


FIGURE 21.25 DuPont's prediction for cost development in relation to the volume of Nafion produced. (DuPont, 2002.)

21.4.1.4 Reinforced Membrane

In order to improve the lifetime of the membrane, DuPont made efforts in the direction of mechanical reinforcement of the PFSA membrane. Generation A reinforced membrane performs better in OCV hold tests and RH load cycle tests compared to PFSA cast membranes.

As can be seen in Figures 21.26 and 21.27, reinforced membranes show an increase in the OCV hold lifetime by a factor of 7. Although chemically stabilized ionomer was not yet used in generation A reinforced membranes, these improvements can still be attributed to improved chemical

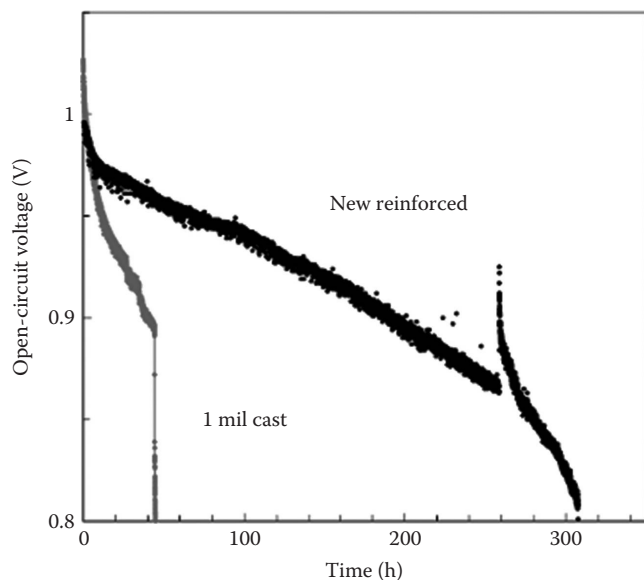


FIGURE 21.26 OCV hold test comparison between Nafion cast membrane and reinforced membrane. (From Choudhury, B., Material challenges in proton exchange membrane fuel cells, *International Symposium on Material Issues in a Hydrogen Economy*, November 12–15, Richmond, VA, 2007.)

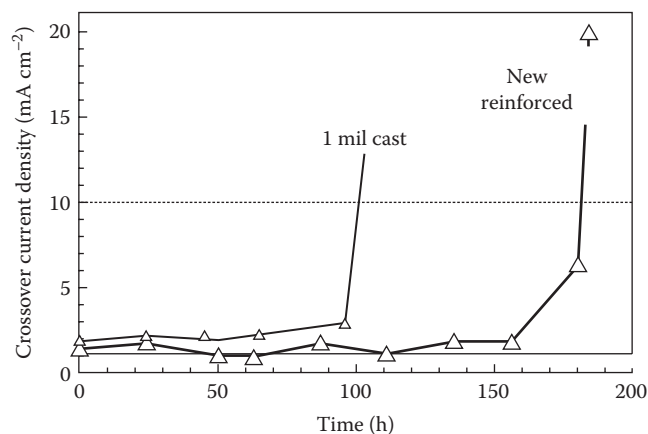
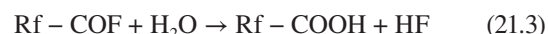
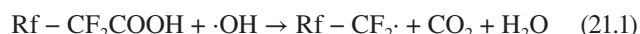


FIGURE 21.27 Hydrogen crossover current density under the long-term RH cycling comparison between Nafion cast membrane and reinforced membrane. (From Choudhury, B., Material challenges in proton exchange membrane fuel cells, *International Symposium on Material Issues in a Hydrogen Economy*, November 12–15, Richmond, VA, 2007.)

stability of the reinforced membrane. In the RH cycling test, also an increase in the lifetime by a factor of 2 was observed. In the case of RH cycling, swelling and shrinking following the wetting and drying cycles cause mechanical stress and ultimately mechanical failure. Reinforced membranes have significantly lower swelling/shrinkage, which leads to less mechanical stress and longer lifetime.⁶⁸

21.4.1.5 Chemical Stabilization

DuPont reported significant progress in the understanding of the chemical degradation of Nafion membranes. Chemical degradation of a PFSA membrane follows through the reaction of H_2O_2 with the membrane. H_2O_2 is generated by the reaction of the crossover oxygen with hydrogen from the anode side. H_2O_2 decomposes in the presence of Fenton's cations to produce $\cdot\text{OH}$ or $\cdot\text{OOH}$ radicals. These radicals preferentially attack reactive end groups of the polymer and initiate chain scission reactions leading to the degradation of the polymer backbone.



Both, ex-situ Fenton's test and in situ fuel cell tests, suggest similar kind of degradation mechanism, as similar polymer fragments were detected under both conditions. The nature of the fragments indicates stepwise degradation mechanism beginning at unstable polymer end groups.

Studies showed that groups with carboxylic acid group at the end, for example, carboxylic acid model compound $\text{CF}_3\text{CF}_2\text{OCF}_2\text{CF}(\text{CF}_3)\text{OCF}_2\text{CF}_2\text{COOH}$, were completely degraded to HF and other fragments. But groups with sulfonic acid chain termination, for example, sulfonic acid model compound $\text{CF}_3\text{CF}_2\text{OCF}_2\text{CF}(\text{CF}_3)\text{OCF}_2\text{CF}_2\text{SO}_3\text{H}$, were less prone to degradation.

In order to solve this chemical stability problem, a new proprietary PFSA ionomer synthesis procedure has been developed at DuPont that results in a reduction of the reactive end groups.¹⁷¹ This approach has been referred as chemical stabilization (CS) technology. Fluoride emission from chemically stabilized polymer in a Fenton's test was found to be eight times lower than a nonchemically stabilized polymer.

21.4.1.6 Fluoride Emission Rate: Reinforced and Chemically Stabilized Membrane

DuPont has claimed to have successfully combined the mechanical and chemical stability strategies in new membranes. Going from a pure PFSA cast membrane to a reinforced PFSA polymer membrane without chemically stabilized ionomer provides significant gains in terms of lower fluoride emission rate (FER). But usage of a chemically stabilized PFSA ionomer for the preparation of reinforced membrane provides an improvement in terms of much lower FER and significantly lower membrane degradation rates as shown in Figure 21.28.

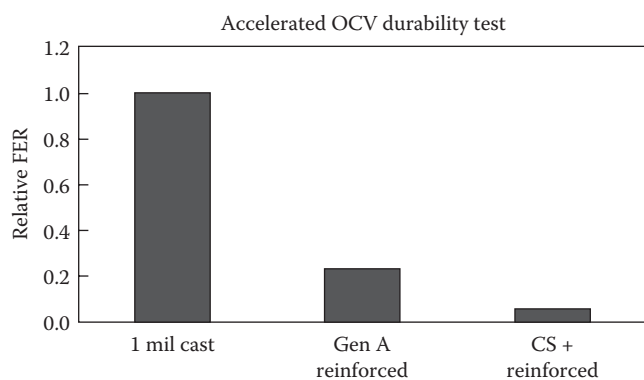


FIGURE 21.28 Relative FER comparison of Nafion cast membrane, generating a reinforced membrane and chemically stabilized reinforced membrane during the accelerated OCV durability test. (DuPont, 2002.)

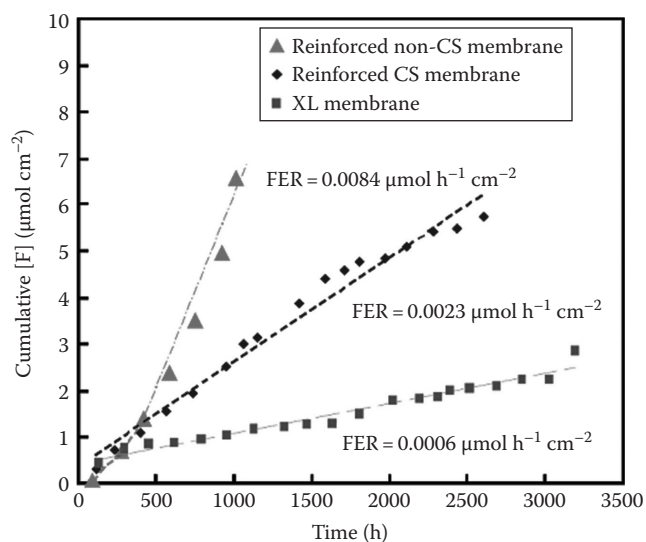


FIGURE 21.29 FER comparison of non-CS membrane reinforced CS membrane and XL membrane during an automotive load cycling test. (DuPont, 2002.)

In the new XL membrane, DuPont has reportedly incorporated advanced chemical stabilization technology that further reduces the number of reactive end groups in the polymer chain and thus further reduces the FER during operation. Due to these advancements in the chemical stabilization technology, XL membrane shows 14 times lower FER than standard reinforced PFSA membrane (see Figure 21.29).

21.4.2 MECHANICALLY REINFORCED PERFLUORINATED MEMBRANES

21.4.2.1 PFSA Ionomer in Expanded Porous PTFE (Gore-Select Membranes)

The company W.L. Gore & Associates (Elkton, MD) develops membranes under the name Gore-Select consisting of a microporous stretched PTFE (expanded PTFE porous sheet) membrane filled with perfluorinated ionomer. The microporous PTFE matrix provides the mechanical strength, and

therefore, the thickness of the membrane can be reduced considerably, and a thickness of 20–40 μm is commonly used leading to lower ionic resistances. The specific resistance of Gore-Select membranes is relatively high compared with nonreinforced membranes, but this is compensated by the small thickness and by lower EW ionomers. The membrane is composed of a micronetwork of nodes and fibrils with a continuous internal void volume in which the ionomer is introduced. The expanded PTFE technology has been refined and applied to a variety of applications including its use as a PEM in membrane electrode assemblies. In the mid-1990s, Gore began to work on expanded PTFE, which was then applied to PEMFCs. Their MEA is covered in U.S. Patent 5547551 issued in 1996.⁶⁹ The fabrication of Gore-Select membranes is described in the patent. The important step is the impregnation with ionomer solution by brush. The company does not intend to actively market Gore-Select but will use it in its catalyzed PRIMEA[®] MEA. Gore claims to be the highest MEA volume supplier in the world with a capacity for membrane and MEA fabrication of 100,000 m^2 per year. Gore has demonstrated a current density of 1200 mA cm^{-2} at 0.6 V at ambient pressure with hydrogen or reformat fuel. Operating temperatures range from ambient to 60°C–80°C. The company is carrying out research to address activation and mass transport limitations and advance the performance of the PRIMEA[®] power assemblies. A current goal is to achieve 400 mA cm^{-2} at 0.8 V. PRIMEA MEAs have been used in a number of PEM vehicle demonstrations, including vehicles such as the NJDOT Venturer, which operates on compressed hydrogen, and the NJDOT Genesis, which uses Millennium Cell's sodium borohydride as a hydrogen storage medium. Currently, PEMFC stack technology is being targeted at three major market sectors: portable power, residential, and transportation. Each market is driven by a different combination of features, such as power density, size, and life-cycle cost. Gore adapts its MEAs to the specific application by optimizing the ionomer for the requirements. In this respect, specifically developed MEAs with increased performance or with improved durability are reported. The names used by W.L. Gore are the PRIMEA[®] series 56x for the next generation of stationary applications (presently 5621), the series PRIMEA[®] 57 for transportation systems, and series 58 for portable applications. The reported properties of the MEAs are listed in Table 21.7.

TABLE 21.7
Properties of W.L. Gore Membrane Development

Stationary Applications, 56x	Transportation Applications, 57	Portable Applications, 58
Highest durability	Highest power density	Highest power density for dry gas operation
Lowest cost per kW h	Lowest cost per kW system	Lowest cost per kW system
Commercially available	Highest operational flexibility	Simplified system design

According to Gore, one of the most important criteria in identifying a practical membrane material for MEA manufacturing and membrane service is tear strength or tear resistance. Cleghorn et al. compared reinforced Gore-Select membranes and nonreinforced Nafion 112 and determined the stress required to propagate a membrane tear using (ASTM) test 1922–94a.⁷⁰ The results indicate that both membrane types are anisotropic and have greater tear resistance in the machine direction and both membrane types also have reduced tear resistance when hydrated. However, Gore-Select membranes reportedly show superior tear-resistant properties compared to Nafion 112 membranes. Even the hydrated transverse direction for the

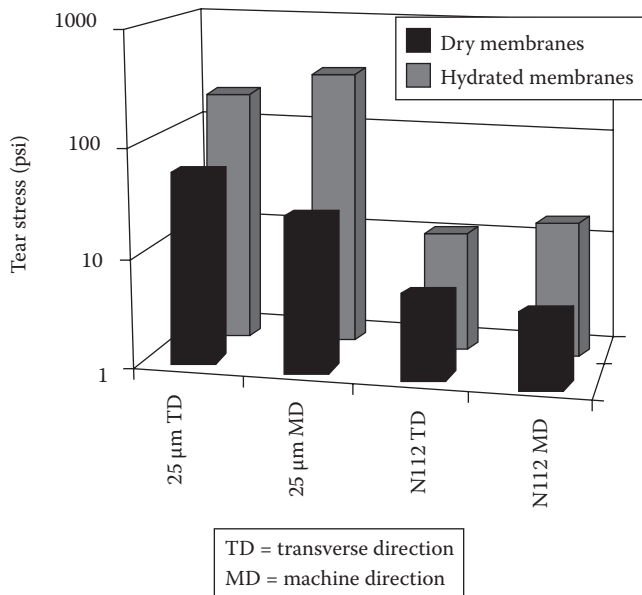


FIGURE 21.30 Comparison of tear strength for hydrated and dry Gore-Select membranes (25 μm) and Nafion 112 membranes in machine and transverse directions. (Reproduced from Cleghorn, S. et al., in: *Handbook of Fuel Cells: Fundamentals, Technology and Applications*, Vielstich, W., Gasteiger, H.A., and Lamm, A., eds., Vol. 3, John Wiley & Sons, Chichester, U.K., 2003. With permission.)

Gore-Select membrane is more tear resistant than the dry transverse direction for Nafion 112 membranes (cf. Figure 21.30).

As can be seen in Figure 21.31, the voltage loss at 800 mA cm⁻² of the PRIMEA 56 MEA is in the range of 5 μV h⁻¹. The development goal is <1 μV h⁻¹ to achieve the 40,000 h requirement for stationary applications. In 2003, Gore reported technology status for automotive applications in comparison to their goals (cf. Table 21.8). Surprisingly, an RH below 50% is indicated as already having been achieved in state-of-the-art membrane electrode assemblies with high-power-density requirements. Gore has reported intensive activity regarding accelerated life test procedures.^{70,71}

Figure 21.32 shows the efforts to reduce noble metal content in MEAs under conditions suitable for transportation applications. Although a significant reduction in Pt has been achieved in the series 57 MEA, further reduction in platinum is required. Gore's low loading development still shows good performance, but it is markedly lower compared to the 57 series.

Gore reported a new composite membrane that performs better than its predecessors at higher operating temperatures and in low-humidity conditions. Higher operating temperatures are desirable because of overall system simplification. But at the same time, membranes must retain enough humidity to be able to have sufficient proton conductivity. For their new membrane, Gore reported better results on both these fronts. In comparison to Nafion 211 membrane, the new Gore membrane shows low RH sensitivity well up to temperatures of 90°C–95°C⁷² (see Figure 21.33).

Gore also reported the results of the RH cycling and related mechanical degradation and decrease in H₂ crossover rates (see Figure 21.34). The new membrane is a reinforced membrane with expanded porous PTFE matrix and improved PFSA polymer proton-conducting material and shows less degradation when put through an RH cycling test. Similarly, the rate of chemical degradation under the OCV hold test was also improved significantly in comparison to the older versions of the Gore membrane.⁷²

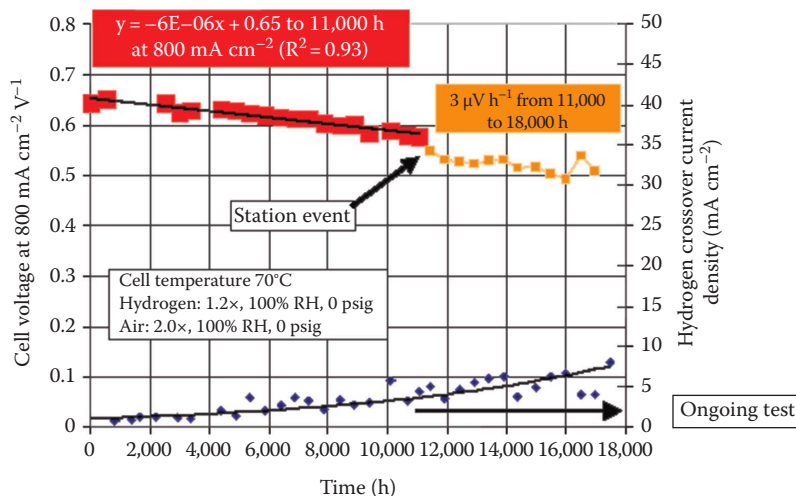


FIGURE 21.31 PRIMEA Series 56 MEA validation life test. Hydrogen fuel—high current density (800 mA cm⁻²). (Courtesy of W.L. Gore & Associates, Elkton, MD.)

TABLE 21.8

MEA Requirements for Commercial Fuel Cell Vehicles—MEA Technology Development Goals

	Current Demonstration Vehicles	
	PRIMEA Series 57 MEA	MEA Needs for Commercial Fuel Cell
Vehicle cost (assume dictated by platinum cost)	1 gpt kW ⁻¹ (at 0.6 V) 75 g for a 75 kW engine	<0.2 gpt kW ⁻¹ (>0.6 V) 15 g for 75 kW engine
Operating conditions (temperature)	T _{cell} 80°C RH < 50% Pressure < 270 kPa	T _{cell} 110°C–120°C RH < 25% Pressure < 150 kPa
Durability (membrane life)	MEA life accelerated conditions approximately 1500 h and <30 μV h ⁻¹ (voltage decay rate)	MEA life of 5000 h; consider freeze/thaw, cold start, stop/start, duty cycle.

Source: Courtesy of W.L. Gore & Associates, Elkton, MD.

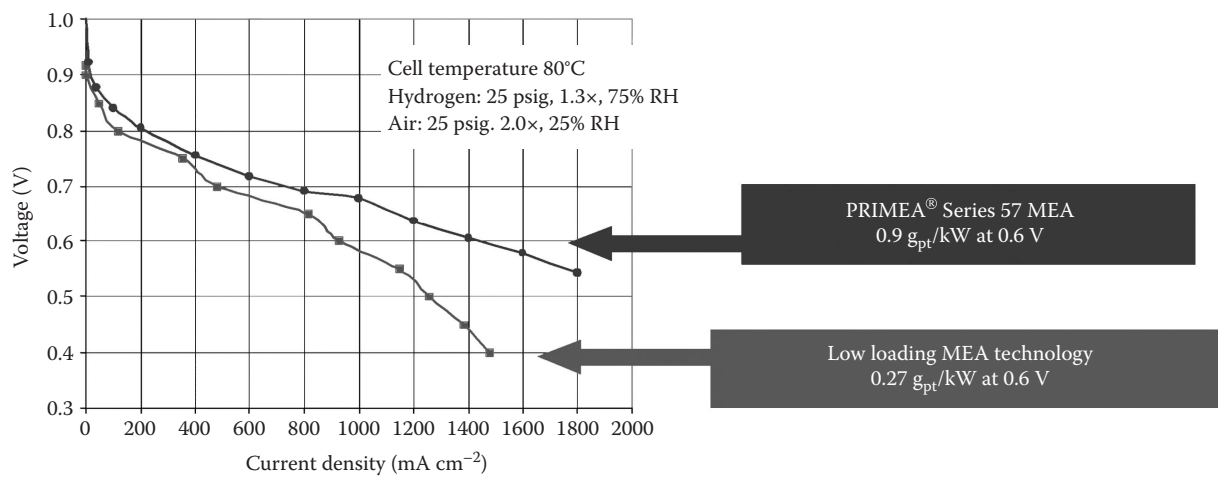


FIGURE 21.32 PRIMEA Series 57 low loading MEA. (Courtesy of W.L. Gore & Associates, Elkton, MD.)

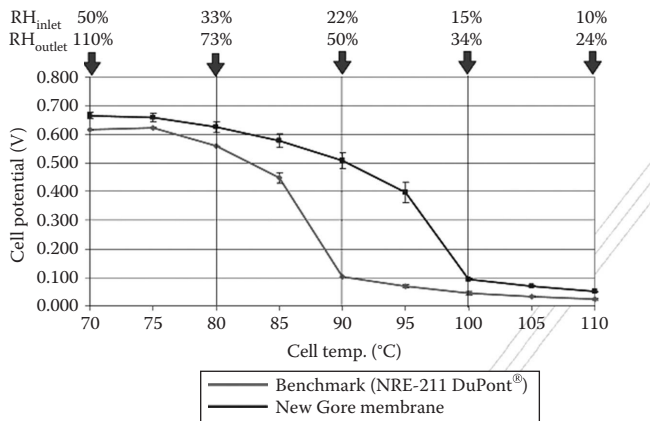


FIGURE 21.33 RH sensitivity at 1200 mA cm⁻²: comparison between NRE-211 and new Gore membrane. (Courtesy of W.L. Gore & Associates, Elkton, MD.)

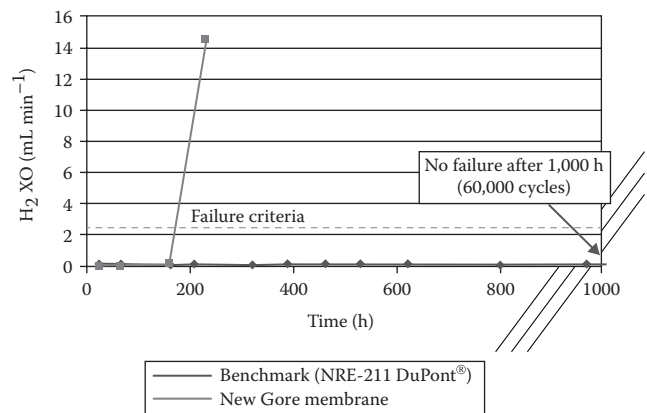


FIGURE 21.34 Hydrogen crossover rate growth as a function of RH cycling and time period under test. (Courtesy of W.L. Gore & Associates, Elkton, MD.)

21.4.2.2 PFSA Ionomer with PTFE Fibril Reinforcement (AGC, Flemion)

AGC manufactures Flemion, which is based on a PTFE fibril reinforcement that was originally developed for chlor-alkali electrolysis. AGC has participated in the R&D programs of

the New Energy and Industrial Technology Development Organization (NEDO) and has developed ion exchange membrane technologies for PEMFCs since 1992. In the first phase of the program, various chemical/physical properties of Flemion membranes were investigated. In the second phase, fundamental properties required for practical use of PEMFCs

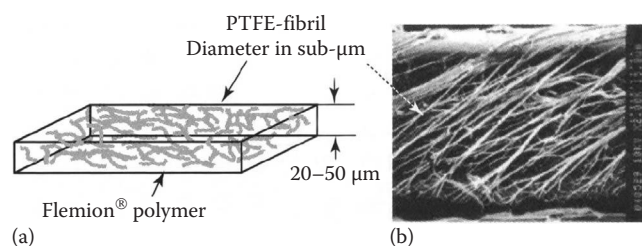


FIGURE 21.35 (a) Schematic representation of a fibril-reinforced membrane and (b) a cross-section image after tearing. (From Hommura, S. et al., *J. Fluor. Chem.*, 120, 151, 2003; Reproduced from Nakao, M. and Yoshitake, M., in: *Handbook of Fuel Cells: Fundamentals, Technology and Applications*, Vielstich, W., Gasteiger, H.A., Lamm, A., eds., Vol. 3, John Wiley & Sons, Chichester, U.K., 2003. With permission.)

were evaluated for Flemion membranes that have various thicknesses and ion exchange capacities (IECs), and AGC successfully developed a new technology for membrane reinforcement. In the third phase of NEDO's program, AGC has been developing some basic technologies for high-power-density-type MEAs and for high-temperature-type MEAs.

Reinforcement of membranes: AGC's fabrication method consists of dispersing a small amount of PTFE fibers in a polymer matrix consisting of a perfluorosulfonic resin with high IEC (EW 909). In addition (according to AGC), a novel stretching method that leads to an evenly enlarged film with less than 50 μm is used. The structure of the fibril reinforcement is shown in Figure 21.35. Two to five percent of the PTFE microfiber weight is dispersed in the perfluorosulfonic resin. Various mechanical properties are controlled by optimizing the fibril content, length, and radii of PTFE fibrils and other parameters. The trade name for AGC membranes is Flemion. The Flemion[®] FR30 is 30 μm thick, and the SH50 is 50 μm thick.⁷³

The key parameter in the preparation of a thin and flat membrane with fibril reinforcement is the uniform dispersion of the fibrils in the matrix. Furthermore, the overall flatness of the membrane is important for coating the electrodes. AGC's new preparation method is disclosed in European Patent EP1139472.^{74,75} A precursor polymer and PTFE powder are

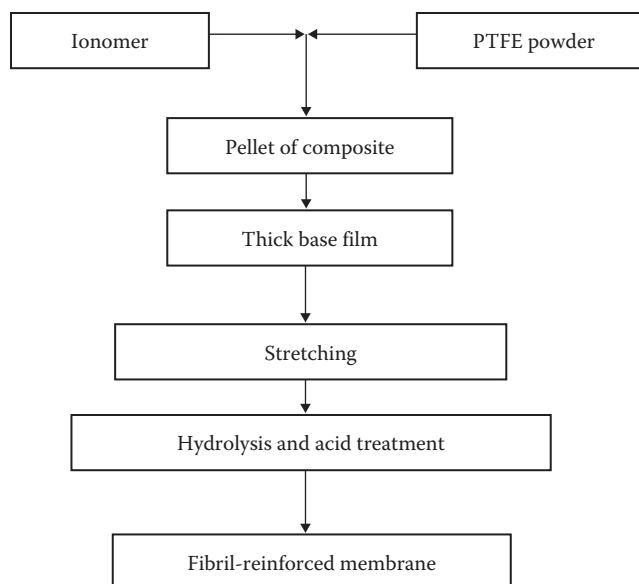
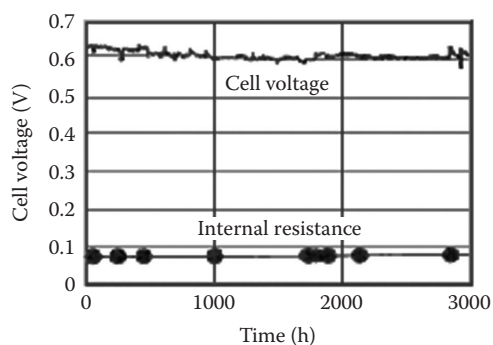


FIGURE 21.36 Fabrication of PTFE fibril-reinforced Flemion. (Reproduced from Nakao, M. and Yoshitake, M., in: *Handbook of Fuel Cells: Fundamentals, Technology and Applications*, Vielstich, W., Gasteiger, H.A., Lamm, A., eds., Vol. 3, John Wiley & Sons, Chichester, U.K., 2003. With permission.)

kneaded, pelletized, and subsequently extruded to make a thicker base film. This base film is stretched (using a supporting film) to form a thin cationic film. This film then undergoes alkali and acid treatments. The process is schematically illustrated in Figure 21.36. The reported durability of the Flemion membranes is also relatively good (cf. Figure 21.37).

AGC's developments concerning high-power-density-type MEAs are represented in Figure 21.38, which shows the structure of an MEA at the cathode side, whereby the cathode is fabricated from catalysts and ionomers. AGC is trying to accommodate all the electrode requirements with improved ionomers and hydrophobic components in the electrode structure. They are developing high-performance MEAs using candidate materials for improving power density such as high-IEC ionomers, new ionomers with high oxygen solubility, and soluble fluoropolymers (Cytos[®]).⁷⁶



Effective area	: 25 cm ²
Current density	: 1 A cm ⁻²
Hydrogen pressure	: 1.5 ata
Air pressure	: 1.5 ata
Temperature	: 80°C
Pt loading	: 0.4 mg cm ⁻²
Humidification temperature	: 80°C

FIGURE 21.37 Durability of fibril-reinforced Flemion. (From Hommura, S. et al., *J. Fluor. Chem.*, 120, 151, 2003; Reproduced from Nakao, M. and Yoshitake, M., in: *Handbook of Fuel Cells: Fundamentals, Technology and Applications*, Vielstich, W., Gasteiger, H.A., Lamm, A., eds., Vol. 3, John Wiley & Sons, Chichester, U.K., 2003. With permission.)

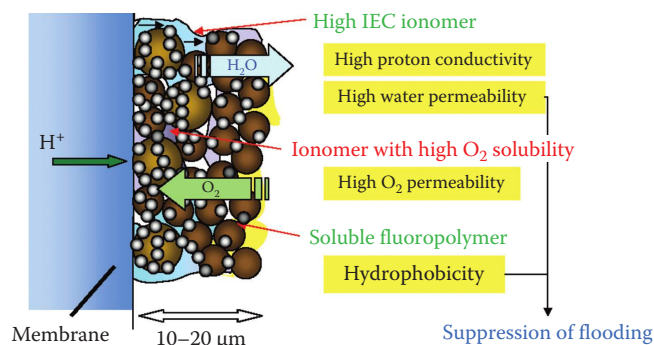


FIGURE 21.38 Pictorial depiction of the development activities of AGC. (From Yamada, K. et al., *Abstracts of the 2003 Fuel Cell Seminar*, 2003.)

21.4.2.3 PFSA Ionomer and PTFE Reinforcement at Asahi Kasei (Aciplex Membranes)

Asahi Kasei develops membranes mainly for chlor-alkali electrolysis technology with Aciplex F PFSA membranes. The Aciplex F membrane is employed in plants with a total production capacity of over 5 million tons of sodium hydroxide per year. Since 1996, Asahi Kasei has been developing Aciplex membranes for PEMFCs under a grant from NEDO in view of the rising expectations for the adoption of PEMFCs as an alternative energy source in both transportation and stationary applications and with the specific purpose of identifying the membrane properties required for durable fuel cell stacks. Asahi Kasei is also focusing its activities on reinforced membranes. Reinforced membranes (Aciplex-S-AH and Aciplex-S-H-EH) of 100, 150, and 200 μm thickness have been reported using reinforcing webs of 150 and 200 denier PTFE, respectively, and modification of the conditions of their hydration to increase their water content, compared to conventional nonreinforced membranes. The dimensional stability of the reinforced membranes, in terms of dimensional change between their wet and dry states, was considerably improved. Shrinkage in drying is reportedly less than 10% for each of the reinforced membranes and 14.9%–18.8% for the nonreinforced membranes. As with the previous reinforced membranes, the tensile strength of the reinforced membranes is about twice that of nonreinforced Aciplex-S membranes. The reinforced membranes also show considerably less creep under stress than the other membranes.⁷⁷

21.4.3 PARTIALLY FLUORINATED IONOMERS

21.4.3.1 FuMA-Tech Membranes

FuMA-Tech is an established manufacturer of ion exchange membranes and belongs to the BWT Group based in Austria. With 65 group companies and some 2700 employees, the Best Water Technology Group (BWT) is the leading water technology company in Europe. FuMA-Tech GmbH develops membranes for PEMFC. FuMA-Tech is the only supplier to offer both fluorinated and nonfluorinated membranes for PEMFCs and DMFCs with application temperatures of up to

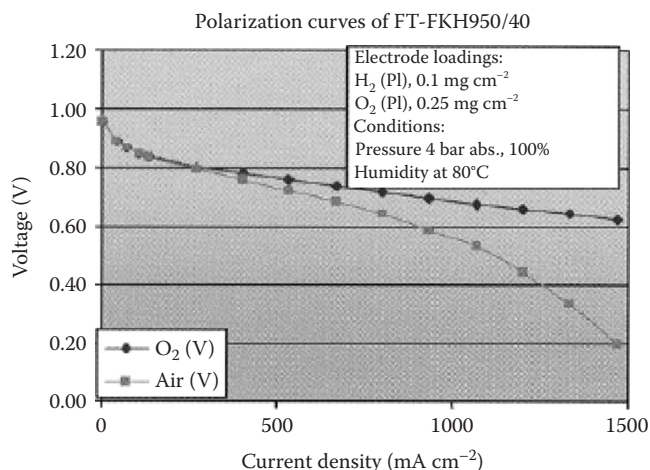


FIGURE 21.39 Performance curves for FT-FKH950/40 and FT-PKH/757/45. (Courtesy of FuMA-Tech, Vaihingen an der Enz, Germany.)

130°C. Catalyzed membranes for fuel cells and water electrolysis are manufactured as well. FuMA-Tech offers two different membrane families for fuel cell applications. For standard applications in hydrogen/air or oxygen environment, the partially fluorinated (highly conductive and chemically stable) FKH series ranging from EW 950 to 1500 is offered. The membranes are available in two different thicknesses and two different configurations (not specified). It is stated that membrane electrode processing by way of a standard hot-pressing protocol is possible and that reliable and reproducible results have been obtained. A second class of partially fluorinated membranes consists of glass fiber reinforced FKH/60GF, which was developed to avoid wrinkling and uncontrolled membrane swelling caused by the solvents in most catalyst ink or paste formulations. Besides this feature, the membrane is reported to be insusceptible to mechanical stress. The FKE membranes using polyketone-type sulfonic acids are a completely different type of membrane, being nonfluorinated and intended for medium-temperature applications above 100°C and DMFCs. According to FuMA-Tech, these membranes are offered in standard sheets measuring 30 cm \times 30–200 cm. Other dimensions and rollware have to be requested.

Curves reported by FuMA-Tech are presented in Figure 21.39.

21.4.3.2 Poly(α , β , γ -Trifluorostyrene) and Copolymers (Ballard Advanced Materials)

Ballard Advanced Materials Corporation (BAM) ionomers are sulfonated copolymers of trifluorostyrene and substituted trifluorostyrene monomers. Ballard Advanced Materials, a subsidiary of Ballard Power Systems, investigated the conducting polymers based on polyphenylquinoxaline (PPQ). These can be sulfonated in a wide range and were referred to as Ballard first-generation (BAM1G) membranes, but these membranes were found to have short durability. To overcome this problem, BAM developed a second generation of advanced membranes

based on two distinct material types. The first consisted of a series of sulfonated poly(2,6-diphenyl 1,4-phenylene oxide). The second series consisted of sulfonated poly(arylether sulfone). But the durability of these membranes was also insufficient. Since the durability of previous membranes was limited, Ballard produced a novel family of sulfonated membranes based on α,β,β -trifluoro-styrene monomers and a series of substituted trifluoro-comonomers.^{78,79} This family of membranes was named BAM 3G. Condensation polymerization techniques that did not involve fluoridation technologies were used. These polymers have low EWs ranging from 375 to 920. Because of this small EW, these membranes exhibited high water uptake as well as good durability.

Furthermore, in 2001, Ballard entered an alliance with Victrex to produce two new membrane alternatives. One membrane is based on sulfonated poly(arylether) ketone (a variant of s-PEEK) supplied by Victrex, which may be better suited to PEM fuel cell fabrication applications. In March 2002, U.S. Patent 6359019 was issued to Ballard Power for a graft-polymeric membrane in which one or more trifluoro-vinylaromatic monomers are radiation graft polymerized to a preformed polymeric base. The structures of BAM membranes have been studied by way of small-angle neutron scattering or SANS.⁸⁰ The study of the ionomer peak position suggests the existence of relatively small ionic domains compared to Nafion, despite large water content. Phase separation in the polymer matrix is possibly crucial for the membrane's mechanical and transport properties.

21.4.3.3 Radiation-Grafted Membranes

Partially fluorinated membranes prepared by radiation grafting are under active research, for example, in the groups at the Paul Scherrer Institute and the Helsinki University of Technology.^{78,81–94} The preparation of the membranes involves an irradiation or e-beam step to produce radical sites in perfluorinated polymer membranes, partially fluorinated polymer membranes, and nonfluorinated base membranes.⁹⁵ Typically, the membranes are swollen with suitable solutions of polymer network-forming compounds (e.g., styrene/divinylbenzene). An interpenetrating polymer grafting network is formed at the radical sites normally by heating up the sample. These membranes are then sulfonated. The preparation process is depicted in Figure 21.40. The advantages of this preparation method are stated as enabling low-cost starting materials, simple chemical reactions, and the possibility to form a cross-linked material directly in its final form. Poly(tetrafluoroethylene) (PTFE), poly(tetrafluoroethylene-co-hexafluoropropylene) (FEP), poly(ethylene-alt-tetrafluoroethylene) (ETFE), poly(vinylidene fluoride) (PVDF), and poly(tetrafluoroethylene-co-perfluorovinylether) (PFA) have all been used as host materials for PSSA grafts. Less investigated alternatives to PSSA include grafting glycidyl methacrylate and methyl styrene with subsequent sulfonation. The exact properties of the membranes may be determined by way of numerous reaction parameters like irradiation dose, thickness of the base polymer film, styrene/divinylbenzene composition, and graft level (determined by ratio of graft

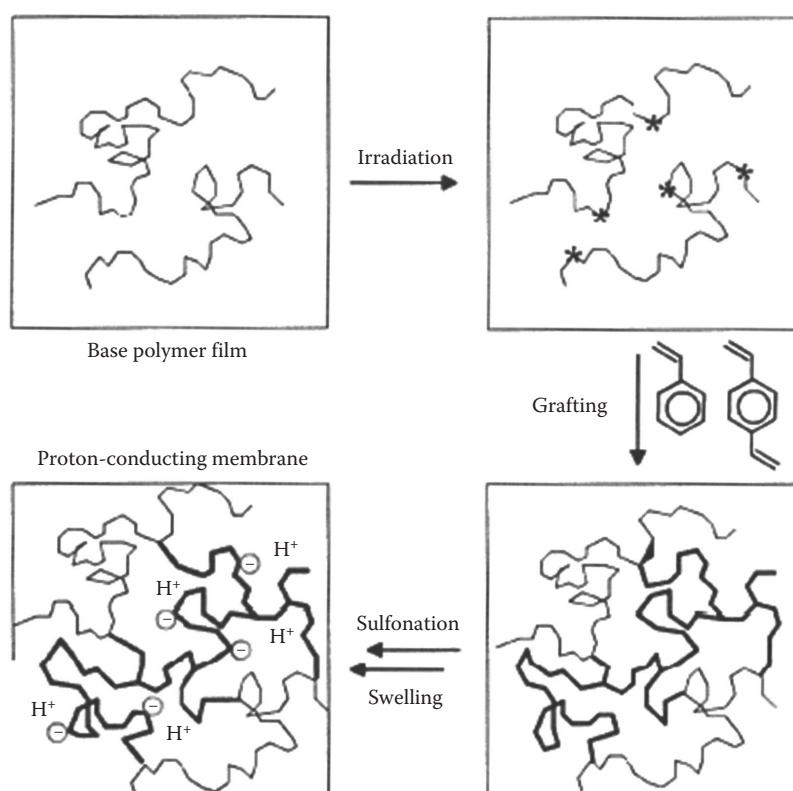


FIGURE 21.40 Diagram of the preparation process for radiation-grafted membranes. (Reproduced from Geiger, A.B. et al., *Proceedings of First European PEFC Forum 2001*, Büchi, F.N., Scherer, G.G., Wokaun, A., eds., 2001. With permission.)

material to base material). From the published work, it can be derived that there are two main obstacles to realizing technical radiation-grafted membranes. The interface between electrodes and membranes has often shown insufficient bonding, and delamination has often been reported. Durability seems to be a critical issue with these membranes.⁷⁸

Decent performance curves in short-term operation have been reported for radiation-grafted membranes in DMFCs. An advantage versus Nafion has been observed by Geiger et al. and by Scott et al. (for higher current densities), but so far, all reported DMFC measurements have been performed for short operation times.^{96,97}

A publication by the Paul Scherrer Institute reports progress in preparing membrane/electrode assemblies for PEMFCs based on radiation-grafted FEP PSSA membranes.⁷⁸ Hot-pressing with Nafion was used to improve the interfaces. These improved MEAs showed performance data comparable to those of MEAs based on Nafion 112 and a service life in H₂/O₂ fuel cells of more than 200 h at 60°C and 500 mA cm⁻².

The long-term performance was found to be stable up to 2000 h—an important improvement on the previously reported service lives in the range of 500 h.

21.4.4 INORGANIC/ORGANIC (FLUORINATED) COMPOSITE IONOMER MEMBRANES

21.4.4.1 Hydrophilic Fillers (SiO₂, TiO₂, ZrO₂) and ORMOSIL Networks

Over the last decade, extensive results have been reported regarding the improvement in the characteristics of known ionomeric membranes by dispersing inside their polymeric matrix, the acids with low solubility (e.g., heteropoly acids), or particles of insoluble solids such as metal oxides, lamellar zirconium phosphates, or phosphonates. A second strategy aims at developing membranes obtained by filling a non-proton-conducting polymeric matrix with ionomers or inorganic particles of high-proton conductivity. The degree of dispersion inside the membrane may vary considerably, leading to nano- or microcomposites or even macrocomposites.

The oldest concept in this respect is Nafion-based membranes that are prepared by recasting Nafion solution and introducing inorganic hydrophilic additives, quite frequently silica or titania particles. This concept was introduced by P. Stonehart and M. Watanabe and is protected and disclosed in U.S. Patent 5523181.⁹⁸ It is clear that the silica and titania particles (e.g., nanoporous, highly hydrophilic SiO₂ from Degussa, *Aerosil*) are completely nonconductive. However, the composite recast Nafion-based membranes containing hydrophilic SiO₂ or TiO₂ particles as well as other inorganic material are expected to increase the water retention and, therefore, to lead toward increased ionic conductivity at elevated temperatures. The interpretation of improved water retention is backed by the experimental result of a higher water uptake of the membranes. The second concept that is supposed to lead to better distribution of the particles in the membrane is based on producing the particles by hydrolysis

in preformed membranes by introducing a precursor (e.g., tetraethoxysilane [TEOS]) into the swollen membrane.^{99–103} The hydrolysis is catalyzed by the sulfonic groups forming an inorganic network in the membranes. Such structures are named ORganically MODified SILicate (ORMOSIL). The Mauritz group has prepared different membranes using this route, namely, Nafion with SiO₂/OH, Nafion with ZrO₂/OH, and Surlyn with SiO₂/OH. The disadvantage is that the inorganic content cannot be varied over a large range, but these membranes are nevertheless promising for application at temperatures over 100°C and, therefore, also for DMFCs. However, structural changes in the membrane during preparation have also been observed. Differing results have been reported: whereas the Watanabe group found a significant improvement in membrane performance without humidification of gases, the Savinell group found no improvement in proton conductivity (although the water content was higher) for nanomodified Nafion prepared following the procedure from Mauritz et al.¹⁰² Recently, reports from Adjemian et al. reported significant improvement in silicon oxide–modified recast Nafion as well as Nafion 115.^{105,106}

Alberti and Casciola have pointed out that it is unlikely that the improved conductivity of composite ionomer membranes is just due to the improved water absorption and retention properties, because the content of the SiO₂ is in the range of 3–10 wt%.¹⁰⁷ The reported increased water uptakes in the range of 20 wt%—if only absorbed in the inorganic particles—would lead to a molar ratio of ~27. Since water is only absorbed on the surface of the nanoparticles, the hydration number of the silanol groups (H₂O/SiO₂) would be much higher than 27. This is unrealistic, as it would mean that the hydration of silanol groups is higher than that of the superacid –SO₃H groups. However, as mentioned before, the structure of the membrane is changed upon metal oxide modification leading, for instance, to a large degree in crystallinity of the polymer backbone. Therefore, the increased water content of metal-oxide-loaded Nafion is probably associated with structural changes in the polymer matrix induced by the presence of the inorganic nanoparticles.

Several groups have reported increased performances for such membranes in DMFC applications due to a decrease in methanol permeation. A maximum power density of 240 mW cm⁻² at 0.4 V was obtained by Arico et al. and Antonucci et al.^{108,109} The reduced methanol permeation of such membranes is, however, controversial.¹¹⁰ The Watanabe group proposed a further self-humidifying composite membrane with highly dispersed nanoparticles of Pt and TiO₂ (or other metal oxide particles).^{111–114} The idea is represented in [Figure 21.41](#) and consists of generating water by permeating hydrogen and oxygen with the catalytic active Pt in the membrane and a water storage function of the hydrophilic particles in the membrane.

This concept enables the operation of PEMFCs without any humidification, which should also be interesting for higher temperatures. The corresponding U–I characteristics are displayed in [Figure 21.42](#). The disadvantage to this concept, however, is that the cost of the membrane is significantly

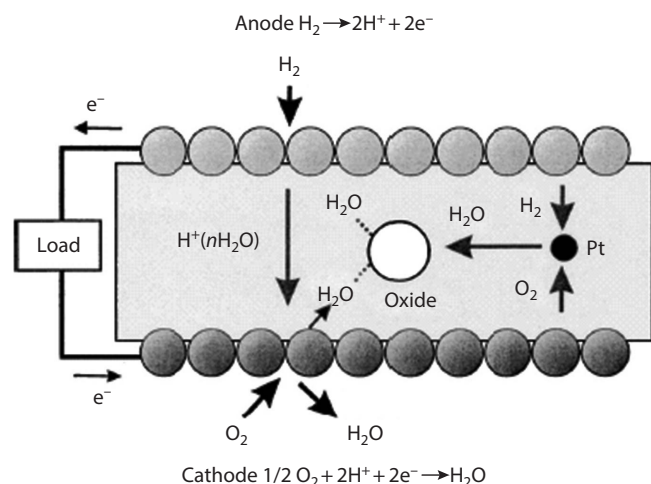


FIGURE 21.41 Operation concept of a PEMFC using self-humidifying Pt-oxide-PEM. (Reproduced from Uchida, H. et al., *J. Electrochem. Soc.*, 150, A57, 2003. With permission of The Electrochemical Society, Inc.)

increased by adding noble metal particles. Composite membranes with nonfluorinated polymer matrices have also been investigated. For instance, high-surface amorphous silica, precipitated from a solution of tetrapropylammonium oligosilicate, was used as a filler of s-PEEK with 1.6 mequiv. g^{-1} IEC.¹¹⁵ In this work, microcomposite membranes containing up to 20 wt% silica were prepared by bulk mixing the finely prepared powder with the polymer solution. The membrane containing 10 wt% silica exhibited the best electrical (conductivity rises to $3 \times 10^{-2} \text{ S cm}^{-1}$ at 100°C for RH in the range of 75%–100%) and mechanical characteristics.

According to a similar synthetic approach reported by Nunes et al., nanocomposite membranes loaded with SiO_2 , TiO_2 , and ZrO_2 were prepared by way of hydrolysis of silanes and metal alkoxides in solutions of s-PEEK and s-PEK.¹¹⁶ While homogeneous dispersions of TiO_2 and ZrO_2 particles were obtained starting from $\text{Ti}(\text{OEt})_4$ and $\text{Zr}(\text{OPr})_4$, the hydrolysis of $\text{Si}(\text{OEt})_4$ led to the formation of larger particles and cavities in the polymeric matrix. However, smaller and better-dispersed silica particles (about 100 nm in size) were formed by using either silanes covalently bonded to the polymer chain or organically modified silanes bearing imidazole groups. A loading of 14–33 wt% metal oxide resulted in a decrease in the membrane permeability to water and methanol by a factor of 30–60 but also resulted in reduced proton conductivity at 25°C . A good balance of low permeability and high conductivity ($3.5\text{--}4.5 \times 10^{-3} \text{ S cm}^{-1}$ against $5 \times 10^{-3} \text{ S cm}^{-1}$ for the unmodified polymer) was achieved by incorporating a mixture of 10–15 wt% ZrO_2 and 20–14 wt% amorphous ZrP into s-PEEK.

21.4.4.2 Properties of Recast Membranes with Inorganic Fillers

Preparation of membranes using the recast method with inorganic hydrophilic ingredients has proved to be a promising approach to manipulate the membrane properties with

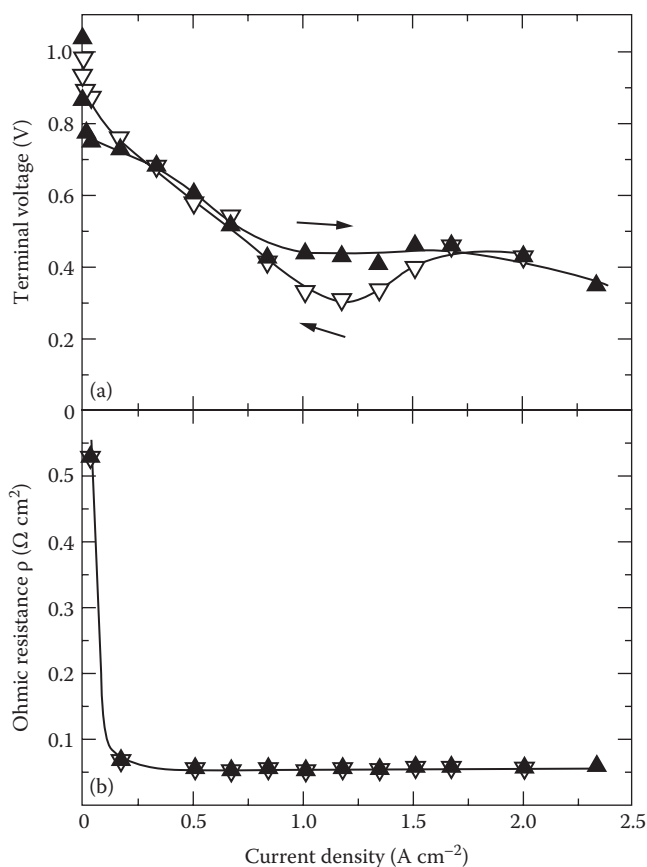


FIGURE 21.42 (a) U-I curve and (b) ohmic resistance of a PEMFC using Pt- TiO_2 -PEM operated at 80°C and ambient pressure with no external humidification at the reactant utilization of H_2 56% and O_2 54%. An OCV was measured at a flow rate of 7 mL min^{-1} for both dry H_2 and dry O_2 . The amount of Pt dispersed in the PEM = 0.1 mg cm^{-2} , the amount of TiO_2 = 0.42 mg cm^{-2} (4 wt%). Full symbols measured on increasing current density, and open symbols measured on decreasing current density. (Reproduced from Uchida, H. et al., *J. Electrochem. Soc.*, 150, A57, 2003. With permission of the Electrochemical Society, Inc.)

respect to liquid permeation (water and methanol), ionic conductivity, and water uptake. This approach was introduced by Stonehart and Watanabe to improve the water management of Nafion membranes in PEMFCs.¹¹⁷ Several investigations by Antonucci et al.¹¹⁸ have also reported an advantage to such composite membranes for DMFC applications due to a decrease in methanol permeation induced by a structural change in the polymer associated with a higher crystallinity. P. Dimitrova et al.^{112,119} reported a detailed characterization of a recast ionomer composite membrane with 4.3% Aerosil A380 (silicon dioxide).

21.4.4.2.1 Water Uptake of Composite Membranes

Recast Nafion-based samples with and without fillers absorb more water compared to the commercial Nafion 117, 115, and 112 membranes. It is observed that the water content rises slightly with the thickness of the membranes investigated. Nafion 112 indicates unexpectedly low water content in the swollen state. It is noted that even after many repetitive

drying–rehydration treatments, the composite membranes contain more water than the commercial membranes. This finding might be explained by the hydrophilicity of the filler, by the altered physical structure of the ionomer backbone or possibly by the stronger interactions between the absorbed water and the modified matrix. In particular, the silica nanoparticles retain water even at high temperatures, and this property may help to prevent the membrane drying during fuel cell operation. Easier water management during fuel cell operation can be anticipated for the composite membranes.

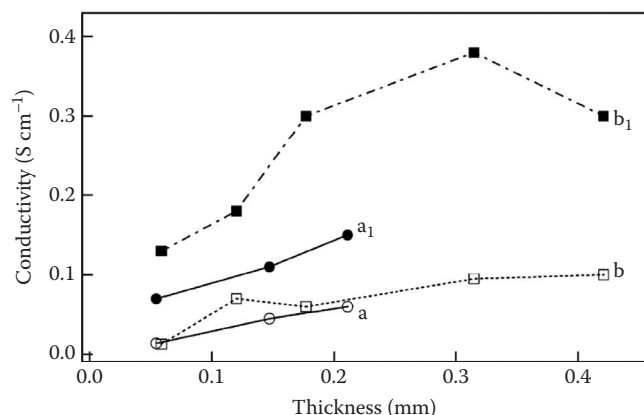


FIGURE 21.43 Conductivity of the membranes as a function of thickness and at different temperatures: (a, a₁, ○, ●) commercial samples N112, N115, and N117 (b, b₁, □, ■) composite membranes. Temperature: at 15°C, plots a and b (open symbols), and at 90°C, plots a₁ and b₁ (full symbols). Lines are for guidance. (Reprinted from *J. Electroanal. Chem.*, 532(1–2), Dimitrova, P., Friedrich, K.A., Vogt, B., and Stimming, U., Transport properties of ionomer composite membranes for direct methanol fuel cells, 75–83, Copyright 2002, with permission from Elsevier.)

21.4.4.2 Proton Conductivity

Figure 21.43 shows the conductivity as a function of thickness of the commercial membranes and the modified recast Nafion membranes for temperatures of 15°C and 90°C. A proton conductivity for composite recast membranes higher than or comparable to commercial membranes is measured at 15°C. At 90°C, this difference becomes significant. These results manifest that the hydrophilic particles assist in humidifying the membrane, leading to higher proton conductivity. It should be noted that the conductivity is not constant with thickness but increases in most samples. The increase in conductivity with thickness, which should not occur for homogeneous material, suggests that the properties of the membrane change with the thickness.

21.4.4.2.3 Methanol Permeation Rate

The methanol permeation measurement illustrates the relationship between the methanol permeation rate and the temperature versus the thickness of the membrane. In the case of thinner samples, the permeation rate changes by a factor of 4 or 5 with a temperature change from 25°C to 65°C, while in the thicker membranes, this factor is about 3. At lower temperatures, the variation of the methanol flux through the membranes versus thickness is small compared to that at 65°C, where this dependence is pronounced. As anticipated, a strong decrease in permeation with thickness is observed in all cases. For the reciprocal quantity, a linear relationship between permeation rate and thickness can be derived approximately as shown in the inset of Figure 21.44. The comparison between the composite membranes and the commercial Nafion (112, 115, and 117) reveals a similar methanol permeation rate at elevated temperature with slightly higher values of the composites.

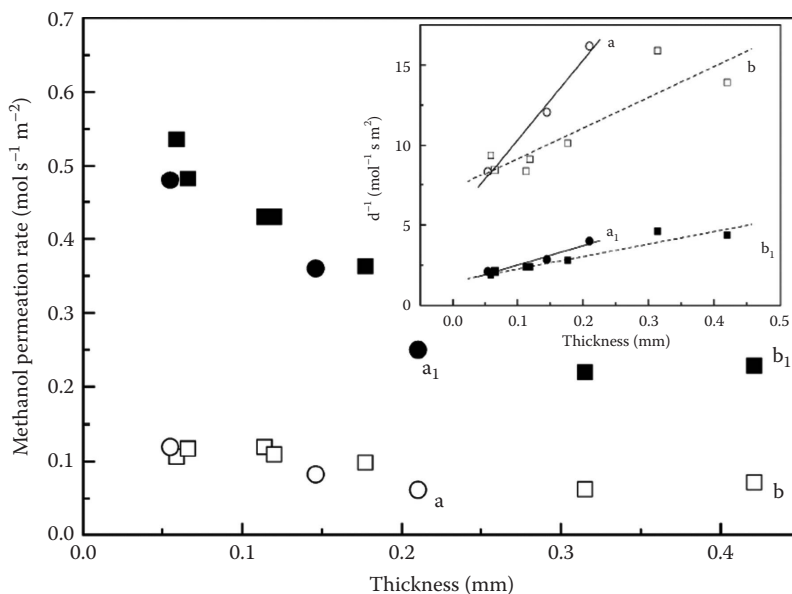


FIGURE 21.44 Methanol permeation rate of the membranes as a function of thickness and at different temperatures: (a, a₁, ○, ●) commercial samples N112, N115, and N117 (b, b₁, □, ■) composite membranes. Temperature: at 25°C, plots a and b (open symbols), and at 65°C, plots a₁ and b₁ (full symbols). (Reprinted from *J. Electroanal. Chem.*, 532(1–2), Dimitrova, P., Friedrich, K.A., Vogt, B., and Stimming, U., Transport properties of ionomer composite membranes for direct methanol fuel cells, 75–83, Copyright 2002, with permission from Elsevier.)

21.4.4.2.3.1 Water Permeation It is favorable for fuel cell operation when reduced methanol transport across the membrane is accompanied by proper water management. In particular, a low water crossover from the anode to the cathode is necessary in order to avoid flooding of the cathode. The dependence of water permeation on the membrane thickness is weak. Only a small decrease in water permeation is observed for the commercial Nafion membranes, whereas the thickness of the recast membranes has no significant influence on the water transport rate. In contrast, the effect of temperature on water permeation is strong. At 65°C, the rates are higher by a factor of 5 compared to those at 25°C.

21.4.4.3 Heteropoly Acid Additive

The heteropoly acids possess a relatively high inherent proton conductivity that increases the overall ionic conductivity of the membrane. Owing to these characteristics, heteropoly acids are suitable membrane fillers for increasing the number of protonic carriers and thus improving the hydrophilic character of the membranes. The major problem with modified membranes is the hydrosolubility of heteropoly acids. Composite Nafion membranes containing heteropoly acids were obtained by simply impregnating preformed membranes with a heteropoly acid solution and mixing a Nafion solution with an appropriate amount of heteropoly acid followed by casting.^{120,121} Nafion recast membranes loaded with silicotungstic acid (STA), phosphotungstic acid (PTA), and phosphomolybdic acid (PMA) were investigated regarding ionic conductivity, water uptake, tensile strength, and thermal behavior.¹²⁰ In comparison with Nafion 117, all these membranes exhibited higher proton conductivity and greater water uptake but exhibited a decreased tensile strength. Water uptake, determined by dipping dried membranes in boiling water, increases from 27% for Nafion 117 to a maximum of 95% for the PMA-based membrane. At 80°C, the heteropoly acid-loaded membranes show a better fuel cell performance than unmodified Nafion 117. The current density at 0.6 V increases from 640 mA cm⁻² for Nafion 117 up to a maximum of 940 mA cm⁻² for PMA-Nafion 117. Composite PTA-Nafion 117 membranes, impregnated with PTA solutions in acetic acid or in molten tetra-*n*-butylammonium chloride, were tested in H₂/O₂ fuel cells working at

1 atm up to 110°C.¹²¹ In comparison with unmodified Nafion 117, these membranes showed a much improved performance that increased with increasing temperature.

Composite membranes with nonfluorinated polymers and heteropoly acid were also prepared. A series of nano-composite membranes made of *s*-PEEK and 60 wt% PTA or PMA were prepared by Homna et al. by mixing the heteropoly acid with a polymer solution in dimethylacetamide.¹²² In comparison with the pure sulfonated polymers, the composite membranes are characterized by a higher glass transition temperature, probably because of the intermolecular interaction between the sulfonic groups and the heteropoly acids, and by much greater hydration at room temperature (up to five times for PTA-loaded *s*-PEEK with 80% degree of sulfonation). Conductivity was determined in the range of 20°C–150°C by using an open cell with concomitant water loss (therefore, lower limit of the membrane conductivity). The composite membranes are generally more conductive than the pure polymer, but the conductivity enhancement decreases with an increasing degree of sulfonation. In all cases, the conductivity dependence on temperature shows a maximum around 120°C. In the investigated temperature range, the highest conductivities were found for the PTA-based membranes (at 120°C from 2 × 10⁻² to 0.1 S cm⁻¹ with an increasing degree of sulfonation from 70% to 80%).

21.4.4.4 Phosphate and Phosphonate Additives

This class of composite membranes is strongly favored by the Alberti group.^{14,107,123–125} The Alberti group has developed an in situ method for formation of layered metal(IV) phosphonates or phosphate-phosphonates. These compounds can be considered organic derivatives of α-ZrP and have the general formula M(IV)(O₃P-G)_{2-x}(O₃P-ArX)_x, where -G may be an inorganic (e.g., -OH), organic (e.g., -CH₂OH), or inorgano-organic group (e.g., -CF₂PO₃H₂). Ar is an aryl group (e.g., phenylene), X is an acid group (e.g., -SO₃H, -PO₃H₂, or -COOH), and *x* is a coefficient that can vary between 0 and 1.5. Important in this respect is that, because of the presence of the electronegative O₃P group attached to the same ring, the -SO₃H group acquires superacid properties. In Table 21.9, the conductivity of some zirconium phosphonates is reported

TABLE 21.9
Conductivity of Some Layered Zirconium Phosphates and Phosphonates (100°C, 95% RH)

	(Φ) S cm ⁻¹	References
α-Zr(O ₃ P-OH) ₂ · H ₂ O (crystalline)	1.8 × 10 ⁻⁵	[223]
γ-ZrPO ₄ [O ₂ P(OH) ₂] · 2H ₂ O (crystalline)	2 × 10 ⁻⁴	[224]
α-Zr(O ₃ P-OH) ₂ · H ₂ O (semicrystalline)	2–7 × 10 ⁻⁴	[225]
Zr(O ₃ P-OH) ₂ · <i>n</i> H ₂ O (amorphous)	1–5 × 10 ⁻³	G. Alberti (unpublished results)
Zr(O ₃ P-OH)1.5(O ₃ P-C ₆ H ₄ SO ₃ H)0.5 (amorphous)	0.9–1.1 × 10 ⁻²	G. Alberti (unpublished results)
α-ZrPO ₄ [O ₂ P(OH) ₂]0.54'[O ₂ P(OH)C ₆ H ₄ SO ₃ H]0.46 · <i>n</i> H ₂ O (crystal)	5 × 10 ⁻²	[224]
Zr(O ₃ P-OH)(O ₃ P-C ₆ H ₄ SO ₃ H) · <i>n</i> H ₂ O (semicrystalline)	0.8–1.1 × 10 ⁻¹	G. Alberti (unpublished results)

Source: Alberti, G. and Casciola, M., *Annu. Rev. Mater. Res.*, 33, 129, 2003.

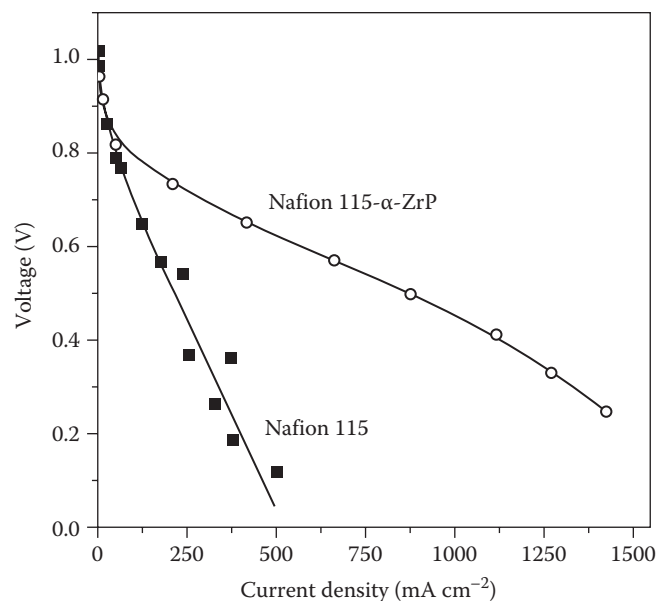


FIGURE 21.45 Polarization curves of PEMFCs based on Nafion 115 and Nafion 115- α -ZrP (123 wt%) at 130°C and 3 atm with reactants humidified at 130°C. (Reprinted from *Electrochim. Acta*, Nafion (R) 115/zirconium phosphate composite membranes for operation of PEMFCs above 100 degrees C., 47, 2002, 1023, Costamagna, P., Yang, C., Bocarsly, A.B., Srinivasan, S. With permission from Elsevier.)

and compared with that of α and γ -zirconium phosphates of varying crystallinity. The conductivity of the sulfophenylene derivatives is much higher than that of the best amorphous ZrP and, for some compositions, is comparable or even greater than that of Nafion 117. The in situ formation of these insoluble layered compounds is based on the experimental observation that their soluble precursors can be formed in proton acceptor solvents commonly used for the solubilization of proton-conducting ionomers (e.g., DMF, NMP, alkanols). The special property of these compounds is that they can easily be transformed into the final insoluble zirconium phosphonates just by drying at 110°C–130°C.

A composite Nafion 115 and recast Nafion with α -ZrP nanoparticles were investigated by Costamagna et al.¹²⁶ At 130°C cell temperature with H_2 and O_2 humidified at 130°C, the nanocomposite membranes displayed much better performance than unmodified Nafion (cf. Figure 21.45). In particular, the polarization curve of a nanocomposite recast membrane at 130°C and 3 atm was equivalent to that of the unmodified recast film at 80°C and 1 atm. Moreover, the composite membranes showed stable behavior over time at 130°C, whereas Nafion was irreversibly degraded under the same conditions. Yang et al. also investigated a Nafion- α -ZrP nanocomposite membrane in a DMFC that exhibited good performance up to about 150°C, with maximum power densities of 380 and 260 $mW\ cm^{-2}$ under oxygen and air feed, respectively.

Composite polyarylene membranes modified by using organic solutions of zirconium phosphonate precursors were investigated by the Alberti group in combination with FuMA-Tech membranes.¹⁰⁷ Preliminary results from Alberti group

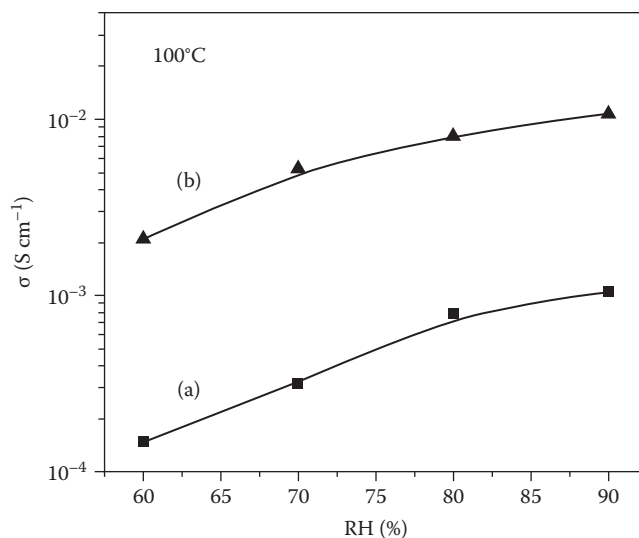


FIGURE 21.46 Conductivity as a function of RH for (a) a high-molecular-weight s-PEK membrane (FuMA-Tech; thickness 50 μm) and (b) the same membrane filled with 35 wt% of $Zr(O_3P-OH)$ ($O_3P-C_6H_4SO_3H$)- nH_2O . (Reprinted with permission from Alberti, G. and Casciola, M., *Ann. Rev. Mater. Res.*, 2003, 33, 129 © 2003 by Annual Reviews, www.annualreviews.org.)

showed that the conductivity of s-PEK membranes of high molecular weight (FuMA-Tech) is enhanced to a great extent in the presence of nanoparticles of zirconium phosphate sulfophenylphosphonates (cf. Figure 21.46). Taking into account that much lower enhancement was instead obtained with α -ZrP nanoparticles, these results seem to confirm the importance of the high proton conductivity and acid strength of the filler. Thus, according to Alberti, superacid zirconium phosphonates deserve further attention as fillers of nanocomposite membranes.¹⁰⁷

21.4.4.4.1 Ammonium Polyphosphate

Ammonium polyphosphate composite-based proton conductors for the intermediate temperature range (200°C–300°C) have been found to possess good proton conductivity (0.1 $S\ cm^{-1}$ at 300°C) under humidified conditions.¹²⁷ This temperature range would not have any kinetics or CO poisoning problem, but improving stability of the proton conductor in fuel cell conditions is still a challenge.^{128–131}

21.4.4.5 Proton-Conducting Membranes Based on Electrolyte-Filled Microporous Matrices/Composite Membranes

Composites enable the mechanical and electrical properties of the membrane to be separated. In most cases, they consist of a matrix (mechanical support) filled with a protonic electrolyte. Varying the electrolyte and optimizing the structure of its mechanical support enable the working conditions of the cell to be adapted. This implies an improvement in the performance of the cell, along with a possible reduction in the cost of the membrane. Successful efforts have been made by some groups in this direction. S. Haufe and U. Stimming¹³² prepared and characterized composite membranes made by

soaking polysulfone fleece and microglass fiber fleece in 5 M sulfuric acid and ionomer electrolytes.

Figure 21.47 shows the conductivity for the various samples in the form of an Arrhenius plot $\log(\sigma T)$ versus $1/T$. The figure reveals that all samples exhibit similar activation energies (0.10–0.19 eV), which correspond to those commonly measured for acids in the liquid state. Moreover, in the investigated temperature regime, the polysulfone fleece soaked with H_2SO_4 had a slightly higher specific conductivity than Nafion 117 membranes. This fact might be considered surprising, since, on the basis of the specific conductivity obtained for the free acids and on the basis of the porosity of the fleece (83%), a much higher conductivity is to be expected. This leads to the conclusion that the pores of the fleeces were not completely filled with H_2SO_4 .

Based on a simple geometric consideration, a comparison between the conductivity of the acid and that of the

impregnated fleeces results in only 7% of the volume of the polysulfone fleece and 11% of the volume of the microglass fiber fleece contributing to the proton conductivity of the composite. Similarly, the filled volume for H_3PO_4 and the fleece impregnated with it amount to 13%. The difference between the conductivity of Nafion 117 and that measured for the fleeces impregnated with Nafion ionomer is, however, smaller, revealing a filled volume of 34% for the polysulfone fleece and 53% for the microglass fiber fleece. These observations suggest that the surface treatment of the fleece may help in optimally impregnating the matrix.

H_2/O_2 fuel cell performance using a polysulfone fleece filled with H_2SO_4 , microglass-fiber fleece filled with Nafion, and a Nafion 117 was found to be comparable. The same kind of composite membranes were also suggested to be a good alternative to Nafion for liquid-feed DMFCs. Peled et al.^{133,134} reported a family of nanoporous proton-conducting membranes (NP-PCMs). These membranes consisted of electronic, nonconductive, nanosized ceramic powder ($\text{SiO}_2/\text{TiO}_2$); a polymer binder (PVDF); and an acid. They have the appearance of plastic, good mechanical properties, nanosized pores (typically smaller than 1.5–3 nm) filled with the acid, and room-temperature conductivity of up to 0.21 S cm^{-1} (twice that of Nafion) at 25°C . Their thickness ranges from 40 to $400 \mu\text{m}$. Their insensitivity to heavy ion impurities and reduced methanol crossover (by order of magnitude) makes them good low-cost candidates for liquid-feed DMFCs.

21.4.4.6 Other Concepts

Creavis's concept is based on ceramic membrane foils already marketed under the trade name CREAMFILTER®. They reportedly combine the characteristics of flexible polymeric membranes and ceramic membranes in a favorable way. The basis of the membrane is a woven or nonwoven support of stainless steel or temperature-tolerant glass fibers. Due to their better chemical stability, stainless steel supports are preferred for filtration applications, whereas nonconducting glass supports are needed for batteries and fuel cells. This support is coated with ceramic materials, for example, alumina or zirconia, and a flexible membrane with microfiltration (MF) properties is realized. The thickness of the membrane is about $80 \mu\text{m}$. This is thin enough for the membrane to retain the flexibility of the support. The pore size of the membrane is in the range of 50–500 nm, depending on the particle size of the ceramic materials. This MF membrane can be modified by superimposing additional layers with smaller particles or active particles onto the first layer. Coating the MF membranes once results in ultrafiltration (UF) membranes with pore sizes between 5 and 50 nm, while coating them twice produces nanofiltration (NF) membranes with pore sizes smaller than 5 nm. To use the CREAMFILTER membranes in a low-temperature fuel cell, the nonconducting MF membrane has to be transferred into a PEM. This can be achieved in a very similar way to the production process of the filtration membrane described earlier. The MF membrane is infiltrated with a solution, suspension, or sol of a proton-conducting material. After this impregnation step,

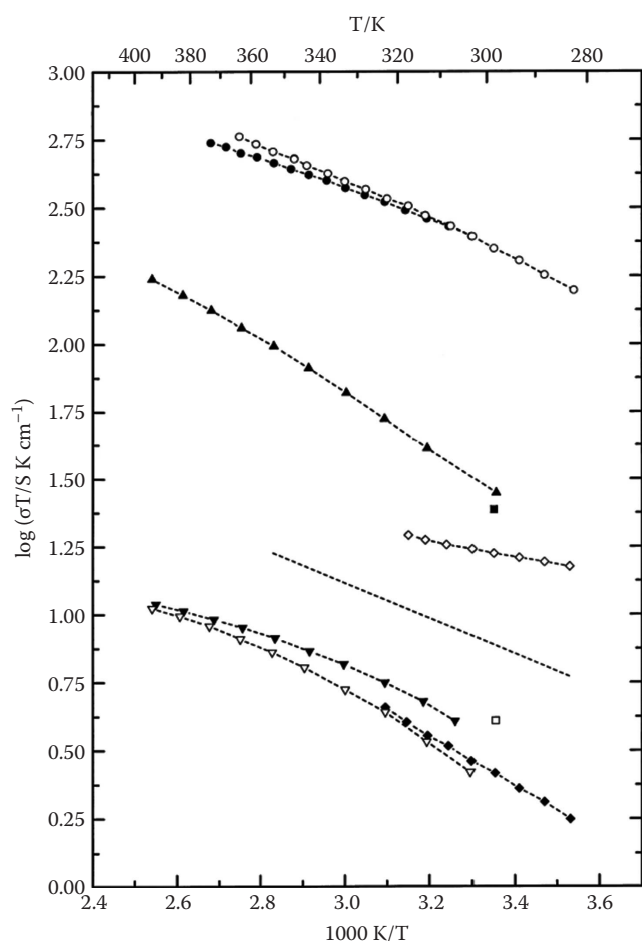


FIGURE 21.47 Arrhenius plots $\log(\sigma T)$ versus $1/T$ of the proton conductivity of $5 \text{ mol dm}^{-3} \text{ H}_2\text{SO}_4$ (●) according to Ref. [218] (○, experimental data); $15 \text{ mol dm}^{-3} \text{ H}_3\text{PO}_4$ (▲); polysulfone fleece filled with $5 \text{ mol dm}^{-3} \text{ H}_2\text{SO}_4$ (◇); polysulfone fleece filled with $15 \text{ mol dm}^{-3} \text{ H}_3\text{PO}_4$ (X) or with $19 \text{ mol dm}^{-3} \text{ H}_3\text{PO}_4$ (B); polysulfone fleece filled with Nafion (Δ); microglass fiber fleece filled with $5 \text{ mol dm}^{-3} \text{ H}_2\text{SO}_4$ (!); and microglass fiber fleece filled with Nafion (□) and Nafion 117 membrane (dotted line, according to: Cappadonia, M. et al., *J. Electroanal. Chem.*, 376, 189, 1994).

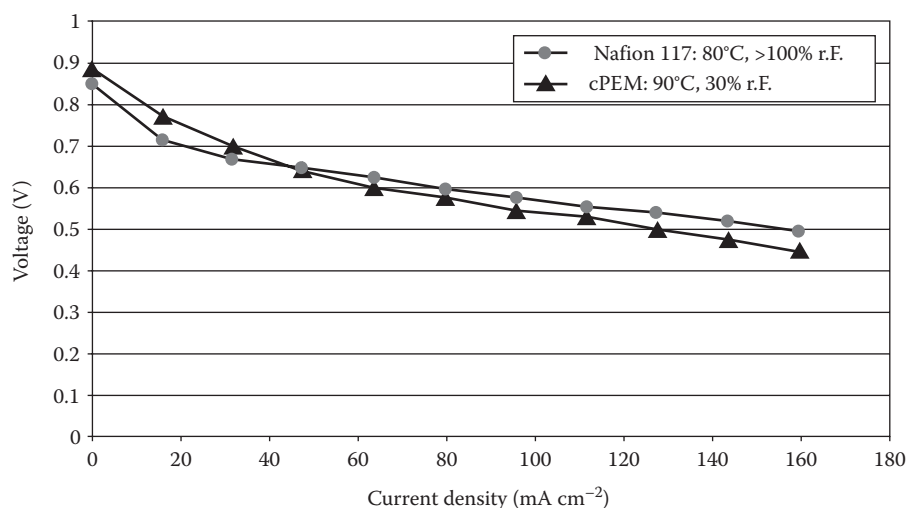


FIGURE 21.48 U–I behavior of a CREAMFILTER PEM, compared to Nafion 117. Note the different working conditions of the membranes. (Reprinted from *Desalination*, 146, 2002, 23–28, S. Augustin et al. With permission from Elsevier.)

the proton-conducting material is immobilized by thermally treating the membrane. From a theoretical point of view, all kinds of proton-conducting materials can be used as active materials for infiltrating CREAMFILTER membranes. Due to the inorganic nature of the support, inorganic compounds are preferably used as active materials. Candidate materials for proton conductors are zirconium phosphates; sulfuric acids based on triethoxy silane compounds; or other Bronsted acids, such as H_3PO_4 or H_2SO_4 . To immobilize these acids, an inorganic sol that contains the acids is typically prepared. The MF membranes are infiltrated with sols that comprise additional metal oxide compounds. During the thermal treatment, the gelation of the sol occurs and the acids are fixed in the gels. The membranes reportedly do not have pores and are absolutely gas tight. The proton conductivity of the membranes is comparable to Nafion membranes. Due to the inorganic nature of the CREAMFILTER® PEMs, these membranes show no swelling and need only a reduced RH to reach high conductivities. Figure 21.48 shows a typical U–I behavior of the membranes. The CREAMFILTER PEM in Figure 21.48 comprises an H_3PO_4 -doped silica gel as the proton-conducting material. Typical working conditions for Nafion are 80°C and an RH of up to 100%. In contrast, the CREAMFILTER membrane works at temperatures of at least 90°C and RHs of about 30%. With this membrane (Figure 21.48), power densities of more than 50 mW cm^{-2} can be achieved (low conductivity of phosphoric acid at 90°C, slow kinetics). Creavis claims that with other proton-conducting membranes, the CREAMFILTER PEM reaches power densities of up to 200 mW cm^{-2} under the same conditions.

21.4.5 POLYMER MEMBRANES WITH INORGANIC ACID IMPREGNATION

Aromatic PBIs are highly thermostable, with melting points $>600^\circ\text{C}$. The PBI commercially available is poly[2,20-(mphenylene)-5,50-bibenzimidazole] (cf. Figure 21.49).

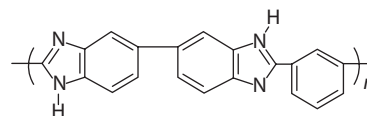


FIGURE 21.49 Chemical structure of poly[2,20-(mphenylene)-5,50-bibenzimidazole].

PBI has a tendency to take up water, thus explaining the low proton conductivity (in the range $\sim 10^{-7} \text{ S cm}^{-1}$) that is observed even for the neat polymer.¹³⁵ PBI is basic (pK value of ~ 5.5), and it readily forms complexes with organic and inorganic bases. It has long been known that PBI can be treated with sulfuric and phosphoric acids, which leads to stabilization as well as to a significant increase in conductivity. The acid uptake reaches 5 mol H_3PO_4 per PBI repeat unit. This quantity is much too large to use the term doped, yet this is the term often inappropriately used to describe PBI–acid complexes. The properties of such impregnated (doped) membranes and their application in PEM fuel cells and in cells using hydrocarbons and methanol as fuels have been investigated systematically since 1994 by Wainright et al.^{15,136–147} Celanese Ventures is the largest (and for a long time the only) producer of PBI and developed this membrane for fuel cell applications. In 2004, their fuel cell activities were spun off into a new and independent company, PEMEAS, which continues to develop MEAs. These MEAs are based on phosphoric acid–doped PBI. A pilot plant for fuel cell MEAs has been established in Höchst, Frankfurt am Main. The main advantage of this system is high-temperature operation over 150°C. Doping the membranes with other acids like hydrochloric acid, perchloric acid, or nitric acid leads to high conductivity.¹⁴³ Different methods are used to form the PBI–acid complex: immersing a PBI membrane in an acid solution of a given concentration for a given length of time is the most popular method. A second possibility is direct casting from a solution of PBI and phosphoric acid in trifluoroacetic acid. A recent variant of this approach uses polyphosphoric acid as

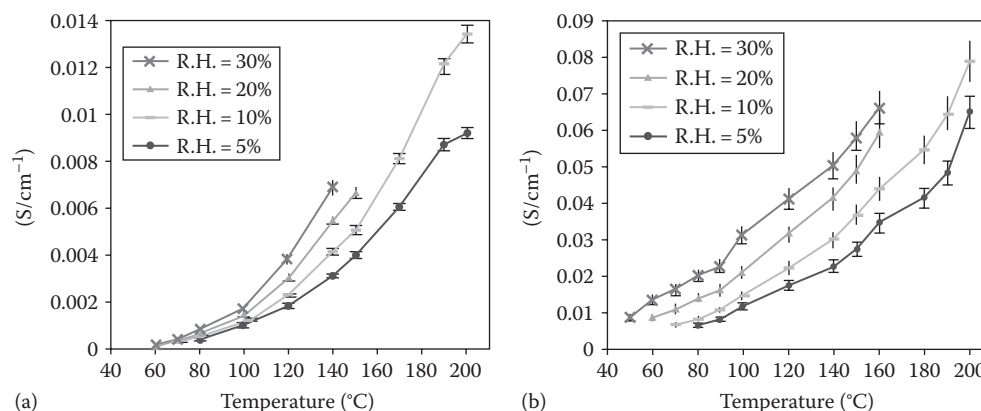


FIGURE 21.50 Conductivity of PBI versus temperature for various RHs. (a) Doping level 300% and (b) doping level 630%.²²⁰

the condensing agent for polymerization and as a membrane casting solvent. Absorption of water after casting leads to in situ hydrolysis of polyphosphoric to phosphoric acid in the membrane.¹³⁵

Whether humidification of PBI in fuel cells is necessary remains an open question. Short-term fuel cell tests yielded no or small performance losses when dry fuels were used or humidification was reduced.^{147,148} However, membrane conductivity does depend on the water activity: as can be seen in Figure 21.50 taken from a presentation by Savinell, the conductivity of PBI (3 H₃PO₄/PBI repeat unit and 6.3 H₃PO₄/PBI repeat unit) depends considerably on RH.¹⁴⁹ However, Celanese (PEMEAS) states in their publications that no humidification is required for their PBI systems.

21.4.5.1 PEMEAS (Celanese) Membranes

PEMEAS, a 2004 spin-off from Celanese AG, has developed a membrane made from the heat-resistant polymer PBI. The PBI membrane marketed by PEMEAS under the brand name Celtec® enables a fuel cell to operate at temperatures of up to 200°C (392°F), while more conventional technologies allow PEMFC operating temperatures of up to 100°C (212°F). Due to the operating temperature, PBI is resistant to CO poisoning of the catalyst and at least 100 ppm CO can be tolerated at 150°C. The need for higher fuel cell operating temperatures, according to Celanese AG, is outlined as follows:

- Higher-operating-temperature PEMFCs operate with smaller cooling elements. This is especially good for automotive applications.
- Higher-operating-temperature membranes enable more efficient heat recovery for stationary applications of PEMFCs.
- Higher temperature-tolerant membranes are more tolerant to CO poisoning. This reduces the need for ultrapure hydrogen feed.

The performance curves reported by Celanese are shown in Figure 21.51. The interfacial bonding of electrode and membrane is also accomplished using PBI/H₃PO₄.

The properties of Celtec® P MEAs, according to Celanese, are given in Table 21.10.

According to Celanese, the MEA and its individual components can be customized in size and shape to meet customer requirements.

Taking the high temperature into account, it is astounding (at least for the authors of this study) that the current densities at high single-cell voltages are comparatively low for PBI. Large losses in the kinetically dominated region of the PBI U–I curve are observed. This is due to the strong adsorption of phosphoric acid on Pt electrocatalyst and may be difficult to avoid. This effect has been investigated regarding the oxygen reduction reaction by the Savinell group and is summarized in Figure 21.52 for solid Pt electrodes with and without polymer films.¹⁴⁵ PBI and Nafion films do not influence the reactivity appreciably, but in nonadsorbing perchloric acid, current density is much higher than in the case of phosphoric acid.

21.4.6 SULFONATED HYDROCARBON POLYMER ELECTROLYTE MEMBRANES

PFSA membranes are widely used in PEMFCs because of their good performance in proton conduction and high durability in corrosive environment. However, PFSA membranes show significant disadvantages in some cost, safety, and operation-related issues, such as the dehydration-caused loss of conductivity, emission of fluorinated exhaust fumes, and the glass transition at relatively low temperature. For these reasons, extensive research has been devoted to developing alternatives to PFSA membranes. Sulfonated hydrocarbon polymer electrolyte membranes (PEMs) are promising candidates. They can be synthesized with relatively inexpensive monomers, and the polymer structures can be built with desired properties using various functional monomers. Sulfonated hydrocarbon PEMs have a significantly lower gas permeability than PFSA membranes. Some of them have high thermal and mechanical stabilities, and they can maintain their mechanical properties and have high water uptakes over a wide temperature range.^{150,151} Despite these advantages, some drawbacks are still observed. Sulfonated

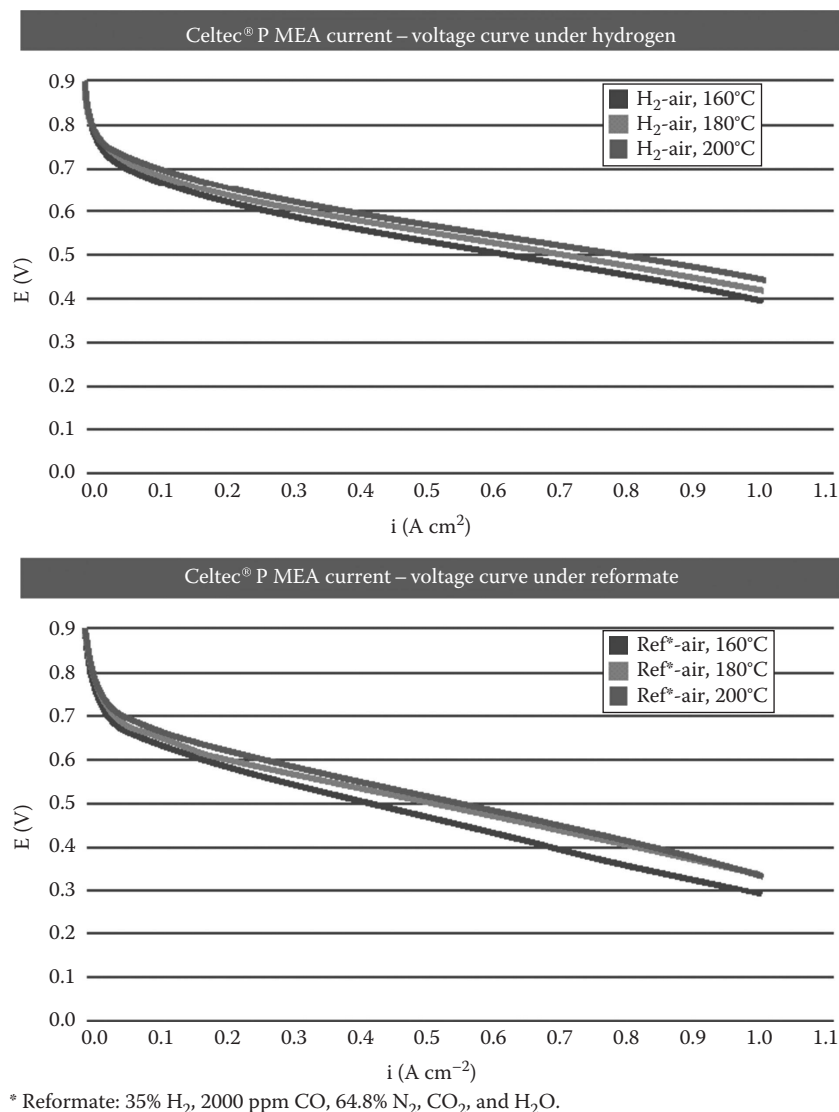


FIGURE 21.51 Celtec P MEA. Active cell area, 45 cm²; air, $\lambda = 2$, 0 bar; H₂, $\lambda = 1.2$, 0 bar; humidification, none. (Courtesy of Celanese AG, Dallas, TX.)

TABLE 21.10
Celtec P MEA Specifications

Performance	0.2 W cm ⁻² at 0.6 V, 180°C, 0 bar, H ₂ /air 0.13 W cm ⁻² at 0.6 V, 180°C, 0 bar, reformat ^a /air
Operational stability (long-term test)	>8,000 h
Drop in voltage in a long-term test	<6 μ V h ⁻¹
Operating temperature	120°C–200°C
CO tolerance	>50,000 ppm
Humidification of reaction gases	Unnecessary

^a Reformat: 35% H₂, 2,000 ppm CO, 64.8% N₂, CO₂, and H₂O.

hydrocarbon PEMs show relatively lower proton conductivities as compared to the Nafion at the same IECs. They exhibit excessive swelling behavior under hydrated conditions because of the weak phase separation between hydrophilic and hydrophobic parts.^{152,64} Furthermore, sulfonated hydrocarbon polymers have lower chemical and oxidative stability as compared to the PFSA membranes for the susceptibility of the sulfonated polymer backbones to chemical attack.¹⁵³ In order to overcome the aforementioned issues, many attempts have been made via the synthesis of copolymers with desirable structures, such as introducing functional side chains, highly sulfonated monomers, or block copolymers.

According to the backbone structures, sulfonated hydrocarbon PEMs can be classified as sulfonated polystyrene copolymers

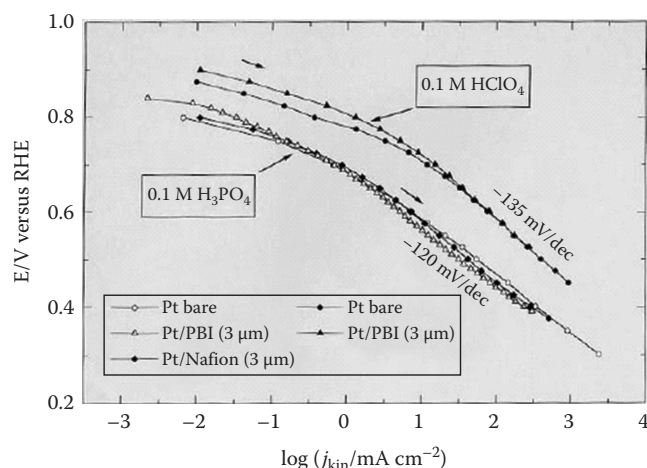


FIGURE 21.52 Tafel plots for O_2 reduction at $25^\circ C$ on oxidized Pt bare electrodes and Pt electrodes with PBI or Nafion film in 0.1 M acid solutions as indicated in the diagram. Scan rate 50 mV s^{-1} . Film thickness indicated in the diagram. (From Savinell, R.F. et al., *Presentation: High Temperature Polymer Electrolyte for PEM Fuel Cells*, 2001.)

(SPSs), sulfonated polyimides (SPIs), sulfonated poly(phenylene)s (SPPs), sulfonated poly(arylene)-type polymers (SPAs), and sulfonated poly(phosphazene)s (SPPhs).¹⁵⁴ They contain hydrophobic blocks (hydrocarbon backbone) and hydrophilic blocks (containing sulfonic acid groups). Sulfonic acid groups, which are commonly employed as hydrophilic functional groups, form well-defined nanosized channels for proton conduction.

Sulfonic acid groups are introduced to the hydrocarbon chains by sulfonation. In the case of sulfonation at aromatic polymer, a sulfonation agent (e.g., concentrated sulfuric acid, chlorosulfonic acid, or acetyl sulfate) reacts on the aromatic ring, and a proton of aromatic rings is substituted by a sulfonic acid group. The reaction takes place site-selectively on the electron-rich site of benzene rings, such as in ortho-position to electron-donating groups. Sulfonic acid groups can be introduced to the already polymerized material, which is called post-polymerization sulfonation method. The Guiver group investigated the sulfonation selectivity of several poly(ether ketone)s (PEKs) via a post-sulfonation approach. PEKs with various side substituents, such as phenyl, methylphenyl, and phenoxyphenyl groups, were found to have controlled sulfonation sites with single substituted sulfonic acid per repeated unit. By adjusting the molecular structures of the host polymers, the sulfonation takes place site-selectively.¹⁵⁵ Kerres et al. did not use the conventional sulfonation agents but sulfonated the polymer by lithiation. It is a four-step reaction containing lithiation, sulfonation, oxidation, and ion exchange. By this procedure, the sulfonic acid group can be inserted into the more hydrolysis-stable part of the molecule, and all polymers that can be lithiated can be subjected to this sulfonation process.¹⁵⁶ The other sulfonation method is direct copolymerization of sulfonated monomers, in which the monomers with sulfonic acid groups are copolymerized with nonsulfonated monomers. The McGrath group synthesized 3,3'-disulfonated

4,4'-dichlorodiphenyl sulfone monomers and prepared a series of sulfonated poly(arylene ether sulfone) (SPAES)-based copolymers.¹⁵⁷ The Guiver group applied commercial sulfonated bisphenol monomers to prepare sulfonated poly(arylene ether) (SPAE)-type copolymers (e.g., sulfonated poly(aryl ether ether ketone) [SPAEKK] and sulfonated poly(aryl ether ether nitril) [SPAEEN]).^{158,159}

In sulfonated hydrocarbon polymers, protons are transported through the proton-conductive channels, which are formed by aggregation of sulfonic acid groups. Most hydrocarbon membranes, especially the fully aromatic ones, possess sulfonic acid groups, which are directly attached to the phenyl rings of the polymer backbone. These sulfonic acid groups cannot aggregate easily, for the aggregation is not just the movement of several independent sulfonic acid groups but requires a sufficient mobility of the entire polymer backbone. There is no doubt that attaching the sulfonic acid groups directly to the backbone is not beneficial to the formation of efficient proton transport channels, at least the aggregation of acid groups is impeded. Attaching the sulfonic acid groups to the backbone via side chains is an efficient strategy to facilitate the formation of proton transport channels. The Guiver group designed comb-shaped SPAES with a new sulfonated side-chain grafting unit containing two or four sulfonic acid groups.^{160,161} The comb-shaped copolymers showed higher proton conductivities ($0.088\text{--}0.096 \text{ S cm}^{-1}$ at $80^\circ C$) compared to a Nafion membrane. Their methanol permeabilities ($1.73\text{--}3.40 \times 10^{-7} \text{ cm}^2 \text{ s}^{-1}$) are several times lower than the ones of Nafion.¹⁶⁰ However, the high initial performance of these comb-shaped polymers declined after MEA durability test, which was believed to be caused by chemical instability of the polystyrene-based side chains containing multiple sulfonic acid groups.¹⁶¹ Na and coworkers synthesized block sulfonated poly(arylene ether ketone) (SPAEK) containing flexible side-chain groups. The side-chain structure and the block structure in the polymers made the sulfonic acid groups more concentrated, and the phase separation between the hydrophobic and the hydrophilic domains became more apparent. The polymer membranes showed the highest proton conductivity of 0.246 S cm^{-1} at $80^\circ C$. Furthermore, they exhibited the lower methanol permeability and lower water swelling as compared to Nafion.¹⁶²

The charge carriers (protons and oxonium ions) in the membrane are created by hydrolytic dissolution of acid groups. High proton conductivity requires a sufficient water content of the membrane. In order to reduce the drastic decrease in the proton conductivity with decreasing water content, the acidity and concentration of the sulfonic acid groups in the hydrophilic domains should be increased.⁶⁴ As a result, the proton conductivity of PEMs with high concentration of sulfonic acid groups (always quantified by IEC) retains relatively high not only under fully hydrated conditions but also under more dry conditions (30% RH). Kreuer and coworkers prepared a series of sulfonated poly(phenylene sulfone)s (SPPSfs), in which the ether units ($-\text{CO}-$) were substituted by sulfone units ($-\text{SO}_2-$) to connect the phenyl rings.¹⁶³⁻¹⁶⁵ These ionomers exhibited increased acidity and

higher hydrolytic stability of the sulfonic acid groups due to the replacement of electron-donating group (ether linkage) by the electron-withdrawing group (sulfone linkage) in their backbone structure. The copolymer-type ionomers¹⁶³ were still insoluble in water with high IEC values in the range of 1.29–2.64 mequiv. g⁻¹. Their proton conductivities were higher than that of Nafion. The homopolymer-type ionomer,^{164,165} which was monosulfonated on each phenyl ring (sPSO₂-220), had an extremely high IEC value in the range of 4.3–4.5 mequiv. g⁻¹. In the dry state, the polymer possessed a remarkably high density (1.75 g cm⁻³) that was nearly as high as the density of pure sulfuric acid (1.83 g cm⁻³). Because of the extremely high charge carrier concentration of sPSO₂-220, it possessed very high proton conductivity, which was

seven times higher than that of Nafion under low-humidity (30% RH) and high-temperature (135°C) conditions. But unfortunately, sPSO₂-220 was soluble in water due to its high IEC. Additionally, a high content of acidic groups in a polymer tends to make it brittle in the dry state, which is a severe problem for the membrane undergoing many swelling–deswelling cycles during operation.¹⁶⁵

Synthesizing the PEMs as a block copolymer is a viable strategy to overcome the problems like poor water insolubility and high brittleness caused by the high content of sulfonic acid group. Figure 21.53 shows the concept for block copolymer membranes. In block copolymers, one segment possesses a high degree of sulfonation that meets the requirements of high proton conductivity; the other separated segment, which

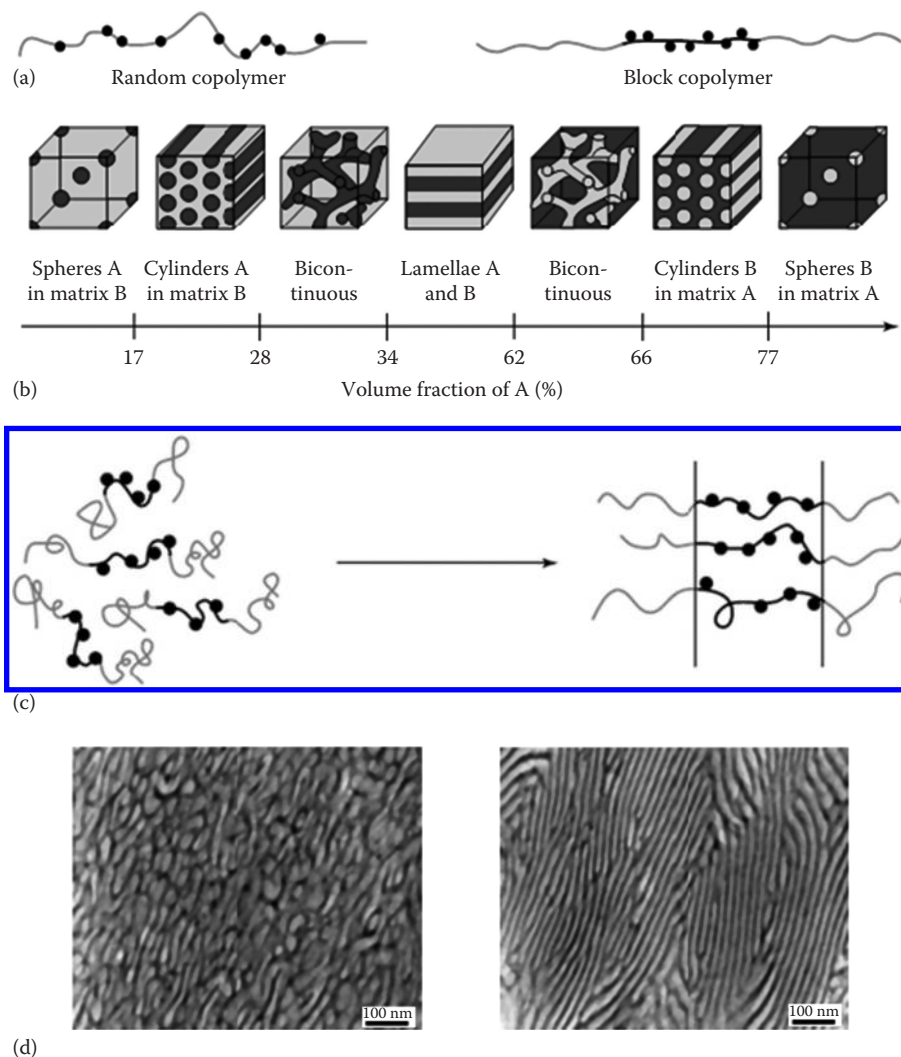


FIGURE 21.53 Concept of block copolymers for fuel cell membranes. (a) Schematic drawings of random and block copolymers; the black sections depict the acid sites. (b) Different thermodynamic equilibrium morphologies, which are discussed for diblock polymers for the strong phase segregation regime; note that the equilibrium morphology among other things depends on the composition of the diblock. (c) Block copolymers can in principle phase segregate into larger domains of the respective blocks; however, the obtainable morphology depends on the preparation conditions; a transition from a disordered to a lamellar morphology is shown. (d) Two morphologies for the same triblock copolymer are shown being different in the order of orientation. (Reprinted from Gross, M. et al., Design rules for the improvement of the performance of hydrocarbon-based membranes for proton exchange membrane fuel cells (PEMFC), in: *Handbook of Fuel Cells: Fundamentals, Technology and Applications*, Vielstich, W., Gasteiger, H.A., Lamm, A., Yokokawa, H., eds., John Wiley & Sons, Ltd., Chichester, U.K., 2010.)

is designed to enhance the mechanical and insoluble properties, has a low degree of sulfonation. Both segments are combined in the block copolymer with microphase separation. The aggregation of highly sulfonated segments forms hydrophilic domains, and the hydrophobic domains are formed by the aggregation of unsulfonated segments. The hydrophobic domains prevent water solubility. Therefore, much higher local sulfonic acid concentrations can be realized as compared to the random copolymers. The Ueda group prepared highly sulfonated multiblock copoly(ether sulfone)s with the IEC in the range of 1.90–2.75 mequiv. g⁻¹. Proton conductivity of all membranes at 80°C and 95% RH was higher than that of Nafion 117. Their multiblock copolymer with IEC of 2.75 mequiv. g⁻¹ exhibited high proton conductivity of 0.0023 S cm⁻¹ even under 30% RH. The phase separation and the high water uptake behavior contributed to the high proton conduction in a wide range of RH.^{166,167} The Watanabe group reported a series of sulfonated block copolymers. In the sulfonated poly(arylene ether sulfone)s (SPAESs) block copolymer, *bis*(4-fluorophenyl) sulfone (FPS) and 2,2-*bis*(4-hydroxy-3,5-dimethylphenyl) propane were used as comonomers for hydrophobic blocks, whereas FPS and 9,9-*bis*(4-hydroxyphenyl)fluorine were used as hydrophilic blocks. The block

copolymers showed stronger phase separation and better mechanical properties than those of the random copolymers. The larger hydrophilic and hydrophobic blocks resulted in higher water uptake and higher proton conductivity. The IEC values of block copolymers were in the range of 1.86–2.20 mequiv. g⁻¹, and the proton conductivities were in the range of 0.02–0.03 S cm⁻¹ at 80°C and 40% RH, which are comparable or higher than that of Nafion membranes.^{168–170}

Park et al.¹⁵⁴ summarized the properties of sulfonated hydrocarbon PEMs shown in Figure 21.54. Nafion 112 with IEC of about 0.91 mequiv. g⁻¹ was used as a reference sample.^{171,172} Hydrocarbon-based random copolymers without specific functionality or side chain were compared with Nafion.¹⁷³ Hydrocarbon-based random copolymers without specific functionality or side chain show similar or lower water uptake values than Nafion with the similar IECs at 25°C. Additionally, they exhibit much lower proton conductivity as compared to Nafion with the same IEC. The poor performance of hydrocarbon-based random copolymer is caused by the inefficient aggregation of sulfonic acid groups that are attached to the backbone directly (without side chain). In contrast, the sulfonic acid groups of Nafion are decorated at the side chains, and even at low IEC value, the

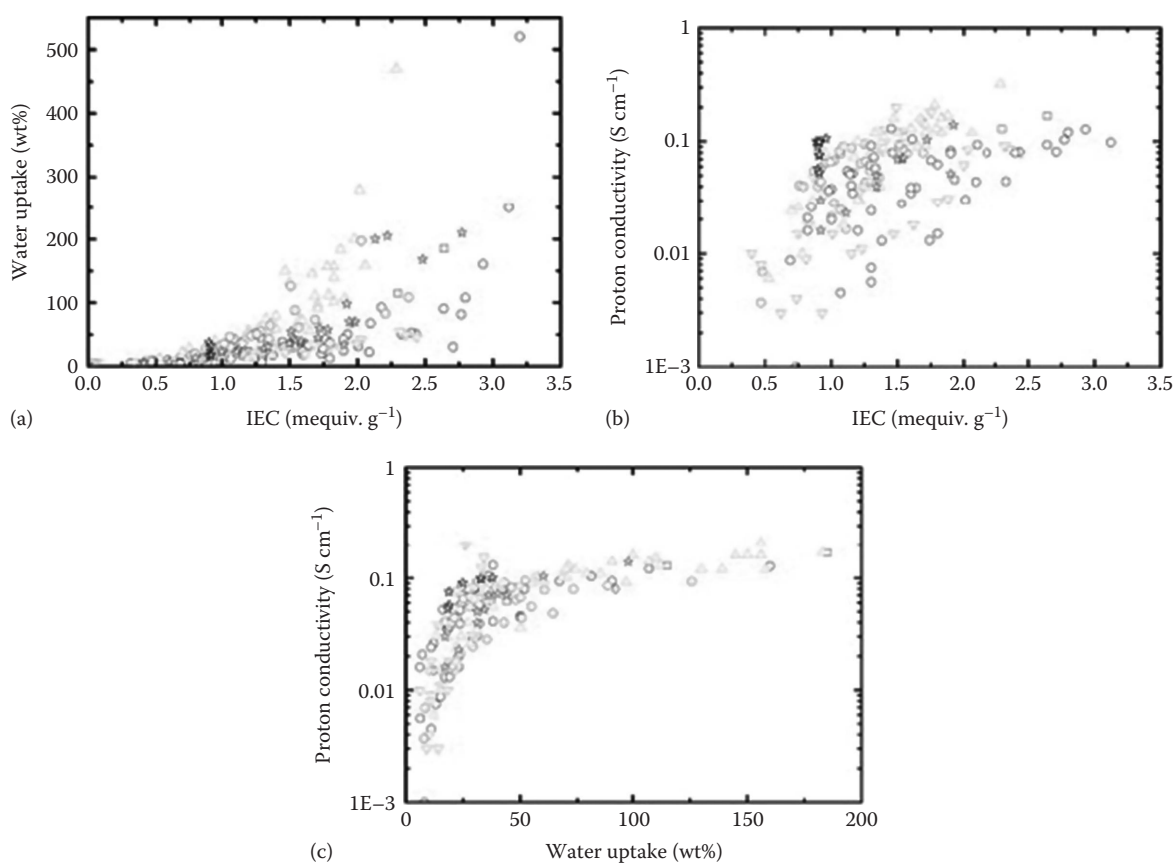


FIGURE 21.54 Performance comparison of various types of sulfonated PEMs at around 25°C: relationship between (a) IEC and water uptake (wt%), (b) IEC and proton conductivity, and (c) water uptake (wt%) and proton conductivity. Symbols: dark stars (Nafion), light stars (the reference sulfonated hydrocarbon PEMs), circles (sulfonated hydrocarbon PEMs with functional groups), up triangles (sulfonated hydrocarbon multiblock PEMs), down triangles (grafted and branched sulfonated hydrocarbon PEMs), squares (sulfonated hydrocarbon PEMs with high IEC), and dot-center circles (sulfonated hydrocarbon PEMs with highly sulfonatable monomers). (From Park, C.H. et al., *Progr. Polym. Sci.*, 36, 1443, 2011.)

sulfonic acid groups can aggregate effectively to form well-connected water channels. As a result, Nafion possesses high proton conductivity even with low water uptake. The poor performance of hydrocarbon-based random copolymers in proton conductivity can be compensated by increasing the content of sulfonic acid groups (increasing IEC). In fact, the practical IEC range of hydrocarbon-based random copolymer is over 1.25 mequiv. g⁻¹.

Sulfonated hydrocarbon PEMs with functional groups have comparably low water uptake at 25°C for given IEC values.^{158,174,175} This demonstrates that the introduction of functional groups can control excessive swelling of the membranes even for those with high IECs under hydrated condition.¹⁵⁴ This is a great potential for the application under fully humidified condition. These membranes exhibit relatively low proton conductivity shown in Figure 21.54b. No matter what the IEC values are, the proton conductivities of them are similar or lower than that of Nafion. According to their backbone chemical structure and functional group type, the proton conductivities disperse in a wide range from 0.002 to 0.1 S cm⁻¹ with the IEC values from 0.5 to 3.5 mequiv. g⁻¹. Most sulfonated hydrocarbon PEMs with functional groups tend to have low proton conductivities. However, some functional groups, such as electron withdrawing fluorine, can increase acidity, which results in a PEM with higher proton conductivity than for the samples without such functional groups.^{176,177}

Via strong phase separation between hydrophobic and hydrophilic segments in multiblock copolymer membranes, the well-connected proton transport channels are effectively formed in the hydrophilic segments, and the mechanical properties are enhanced by the carefully designed hydrophobic segments. Multiblock copolymers have relatively high water uptake values among sulfonated hydrocarbon PEMs, even for the same IEC values. High water uptake indicates a high water affinity; as a result, water molecules can be confined within PEMs strongly to maintain water channels for proton transport, even under low humidity and high temperature conditions. Multiblock PEMs have comparatively the highest level of proton conductivity (over 0.1–0.3 S cm⁻¹ at 25°C) of all sulfonated hydrocarbon PEMs. Additionally, most have comparable or higher proton conductivities than Nafion for IEC values greater than 1.2 mequiv. g⁻¹. Because of their well-defined phase-separated morphology, they exhibit low dimensional swelling despite their high water uptake. Consequently, sulfonated hydrocarbon multiblock PEMs are one of the most attractive design strategies for high-performance PEMs.¹⁷⁸

Most of grafted and branched sulfonated hydrocarbon PEMs have lower water uptake values as compared to other sulfonated hydrocarbon PEMs, so they exhibit great dimensional stability. In the case of the IEC values below 1.3 mequiv. g⁻¹, their proton conductivities are relatively lower than other PEMs. However, when the IEC values are over 1.3 mequiv. g⁻¹, their proton conductivities increase drastically to very high values (0.1–0.2 S cm⁻¹ at 25°C). This behavior indicates that flexible side chains containing sulfonic acid groups help with the formation of water channels for

proton transport in relatively high humidity conditions. In order to apply the grafted and branched sulfonated hydrocarbon PEMs at reduced humidity, a promising approach is to increase the number of sulfonic acid groups in side chains. Furthermore, low chemical stability of side chains in these PEMs is a significant issue. Molecular design of chemically stable side chains is necessary for actual PEMFC application of grafted and branched sulfonated hydrocarbon PEMs.^{160,179}

Sulfonated hydrocarbon PEMs with very high IEC values (containing extremely high content of sulfonic acid groups) do not show such high proton conductivities despite their high IEC values. Considering water uptake and proton conductivity, this type of PEMs has lower performance than others. However, they are originally designed for high-temperature (over 100°C) and low-humidity (around 30% RH) conditions. One of these PEMs shows extremely high IEC of 4.3 mequiv. g⁻¹ and seven times higher proton conductivity than Nafion at high temperature (135°C) and low humidity (30% RH).¹⁶⁵

Sulfonated hydrocarbon PEMs synthesized from highly sulfonatable monomer (such as tetraphenylphenylene ether with up to four sulfonic acid groups¹⁸⁰) have relatively low IEC (below 1.7 mequiv. g⁻¹), while their water uptakes and proton conductivities are higher than those of other sulfonated hydrocarbon PEMs and almost similar to those of sulfonated multiblock PEMs. The high water uptake and proton conductivity of these types of PEMs result from the structural characteristics that have both the advantages of multiblock copolymers and grafted and branched PEMs. But, in practice, the content in sulfonatable monomers should be limited to prevent brittleness of the membranes, for most of the highly sulfonatable monomers contain rigid aromatic structures. In order to solve this problem, introduction of flexible linkages into the highly sulfonatable monomers is a possible way.^{181,182}

21.5 SUMMARY

A lot of research has been carried out in the past decade to develop membranes for the whole spectrum of applications, namely, automotive, stationary, and portable applications. PFSA-based membranes have played the most prominent role until now. Much research has been conducted into the details of proton transport through different polymers and into methods of improving their properties, but a viable and inexpensive substitute to Nafion has yet to be developed. On the other hand, different approaches using PTFE fibril reinforcements have been successfully applied to PFSA-based membranes to make them more mechanically and thermally stable and thus to enhance durability. Such membranes are also reported to have better humidity and heat management characteristics besides lower specific protonic resistance and high power densities. Alternative approaches to modify the properties of PFSA-based membranes by impregnating inorganic fillers have also been reported to produce favorable results. But such membranes still await wide adoption. For liquid-phase operation (as in DMFCs), very inexpensive membranes based on nanoporous inorganic support matrices filled with liquid electrolytes have also shown good potential.

PFSA-based membranes cannot be used in the high-temperature range. A good alternative for the high-temperature range critical to automotive applications is the inorganic, acid-doped, PBI-based membrane from Celanese AG. In spite of all these improvements, a lot of work is still needed to improve various membrane characteristics that would make designing fuel cell-based systems much simpler and would eliminate the need for several BOP components, which adds to the complexity of the fuel cell systems.

REFERENCES

1. S. Srinivasan, Fuel cells for extraterrestrial and terrestrial applications. *Journal of the Electrochemical Society* 1989, 136(2), C41–C48.
2. J. Larminie, A. Dicks, *Fuel Cell Systems Explained*. New York: John Wiley & Sons, 2000.
3. L. Carrette, K.A. Friedrich, U. Stimming, Fuel cells—Fundamentals and applications. *Fuel Cells* 2001, 1, 5.
4. V. Metha, J.S. Cooper, Review and analysis of PEM fuel cell design and manufacturing. *Journal of Power Sources* 2003, 114, 32.
5. K. Kordesch, G. Simader, *Fuel Cells and Their Applications*. New York: John Wiley & Sons, 2000.
6. A.B. Stambouli, E. Traversa, Fuel cells, an alternative to standard sources of energy. *Journal of Power Sources* 2000, 86, 23.
7. A.B. LaConti, M. Hamdan, R.C. McDonald, In *Handbook of Fuel Cells: Fundamentals, Technology and Applications*, W. Vielstich, H.A. Gasteiger, A. Lamm, eds., Vol. 3, pp. 647–662. Chichester, U.K.: John Wiley & Sons, 2003.
8. M. Doyle, G. Rajendran, In *Handbook of Fuel Cells: Fundamentals, Technology and Applications*, W. Vielstich, H.A. Gasteiger, A. Lamm, eds., Vol. 3, pp. 351–395. Chichester, U.K.: John Wiley & Sons, 2003.
9. S. Gottesfeld, T.A. Zawodzinski, Polymer electrolyte fuel cells. In *Advances in Electrochemical Science and Engineering*, R.C. Alkire, H. Gerischer, D.M. Kolb, C.W. Tobias, eds., Vol. 5. Weinheim, Germany: Wiley-VCH, 1997.
10. W. Vielstich, H.A. Gasteiger, A. Lamm, eds., *Handbook of Fuel Cells: Fundamentals, Technology and Applications*, Vols. 3 and 4. Chichester, U.K.: John Wiley & Sons, 2003.
11. D.A. Masten, A.D. Bosco, In *Handbook of Fuel Cells Fundamentals: Technology and Applications*, W. Vielstich, H.A. Gasteiger, A. Lamm, eds., Vol. 4. Chichester, U.K.: John Wiley & Sons, 2003.
12. H.A. Gasteiger, M.F. Mathias, *Proton Conducting Membrane Fuel Cells III Symposium*. The Electrochemical Society of America, 2003.
13. H.A. Gasteiger, J.E. Panels, S.G. Yan, Dependence of PEM fuel cell performance on catalyst loading. *Journal of Power Sources* 2004, 127, 162–171.
14. G. Alberti, M. Casciola, L. Massinelli, B. Bauer, Polymeric proton conducting membranes for medium temperature fuel cells (110–160 degrees C). *Journal of Membrane Science* 2001, 185, 73–81.
15. Y.L. Ma, J.S. Wainright, M.H. Litt, R.F. Savinell, Conductivity of PBI membranes for high-temperature polymer electrolyte fuel cells. *Journal of the Electrochemical Society* 2004, 151, A8–A16.
16. M. Watanabe, Y. Satoh, C. Shimura, Management of the water-content in polymer electrolyte membranes with porous fiber wicks. *Journal of the Electrochemical Society* 1993, 140, 3190–3193.
17. S.H. Ge, X.G. Li, I.M. Hsing, Water management in PEMFCs using absorbent wicks. *Journal of the Electrochemical Society* 2004, 151(9), B523–B528.
18. S.H. Ge, X.G. Li, I.M. Hsing, Internally humidified polymer electrolyte fuel cells using water absorbing sponge. *Electrochimica Acta* 2005, 50(9), 1909–1916.
19. R.B. Hodgdon, J.R. Boyack, A.B. Laconti, *The degradation of polystyrene sulfonic acid*, TIS Report 65DE 5. Lynn, MA: General Electric Company, 1966.
20. A.B. Laconti, A.R. Fragala, J.R. Boyack, Solid polymer electrolyte electrochemical cells: Electrode and other material consideration. In *Proceeding of the Symposium on Electrode Materials and Process for Energy Conversion and Storage*, J.D.E. McIntyre, S. Srinivasan, F.G. Wills, eds., p. 354. Princeton, NJ: The Electrochemical Society, Inc., 1977.
21. A.B. Laconti, Hydrogen and oxygen fuel cell development. In *The MIT/Marine Industry Collegium, Power Systems for Small Underwater Vehicles*, J. Moore, Jr., ed. Cambridge, MA: MIT Sea Grant Program, 1988.
22. G.G. Scherer, Polymer membranes for fuel-cells. *Berichte der Bunsen-Gesellschaft: Physical Chemistry Chemical Physics* 1990, 94, 1008.
23. G.G. Scherer, *Berichte der Bunsen-Gesellschaft: Physical Chemistry Chemical Physics* 1990, 94, 145.
24. Z.G. Qi, A. Kaufman, Improvement of water management by a microporous sublayer for PEM fuel cells. *Journal of Power Sources* 2002, 109(1), 38–46.
25. U. Pasaogullari, C.Y. Wang, K.S. Chen, Two-phase transport in polymer electrolyte fuel cells with bilayer cathode gas diffusion media. *Journal of the Electrochemical Society* 2005, 152(8), A1574–A1582.
26. U. Pasaogullari, C.Y. Wang, Liquid water transport in gas diffusion layer of polymer electrolyte fuel cells. *Journal of the Electrochemical Society* 2004, 151(3), A399–A406.
27. U. Pasaogullari, C.Y. Wang, Two-phase transport and the role of micro-porous layer in polymer electrolyte fuel cells. *Electrochimica Acta* 2004, 49(25), 4359–4369.
28. X. Ren, P.F. Mutolo, F.W. Kovacs, S. Gottesfeld, Modified diffusion layer for use in a fuel cell system, U.S. Patent 6890680, 2005.
29. P. Stonehart, Development of advanced noble metal-alloy electrocatalysts for phosphoric-acid fuel-cells (PaFc). *Berichte der Bunsengesellschaft fur Physikalische Chemie* 1990, 94, 913–921.
30. P. Gode, G. Lindbergh, G. Sundholm, In-situ measurements of gas permeability in fuel cell membranes using a cylindrical microelectrode. *Journal of Electroanalytical Chemistry* 2002, 518, 115–122.
31. F.N. Buchi, M. Wakizoe, S. Srinivasan, Microelectrode investigation of oxygen permeation in perfluorinated proton exchange membranes with different equivalent weights. *Journal of the Electrochemical Society* 1996, 143, 927–932.
32. L. Zhang, C.S. Ma, S. Mukerjee, Oxygen permeation studies on alternative proton exchange membranes designed for elevated temperature operation. *Electrochimica Acta* 2003, 48, 1845–1859.
33. V.I. Basura, C. Chuy, P.D. Beattie, S. Holdcroft, Effect of equivalent weight on electrochemical mass transport properties of oxygen in proton exchange membranes based on sulfonated alpha,beta,beta-trifluorostyrene (BAM (R)) and sulfonated styrene-(ethylene-butylene)-styrene triblock (DAIS-analytical) copolymers. *Journal of Electroanalytical Chemistry* 2001, 501, 77–88.

34. K. Ota, Y. Inoue, N. Motohira, N. Kamiya, Hydrogen oxidation and oxygen reduction at Pt microelectrode on polymer electrolytes. *Journal of New Materials for Electrochemical Systems* 2000, 3, 193–198.
35. W.J. Liu, B.L. Wu, C.S. Cha, Surface diffusion and the spillover of H-adatoms and oxygen-containing surface species on the surface of carbon black and Pt/C porous electrodes. *Journal of Electroanalytical Chemistry* 1999, 476, 101–108.
36. M. Inaba, T. Kuroe, Z. Ogumi, Z. Takehara, K. Katakura, S. Ichikawa, Y. Yamamoto, Oxygen permeation through perfluorinated carboxylate ion-exchange membranes. *Electrochimica Acta* 1993, 38, 1727–1731.
37. D. Raistrick, J.W. Van Zee, R.E. White, K. Kinoshita, H.S. Burney, *Symposium on Diaphragms, Separators and Ion Exchange Membranes*. Pennington, NJ: The Electrochemical Society, 1986.
38. F.N. Büchi, G.G. Scherer, Investigation of the transversal water profile in nafion membranes in polymer electrolyte fuel cells. *Journal of the Electrochemical Society* 2001, 148, A183–A188.
39. P. Schroeder, *Zeitschrift für Physikalische Chemie* 1903, 45, 75.
40. K. Broka, P. Ekdunge, Oxygen and hydrogen permeation properties and water uptake of Nafion(R) 117 membrane and recast film for PEM fuel cell. *Journal of Applied Electrochemistry* 1997, 27, 117–123.
41. A. Heinzl, V.M. Barragan, A review of the state-of-the-art of the methanol crossover in direct methanol fuel cells. *Journal of Power Sources* 1999, 84(1), 70–74.
42. X. Ren, P. Zelenay, S. Thomas, J. Davey, S. Gottesfeld, Recent advances in direct methanol fuel cells at Los Alamos National Laboratory. *Journal of Power Sources* 2000, 86, 111–116.
43. X. Ren, T.E. Springer, S. Gottesfeld, Water and methanol uptakes in nafion membranes and membrane effects on direct methanol cell performance. *Journal of the Electrochemical Society* 2000, 147(1), 92–98.
44. X.M. Ren, T.E. Springer, T.A. Zawodzinski, S. Gottesfeld, Methanol transport through nafion membranes—Electro-osmotic drag effects on potential step measurements. *Journal of the Electrochemical Society* 2000, 147(2), 466–474.
45. X. Ren, T. Zawodzinski, S. Gottesfeld, Water and methanol transport in membranes for direct methanol fuel cells. *Abstracts of Papers of the American Chemical Society* 1999, 217, U490.
46. X.M. Ren, W. Henderson, S. Gottesfeld, Electro-osmotic drag of water in ionomeric membranes—New measurements employing a direct methanol fuel cell. *Journal of the Electrochemical Society* 1997, 144(9), L267–L270.
47. T.A. Zawodzinski, J. Davey, J. Valerio, S. Gottesfeld, The water-content dependence of electroosmotic drag in proton-conducting polymer electrolytes. *Electrochimica Acta* 1995, 40(3), 297–302.
48. S. Gottesfeld, Polymer electrolyte fuel-cells. *Electrochimica Acta* 1995, 40(3), 283–283.
49. X.M. Ren, S. Gottesfeld, Electro-osmotic drag of water in poly(perfluorosulfonic acid) membranes. *Journal of the Electrochemical Society* 2001, 148(1), A87–A93.
50. T.A. Zawodzinski, T.E. Springer, J. Davey, R. Jestel, C. Lopez, J. Valerio, S. Gottesfeld, A comparative-study of water-uptake by and transport through ionomeric fuel-cell membranes. *Journal of the Electrochemical Society* 1993, 140(7), 1981–1985.
51. T.A. Zawodzinski, T.E. Springer, F. Uribe, S. Gottesfeld, Characterization of polymer electrolytes for fuel-cell applications. *Solid State Ionics* 1993, 60(1–3), 199–211.
52. T.A. Zawodzinski, C. Derouin, S. Radzinski, R.J. Sherman, V.T. Smith, T.E. Springer, S. Gottesfeld, Water-uptake by and transport through nafion(R) 117 membranes. *Journal of the Electrochemical Society* 1993, 140(4), 1041–1047.
53. T.A. Zawodzinski, J. Davey, J. Valerio, S. Gottesfeld, Water transport-properties of various fuel-cell ionomers. *Abstracts of Papers of the American Chemical Society* 1993, 205, 75-PMSE.
54. T.A. Zawodzinski, S. Gottesfeld, S. Shoichet, T.J. McCarthy, The contact-angle between water and the surface of perfluoro-sulfonic acid membranes. *Journal of Applied Electrochemistry* 1993, 23(1), 86–88.
55. H. Dohle, H. Schmitz, T. Bewer, J. Mergel, D. Stolten, *Journal of Power Sources* 2002, 106, 313–322.
56. H. Dohle, J. Mergel, D. Stolten, *Journal of Power Sources* 2002, 111, 268–282.
57. M. Cappadonia, J.W. Erning, U. Stimming, Proton conduction of nafion((R))-117 membrane between 140 K and room-temperature. *Journal of Electroanalytical Chemistry* 1994, 376(1–2), 189–193.
58. M. Cappadonia, J.W. Erning, S.M.S. Niaki, U. Stimming, Conductance of nafion-117 membranes as a function of temperature and water-content. *Solid State Ionics* 1995, 77, 65–69.
59. S.J. Paddison, G. Bender, K.D. Kreuer, N. Nicoloso, T.A. Zawodzinski, The microwave region of the dielectric spectrum of hydrated Nafion (R) and other sulfonated membranes. *Journal of New Materials for Electrochemical Systems* 2000, 3, 291–300.
60. T.D. Gierke, G.E. Munn, F.C. Wilson, The morphology in nafion perfluorinated membrane products, as determined by wide-angle and small-angle x-ray studies. *Journal of Polymer Science Part B—Polymer Physics* 1981, 19, 1687–1704.
61. M. Eikerling, Y.I. Kharkats, A.A. Kornyshev, Y.M. Volkovich, Phenomenological theory of electro-osmotic effect and water management in polymer electrolyte proton-conducting membranes. *Journal of the Electrochemical Society* 1998, 145, 2684–2699.
62. S.J. Paddison, Proton conduction mechanisms at low degrees of hydration in sulfonic acid-based polymer electrolyte membranes. *Annual Review of Materials Research* 2003, 33, 289–319.
63. J.A. Keres, Development of ionomer membranes for fuel cells. *Journal of Membrane Science* 2001, 185, 3–27.
64. K.D. Kreuer, On the development of proton conducting polymer membranes for hydrogen and methanol fuel cells. *Journal of Membrane Science* 2001, 185, 29–39.
65. M. Elomaa, S. Hietala, M. Paronen, N. Walsby, K. Jokela, R. Serimaa, M. Torkkeli, T. Lehtinen, G. Sundholm, F. Sundholm, The state of water and the nature of ion clusters in crosslinked proton conducting membranes of styrene grafted and sulfonated poly(vinylidene fluoride). *Journal of Materials Chemistry* 2000, 10, 2678–2684.
66. M. Kawahara, M. Rikukawa, K. Sanui, Relationship between absorbed water and proton conductivity in sulfopropylated poly(benzimidazole). *Polymers for Advanced Technologies* 2000, 11, 544–547.
67. K.D. Kreuer, In *Handbook of Fuel Cells: Fundamentals, Technology and Applications*, W. Vielstich, H.A. Gasteiger, A. Lamm, eds., Vol. 3, pp. 420–436. Chichester, U.K.: John Wiley & Sons, 2003.
68. B. Choudhury, Material challenges in proton exchange membrane fuel cells. *International Symposium on Material Issues in a Hydrogen Economy*, November 12–15, 2007, Richmond, VA, 2007.

69. B. Bahar, A. Hobson, J. Kolde, D. Zuckerbrod, U.S. Patent 5547551, March 15, 1995, 1996.
70. S. Cleghorn, J. Kolde, W. Liu, In *Handbook of Fuel Cells Fundamentals, Technology and Applications*, W. Vielstich, H.A. Gasteiger, A. Lamm, eds., Vol. 3. Chichester, U.K.: John Wiley & Sons, 2003.
71. W. Liu, K. Ruth, G. Rusch, Membrane durability in PEM fuel cells. *Journal of New Materials for Electrochemical Systems* 2001, 4, 227–232.
72. M.G. Simon Cleghorn, W. Liu, J. Pires, J. Kolde, *Gore's Development Path to a Commercial Automotive Membrane Electrode Assembly*, 2007.
73. S. Hommura, Y. Kunisa, I. Terada, M. Yoshitake, Characterization of fibril reinforced membranes for fuel cells. *Journal of Fluorine Chemistry* 2003, 120, 151–155.
74. Y. Higuchi, I. Terada, H. Shimoda, S. Hommura, U.S. Patent EP1139472, 2001.
75. Y. Higuchi, I. Terada, H. Shimoda, S. Hommura, U.S. Patent US2001/00226883, 2001.
76. K. Yamada, Y. Kunisa, M. Tsushima, M. Kawamoto, Y. Takimoto, J.-I. Tayanagi, M. Yoshitake, *Abstracts of the 2003 Fuel Cell Seminar*, 2003.
77. M. Wakizoe, T. Kodani, T. Ota, *Abstracts of the 2003 Fuel Cell Seminar*, 2003.
78. J. Huslage, T. Rager, B. Schnyder, A. Tsukada, Radiation-grafted membrane/electrode assemblies with improved interface, *Electrochimica Acta* 2002, 48, 247–254.
79. J. Wei, C. Stone, A.E. Steck, U.S. Patent WO 95/08581, 1995.
80. G. Gebel, O. Diat, C. Stone, Microstructure of BAM (R) membranes: A small-angle neutron scattering study. *Journal of New Materials for Electrochemical Systems* 2003, 6, 17–23.
81. H.P. Brack, M. Wyler, G. Peter, G.G. Scherer, A contact angle investigation of the surface properties of selected proton-conducting radiation-grafted membranes. *Journal of Membrane Science* 2003, 214, 1–19.
82. S. Holmberg, P. Holmlund, C.E. Wilen, T. Kallio, G. Sundholm, F. Sundholm, Synthesis of proton-conducting membranes by the utilization of preirradiation grafting and atom transfer radical polymerization techniques. *Journal of Polymer Science Part A—Polymer Chemistry* 2002, 40, 591–600.
83. H.P. Brack, H.G. Buhner, L. Bonorand, G.G. Scherer, Grafting of pre-irradiated poly(ethylene-alt-tetrafluoroethylene) films with styrene: Influence of base polymer film properties and processing parameters. *Journal of Materials Chemistry* 2000, 10, 1795–1803.
84. H.P. Brack, F.N. Buchi, J. Huslage, M. Rota, G.G. Scherer, Development of radiation-grafted membranes for fuel cell applications based on poly(ethylene-alt-tetrafluoroethylene), ACS Symposium Series, 2000, pp. 174–188.
85. B. Gupta, G.G. Scherer, J.G. Highfield, Thermal stability of proton exchange membranes prepared by grafting of styrene into pre-irradiated FEP films and the effect of crosslinking. *Angewandte Makromolekulare Chemie* 1998, 256, 81–84.
86. G.G. Scherer, Interfacial aspects in the development of polymer electrolyte fuel cells. *Solid State Ionics* 1997, 94, 249–257.
87. B. Gupta, F.N. Buchi, G.G. Scherer, A. Chapiro, Crosslinked ion exchange membranes by radiation grafting of styrene/divinylbenzene into FEP films. *Journal of Membrane Science* 1996, 118, 231–238.
88. B. Gupta, F.N. Buchi, M. Staub, D. Grman, G.G. Scherer, Cation exchange membranes by pre-irradiation grafting of styrene into FEP films. 2. Properties of copolymer membranes. *Journal of Polymer Science Part A—Polymer Chemistry* 1996, 34, 1873–1880.
89. F.N. Buchi, B. Gupta, O. Haas, G.G. Scherer, Performance of differently cross-linked, partially fluorinated proton-exchange membranes in polymer electrolyte fuel-cells. *Journal of the Electrochemical Society* 1995, 142, 3044–3048.
90. B. Gupta, O. Haas, G.G. Scherer, Proton-exchange membranes by radiation grafting of styrene onto FEP films.4. Evaluation of the states of water. *Journal of Applied Polymer Science* 1995, 57, 855–862.
91. B. Gupta, M. Staub, G.G. Scherer, D. Grman, Surface non-homogeneity in radiation grafted FEP-g-polystyrenesulfonic acid proton-exchange membranes. *Journal of Polymer Science Part A—Polymer Chemistry* 1995, 33, 1545–1549.
92. F.N. Buchi, B. Gupta, O. Haas, G.G. Scherer, Study of radiation-grafted FEP-G-polystyrene membranes as polymer electrolytes in fuel-cells. *Electrochimica Acta* 1995, 40, 345–353.
93. G.G. Scherer, F.N. Buchi, B. Gupta, Radiation grafted membranes for polymer electrolyte fuel-cells, ex situ and in situ characterization. *Abstracts of Papers of the American Chemical Society* 1993, 205, 74-PMSE.
94. G.G. Scherer, E. Killer, D. Grman, Radiation grafted membranes—Some structural investigations in relation to their behavior in ion-exchange-membrane water electrolysis cells. *International Journal of Hydrogen Energy* 1992, 17, 115–123.
95. N. Walsby, *Preparation and Characterisation of Radiation-Grafted Membranes for Fuel Cells*. Helsinki, Finland, 2001.
96. A.B. Geiger, T. Rager, L. Matejek, G.G. Scherer, A. Wokaun, *Proceedings of First European PEFC Forum 2001*, F.N. Büchi, G.G. Scherer, A. Wokaun, eds., 2001.
97. K. Scott, W.M. Taama, P. Argyropoulos, Performance of the direct methanol fuel cell with radiation-grafted polymer membranes. *Journal of Membrane Science* 2000, 171, 119–130.
98. P. Stonehart, M. Watanabe, S. Associates., U.S. Patent 5523181, 1993.
99. S.K. Young, W.L. Jarrett, K.A. Mauritz, Studies of the aging of Nafion (R)/silicate nanocomposites using Si-29 solid state NMR spectroscopy. *Polymer Engineering and Science* 2001, 41, 1529–1539.
100. K.A. Mauritz, Organic–inorganic hybrid materials: Perfluorinated ionomers as sol–gel polymerization templates for inorganic alkoxides. *Materials Science and Engineering C—Biomimetic and Supramolecular Systems* 1998, 6, 121–133.
101. M.A.F. Robertson, K.A. Mauritz, Infrared investigation of the silicon oxide phase in [perfluoro-carboxylate/sulfonate (bilayer)]/[silicon oxide] nanocomposite membranes. *Journal of Polymer Science Part B—Polymer Physics* 1998, 36, 595–606.
102. P.L. Shao, K.A. Mauritz, R.B. Moore, [Perfluorosulfonate ionomer] [SiO₂–TiO₂] nanocomposites via polymer-in situ sol–gel chemistry: Sequential alkoxide procedure. *Journal of Polymer Science Part B—Polymer Physics* 1996, 34, 873–882.
103. P.L. Shao, K.A. Mauritz, R.B. Moore, [Perfluorosulfonate ionomer] [mixed inorganic oxide] nanocomposites via polymer in-situ sol-gel chemistry. *Chemistry of Materials* 1995, 7, 192–200.
104. N. Miyake, J.S. Wainright, R.F. Savinell, Evaluation of a sol-gel derived Nafion/silica hybrid membrane for polymer electrolyte membrane fuel cell applications—II. Methanol uptake and methanol permeability. *Journal of the Electrochemical Society* 2001, 148, A905–A909.
105. K.T. Adjemian, S. Srinivasan, J. Benziger, A.B. Bocarsly, Investigation of PEMFC operation above 100 degrees C employing perfluorosulfonic acid silicon oxide composite membranes. *Journal of Power Sources* 2002, 109, 356–364.

106. K.T. Adjemian, S.J. Lee, S. Srinivasan, J. Benziger, A.B. Bocarsly, Silicon oxide Nafion composite membranes for proton-exchange membrane fuel cell operation at 80–140 degrees C. *Journal of the Electrochemical Society* 2002, 149, A256–A261.
107. G. Alberti, M. Casciola, Composite membranes for medium-temperature PEM fuel cells. *Annual Review of Materials Research* 2003, 33, 129–154.
108. A.S. Arico, V. Baglio, V. Di Blasio, A. Di Blasi, E. Modica, P.L. Antonucci, V. Antonucci, Surface properties of inorganic fillers for application in composite membranes-direct methanol fuel cells. *Journal of Power Sources* 2004, 128, 113–118.
109. P.L. Antonucci, A.S. Arico, P. Creti, E. Ramunni, V. Antonucci, Investigation of a direct methanol fuel cell based on a composite Nafion (R)-silica electrolyte for high temperature operation. *Solid State Ionics* 1999, 125, 431–437.
110. P. Dimitrova, K.A. Friedrich, U. Stimming, B. Vogt, Modified Nafion((R))-based membranes for use in direct methanol fuel cells. *Solid State Ionics* 2002, 150, 115–122.
111. H. Uchida, Y. Ueno, H. Hagihara, M. Watanabe, Self-humidifying electrolyte membranes for fuel cells—Preparation of highly dispersed TiO₂ particles in Nafion 112. *Journal of the Electrochemical Society* 2003, 150, A57–A62.
112. H. Uchida, Y. Mizuno, M. Watanabe, Suppression of methanol crossover and distribution of ohmic resistance in Pt-dispersed PEMs under DMFC operation. *Journal of the Electrochemical Society* 2002, 149, A682–A687.
113. H. Uchida, Y. Mizuno, M. Watanabe, Suppression of methanol crossover in Pt-dispersed polymer electrolyte membrane for direct methanol fuel cells. *Chemistry Letters* 2000, 11, 1268–1269.
114. M. Watanabe, H. Uchida, H. Igarashi, Effects of polymer electrolyte membrane's property on fuel cell performances. *Macromolecular Symposia* 2000, 156, 223–230.
115. B. Bonnet, D.J. Jones, J. Roziere, L. Tchicaya, G. Alberti, M. Casciola, L. Massinelli, B. Bauer, A. Peraio, E. Ramunni, Hybrid organic-inorganic membranes for a medium temperature fuel cell. *Journal of New Materials for Electrochemical Systems* 2000, 3, 87–92.
116. S.P. Nunes, B. Ruffmann, E. Rikowski, S. Vetter, K. Richau, Inorganic modification of proton conductive polymer membranes for direct methanol fuel cells. *Journal of Membrane Science* 2002, 203, 215–225.
117. M. Watanabe, H. Uchida, Y. Seki, M. Emori, P. Stonehart, Self-humidifying polymer electrolyte membranes for fuel cells. *Journal of the Electrochemical Society* 1996, 143(12), 3847–3852.
118. P.L. Antonucci, A.S. Arico, P. Creti, E. Ramunni, V. Antonucci, Investigation of a direct methanol fuel cell based on a composite Nafion (R)-silica electrolyte for high temperature operation. *Solid State Ionics* 1999, 125(1–4), 431–437.
119. P. Dimitrova, K.A. Friedrich, B. Vogt, U. Stimming, Transport properties of ionomer composite membranes for direct methanol fuel cells. *Journal of Electroanalytical Chemistry* 2002, 532(1–2), 75–83.
120. B. Tazi, O. Savadogo, Effect of various heteropolyacids (HPAs) on the characteristics of Nafion((R))—HPAS membranes and their H-2/O-2 polymer electrolyte fuel cell parameters. *Journal of New Materials for Electrochemical Systems* 2001, 4, 187–196.
121. S. Malhotra, R. Datta, Membrane-supported nonvolatile acidic electrolytes allow higher temperature operation of proton-exchange membrane fuel cells. *Journal of the Electrochemical Society* 1997, 144, L23–L26.
122. I. Honma, H. Nakajima, S. Nomura, High temperature proton conducting hybrid polymer electrolyte membranes. *Solid State Ionics* 2002, 154, 707–712.
123. G. Alberti, M. Casciola, R. Palombari, Inorgano-organic proton conducting membranes for fuel cells and sensors at medium temperatures. *Journal of Membrane Science* 2000, 172, 233–239.
124. G. Alberti, U. Costantino, M. Casciola, S. Ferroni, L. Massinelli, P. Staiti, Preparation, characterization and proton conductivity of titanium phosphate sulfophenylphosphonate. *Solid State Ionics* 2001, 145, 249–255.
125. G. Alberti, M. Casciola, Solid state protonic conductors, present main applications and future prospects. *Solid State Ionics* 2001, 145, 3–16.
126. P. Costamagna, C. Yang, A.B. Bocarsly, S. Srinivasan, Nafion (R) 115/zirconium phosphate composite membranes for operation of PEMFCs above 100 degrees C. *Electrochimica Acta* 2002, 47, 1023–1033.
127. S. Haufe, D. Prochnow, D. Schneider, O. Geier, D. Freude, U. Stimming, Polyphosphate composite: Conductivity and NMR studies. *Solid State Ionics* 2005, 176(9–10), 955–963.
128. M. Cappadonia, O. Niemzig, U. Stimming, Preliminary study on the ionic conductivity of a polyphosphate composite. *Solid State Ionics* 1999, 125(1–4), 333–337.
129. T. Matsui, S. Takeshita, Y. Iriyama, T. Abe, M. Inaba, Z. Ogumi, Proton conductivity of (NH₄)₂TiP₄O₁₃-based material for intermediate temperature fuel cells. *Electrochemistry Communications* 2004, 6(2), 180–182.
130. T. Matsui, S. Takeshita, Y. Iriyama, T. Abe, Z. Ogumi, Proton-conductive electrolyte consisting of NH₄PO₃/TiP₂O₇ for intermediate-temperature fuel cells. *Journal of the Electrochemical Society* 2005, 152(1), A167–A170.
131. T. Uma, H.Y. Tu, D. Freude, D. Schneider, U. Stimming, Characterisation of intermediate temperature polyphosphate composites. *Journal of Materials Science* 2005, 40(1), 227–230.
132. S. Haufe, U. Stimming, *Journal of Membrane Science* 2001, 185, 95–103.
133. E. Peled, T. Duvdevani, A. Melman, A novel proton-conducting membrane. *Electrochemical and Solid-State Letters* 1998, 1(5), 210–211.
134. E. Peled, T. Duvdevani, A. Aharon, A. Melman, A direct methanol fuel cell based on a novel low-cost nanoporous proton-conducting membrane. *Electrochemical and Solid-State Letters* 2000, 3(12), 525–528.
135. J. Roziere, D.J. Jones, Non-fluorinated polymer materials for proton exchange membrane fuel cells. *Annual Review of Materials Research* 2003, 33, 503–555.
136. J.S. Wainright, M.H. Litt, R.F. Savinell, In *Handbook of Fuel Cells: Fundamentals, Technology and Applications*, W. Vielstich, H.A. Gasteiger, A. Lamm, eds., Vol. 3. Chichester, U.K.: John Wiley & Sons, 2003.
137. A. Schechter, R.F. Savinell, Imidazole and 1-methyl imidazole in phosphoric acid doped polybenzimidazole, electrolyte for fuel cells. *Solid State Ionics* 2002, 147, 181–187.
138. R.H. He, Q.F. Li, G. Xiao, N.J. Bjerrum, Proton conductivity of phosphoric acid doped polybenzimidazole and its composites with inorganic proton conductors. *Journal of Membrane Science* 2003, 226, 169–184.
139. B. Xing, O. Savadogo, Hydrogen/oxygen polymer electrolyte membrane fuel cells (PEMFCs) based on alkaline-doped polybenzimidazole (PBI). *Electrochemistry Communications* 2000, 2, 697–702.
140. Q.F. Li, H.A. Hjuler, N.J. Bjerrum, Oxygen reduction on carbon supported platinum catalysts in high temperature polymer electrolytes. *Electrochimica Acta* 2000, 45, 4219–4226.

141. O. Savadogo, B. Xing, Hydrogen/oxygen polymer electrolyte membrane fuel cell (PEMFC) based on acid-doped polybenzimidazole (PBI). *Journal of New Materials for Electrochemical Systems* 2000, 3, 343–347.
142. P. Staiti, M. Minutoli, S. Hocevar, Membranes based on phosphotungstic acid and polybenzimidazole for fuel cell application. *Journal of Power Sources* 2000, 90, 231–235.
143. B.Z. Xing, O. Savadogo, The effect of acid doping on the conductivity of polybenzimidazole (PBI). *Journal of New Materials for Electrochemical Systems* 1999, 2, 95–101.
144. M. Kawahara, J. Morita, M. Rikukawa, K. Sanui, N. Ogata, Synthesis and proton conductivity of thermally stable polymer electrolyte: Poly(benzimidazole) complexes with strong acid molecules. *Electrochimica Acta* 2000, 45, 1395–1398.
145. S.K. Zecevic, J.S. Wainright, M.H. Litt, S.L. Gojkovic, R.F. Savinell, Kinetics of O₂ reduction on a Pt electrode covered with a thin film of solid polymer electrolyte. *Journal of the Electrochemical Society* 1997, 144, 2973–2982.
146. S.R. Samms, S. Wasmus, R.F. Savinell, Thermal stability of proton conducting acid doped polybenzimidazole in simulated fuel cell environments. *Journal of the Electrochemical Society* 1996, 143, 1225–1232.
147. J.T. Wang, R.F. Savinell, J. Wainright, M. Litt, H. Yu, A H₂/O₂ fuel cell using acid doped polybenzimidazole as polymer electrolyte. *Electrochimica Acta* 1996, 41, 193–197.
148. Q.F. Li, H.A. Hjuler, N.J. Bjerrum, Phosphoric acid doped polybenzimidazole membranes: Physicochemical characterization and fuel cell applications. *Journal of Applied Electrochemistry* 2001, 31, 773–779.
149. R.F. Savinell, M.H. Litt, J.S. Wainright, In *Presentation: High Temperature Polymer Electrolyte for Pem Fuel Cells*, 2001.
150. M. Rikukawa, K. Sanui, Proton-conducting polymer electrolyte membranes based on hydrocarbon polymers. *Progress in Polymer Science* 2000, 25(10), 1463–1502.
151. M.A. Hickner, H. Ghassemi, Y.S. Kim, B.R. Einsla, J.E. McGrath, Alternative polymer systems for proton exchange membranes (PEMs). *Chemical Reviews* 2004, 104(10), 4587–4612.
152. C.H. Park, C.H. Lee, J.-Y. Sohn, H.B. Park, M.D. Guiver, Y.M. Lee, Phase separation and water channel formation in sulfonated block copolyimide. *The Journal of Physical Chemistry B* 2010, 114(37), 12036–12045.
153. Y. Yin, O. Yamada, K. Tanaka, K.-I. Okamoto, On the development of naphthalene-based sulfonated polyimide membranes for fuel cell applications. *Polymer Journal* 2006, 38(3), 197–219.
154. C.H. Park, C.H. Lee, M.D. Guiver, Y.M. Lee, Sulfonated hydrocarbon membranes for medium-temperature and low-humidity proton exchange membrane fuel cells (PEMFCs). *Progress in Polymer Science* 2011, 36(11), 1443–1498.
155. B. Liu, G.P. Robertson, D.-S. Kim, M.D. Guiver, W. Hu, Z. Jiang, Aromatic poly(ether ketone)s with pendant sulfonic acid phenyl groups prepared by a mild sulfonation method for proton exchange membranes. *Macromolecules* 2007, 40(6), 1934–1944.
156. J. Kerres, W. Cui, S. Reichle, New sulfonated engineering polymers via the metalation route. I. Sulfonated poly(ethersulfone) PSU Udel® via metalation-sulfination-oxidation. *Journal of Polymer Science Part A: Polymer Chemistry* 1996, 34(12), 2421–2438.
157. F. Wang, M. Hickner, Y.S. Kim, T.A. Zawodzinski, J.E. McGrath, Direct polymerization of sulfonated poly(arylene ether sulfone) random (statistical) copolymers: Candidates for new proton exchange membranes. *Journal of Membrane Science* 2002, 197(1–2), 231–242.
158. Y. Gao, G.P. Robertson, M.D. Guiver, S.D. Mikhailenko, X. Li, S. Kaliaguine, Synthesis of poly(arylene ether ether ketone ketone) copolymers containing pendant sulfonic acid groups bonded to naphthalene as proton exchange membrane materials. *Macromolecules* 2004, 37(18), 6748–6754.
159. Y. Gao, G.P. Robertson, M.D. Guiver, S.D. Mikhailenko, X. Li, S. Kaliaguine, Synthesis of copoly(aryl ether ether nitrile)s containing sulfonic acid groups for PEM application. *Macromolecules* 2005, 38(8), 3237–3245.
160. D.S. Kim, G.P. Robertson, M.D. Guiver, Comb-shaped poly(arylene ether sulfone)s as proton exchange membranes. *Macromolecules* 2008, 41(6), 2126–2134.
161. D.S. Kim, Y.S. Kim, M.D. Guiver, J. Ding, B.S. Pivovar, Highly fluorinated comb-shaped copolymer as proton exchange membranes (PEMs): Fuel cell performance. *Journal of Power Sources* 2008, 182(1), 100–105.
162. T. Na, K. Shao, J. Zhu, H. Sun, Z. Liu, C. Zhao, Z. Zhang, C.M. Lew, G. Zhang, Block sulfonated poly(arylene ether ketone) containing flexible side-chain groups for direct methanol fuel cells usage. *Journal of Membrane Science* 2012, 417–418(0), 61–68.
163. M. Schuster, K.-D. Kreuer, H.T. Andersen, J. Maier, Sulfonated poly(phenylene sulfone) polymers as hydrolytically and thermooxidatively stable proton conducting ionomers. *Macromolecules* 2007, 40(3), 598–607.
164. M. Schuster, C.C. de Araujo, V. Atanasov, H.T. Andersen, K.-D. Kreuer, J. Maier, Highly sulfonated poly(phenylene sulfone): Preparation and stability issues. *Macromolecules* 2009, 42(8), 3129–3137.
165. C.C. de Araujo, K.D. Kreuer, M. Schuster, G. Portale, H. Mendil-Jakani, G. Gebel, J. Maier, Poly(p-phenylene sulfone)s with high ion exchange capacity: Ionomers with unique microstructural and transport features. *Physical Chemistry Chemical Physics* 2009, 11(17), 3305–3312.
166. K. Nakabayashi, T. Higashihara, M. Ueda, Highly sulfonated multiblock copoly(ether sulfone)s for fuel cell membranes. *Journal of Polymer Science Part A: Polymer Chemistry* 2010, 48(13), 2757–2764.
167. K. Nakabayashi, T. Higashihara, M. Ueda, Polymer electrolyte membranes based on cross-linked highly sulfonated multiblock copoly(ether sulfone)s. *Macromolecules* 2010, 43(13), 5756–5761.
168. B. Bae, K. Miyatake, M. Watanabe, Synthesis and properties of sulfonated block copolymers having fluorenyl groups for fuel-cell applications. *ACS Applied Materials and Interfaces* 2009, 1(6), 1279–1286.
169. B. Bae, K. Miyatake, M. Watanabe, Sulfonated poly(arylene ether sulfone ketone) multiblock copolymers with highly sulfonated block. Synthesis and properties. *Macromolecules* 2010, 43(6), 2684–2691.
170. B. Bae, T. Yoda, K. Miyatake, H. Uchida, M. Watanabe, Proton-conductive aromatic ionomers containing highly sulfonated blocks for high-temperature-operable fuel cells. *Angewandte Chemie International Edition* 2010, 49(2), 317–320.
171. K. Miyatake, Y. Chikashige, M. Watanabe, Novel sulfonated poly(arylene ether): A proton conductive polymer electrolyte designed for fuel cells. *Macromolecules* 2003, 36(26), 9691–9693.
172. Y. Chikashige, Y. Chikyu, K. Miyatake, M. Watanabe, Poly(arylene ether) ionomers containing sulfluorenyl groups for fuel cell applications. *Macromolecules* 2005, 38(16), 7121–7126.
173. H. Ghassemi, J.E. McGrath, T.A. Zawodzinski, Jr., Multiblock sulfonated-fluorinated poly(arylene ether)s for a proton exchange membrane fuel cell. *Polymer* 2006, 47(11), 4132–4139.

174. M.J. Sumner, W.L. Harrison, R.M. Weyers, Y.S. Kim, J.E. McGrath, J.S. Riffle, A. Brink, M.H. Brink, Novel proton conducting sulfonated poly(arylene ether) copolymers containing aromatic nitriles. *Journal of Membrane Science* 2004, 239(2), 199–211.
175. Y.S. Kim, B. Einsla, M. Sankir, W. Harrison, B.S. Pivovar, Structure–property–performance relationships of sulfonated poly(arylene ether sulfone)s as a polymer electrolyte for fuel cell applications. *Polymer* 2006, 47(11), 4026–4035.
176. Y. Sakaguchi, A. Kaji, K. Kitamura, S. Takase, K. Omote, Y. Asako, K. Kimura, Polymer electrolyte membranes derived from novel fluorine-containing poly(arylene ether ketone)s by controlled post-sulfonation. *Polymer* 2012, 53(20), 4388–4398.
177. Z. Li, J. Ding, G.P. Robertson, M.D. Guiver, A novel bisphenol monomer with grafting capability and the resulting poly(arylene ether sulfone)s. *Macromolecules* 2006, 39(20), 6990–6996.
178. A.S. Badami, O. Lane, H.-S. Lee, A. Roy, J.E. McGrath, Fundamental investigations of the effect of the linkage group on the behavior of hydrophilic–hydrophobic poly(arylene ether sulfone) multiblock copolymers for proton exchange membrane fuel cells. *Journal of Membrane Science* 2009, 333(1–2), 1–11.
179. J. Ding, C. Chuy, S. Holdcroft, Solid polymer electrolytes based on ionic graft polymers: Effect of graft chain length on nano-structured, ionic networks. *Advanced Functional Materials* 2002, 12(5), 389–394.
180. K. Miyatake, A.S. Hay, Synthesis and properties of poly(arylene ether)s bearing sulfonic acid groups on pendant phenyl rings. *Journal of Polymer Science Part A: Polymer Chemistry* 2001, 39(19), 3211–3217.
181. S. Matsumura, A.R. Hlil, M.A.K. Al-Souz, J. Gaudet, D. Guay, A.S. Hay, Ionomers for proton exchange membrane fuel cells by sulfonation of novel dendritic multiblock copoly(ether-sulfone)s. *Journal of Polymer Science Part A: Polymer Chemistry* 2009, 47(20), 5461–5473.
182. S. Matsumura, A.R. Hlil, C. Lepiller, J. Gaudet, D. Guay, A.S. Hay, Ionomers for proton exchange membrane fuel cells with sulfonic acid groups on the end groups: Novel linear aromatic poly(sulfide–ketone)s. *Macromolecules* 2007, 41(2), 277–280.
183. T.A. Zawodzinski, M. Neeman, L.O. Sillerud, S. Gottesfeld, Determination of water diffusion-coefficients in perfluorosulfonate ionomeric membranes. *Journal of Physical Chemistry* 1991, 95, 6040–6044.
184. P.L. Spedding, Electrical conductance of molten alkali carbonate binary-mixtures. *Journal of Electrochemical Society* 1973, 120, 1049–1052.
185. A.L. Horvath, *Handbook of Aqueous Electrolyte Solutions*. Chichester, U.K.: Ellis Horwood Ltd., 1985.
186. N.P. Brandon, S. Skinner, B.C.H. Steele, Recent advances in materials for fuel cells. *Annual Review of Materials Research* 2003, 33, 183–213.
187. G. Alberti, M. Casciola, L. Massinelli, B. Bauer, Polymeric proton conducting membranes for medium temperature fuel cells (110–160 degrees C). *Journal of Membrane Science* 2001, 185, 73–81.
188. S.S. Kocha, In *Handbook of Fuel Cells: Fundamentals, Technology and Applications*, W. Vielstich, H.A. Gasteiger, A. Lamm, eds. Chichester, U.K.: John Wiley & Sons, 2003.
189. T. Sakai, H. Takenaka, E. Torikai, Gas-diffusion in the dried and hydrated nafions. *Journal of the Electrochemical Society* 1986, 133, 88–92.
190. T. Sakai, H. Takenaka, N. Wakabayashi, Y. Kawami, E. Torikai, Gas permeation properties of solid polymer electrolyte (SPE) membranes. *Journal of the Electrochemical Society* 1985, 132, 1328–1332.
191. K. Broka, P. Ekdunge, Modelling the PEM fuel cell cathode. *Journal of Applied Electrochemistry* 1997, 27, 281–289.
192. Z. Ogumi, Z. Takehara, S. Yoshizawa, Gas permeation in SPE method.1. Oxygen permeation through nafion and neosepta. *Journal of the Electrochemical Society* 1984, 131, 769–773.
193. G. Alberti, M. Casciola, Composite membranes for medium-temperature PEM fuel cells. *Annual Review of Materials Research* 2003, 33, 129–154.
194. A.N. Campbell, E.M. Kartzmark, D. Bisset, M.E. Bednas, The conductances of aqueous solutions of sulphuric acid at 50-degrees and 75-degrees. *Canadian Journal of Chemistry-Revue Canadienne De Chimie* 1953, 31, 303–305.
195. R. F. Savinell, M. H. Litt, J. S. Wainright, *Presentation: High Temperature Polymer Electrolyte for PEM Fuel Cells*, 2001.
196. M. Gross, G. Maier, T. Fuller, S. MacJinnon, C. Gittleman, Design rules for the improvement of the performance of hydrocarbon-based membranes for proton exchange membrane fuel cells (PEMFC). In *Handbook of Fuel Cells: Fundamentals, Technology and Applications*, W. Vielstich, H.A. Gasteiger, A. Lamm, H. Yokokawa, eds. Chichester, U.K.: John Wiley & Sons, Ltd., 2010.
197. C.H. Park, C.H. Lee, M.D. Guiver, Y.M. Lee, Sulfonated hydrocarbon membranes for medium-temperature and low-humidity proton exchange membrane fuel cells (PEMFCs). *Progress in Polymer Science* 2011, 36, 1443–1498.
198. M. Casciola, F. Marmottini, A. Peraio, *Solid State Ionics* 1993, 61, 125.
199. G. Alberti, L. Boccali, M. Casciola, L. Massinelli, E. Montoneri, *Solid State Ionics* 1996, 84, 97.
200. G. Alberti, *Semaine D'étude Sur le Thème Membranes Biologiques et Artificielles et la Desalinisation de L'eau*, R. Passino, eds., pp. 629–669. Città del Vaticano: Pontificia Accad. d. Sci. 17, 1975.